

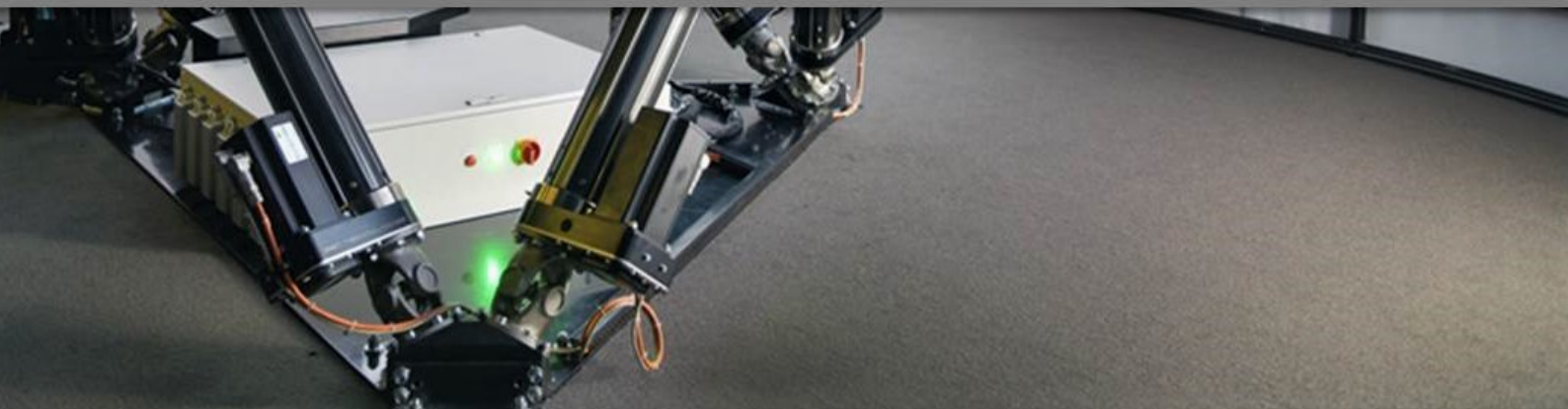


Technische Universiteit Delft

## Highly Automated Driving

Transitions of control authority using  
Haptic Shared Control

K. M. van Dintel





# Highly Automated Driving

## Transitions of control authority using Haptic Shared Control

by

**K. M. van Dintel**

to obtain the degree of Master of Science  
at the Delft University of Technology,  
to be defended publicly on Monday December 23, 2019 at 13:00 PM.

Student number: 4213270  
Project duration: January 23, 2019 – December 23, 2019  
Thesis committee: Prof. dr. ir. D. A. Abbink, TU Delft, supervisor  
Dr. ir. S. M. Petermeijer, TU Delft, supervisor  
Dr. ir. E. J. H. de Vries, Cruden BV, supervisor  
Dr. ir. D. H. Plettenburg, TU Delft, external member

An electronic version of this thesis is available at <http://repository.tudelft.nl/>.

Cover photo © Audi AG 2016

The work in this thesis was supported by Cruden BV. Their cooperation is hereby gratefully acknowledged.



# Preface

Dear reader, thank you for taking the time and interest to read my master thesis. Self-driving cars is one of the hot topics in the 21<sup>st</sup> century, and raises many question. One of these questions is: "How will the role of human change, when they are no longer actively engaged with the driving task?" Therefore, in the past year I have done research on the transitions from highly automated driving back to manual control, with the aim to make a valuable contribution to our understanding of the interaction between human and machine.

I would like to express my gratitude to my supervisors David Abbink and Bastiaan Petermeijer for their sincere enthusiasm throughout the project. This really helped me to keep motivated and proud of the work. I would also like to thank Edwin de Vries for his guidance during the project and for encouraging me to take a critical view of my work. This helped me to approach the work from different angles with a fresh mindset. I would like to show my appreciation to Jelle van Doornik for providing me with technical support whenever I had issues with the simulator.

Furthermore, I would like to thank my friends, family and Renske for supporting me throughout my research and for enduring my sometimes tiring monologues about the subject.

*K. M. van Dintel*  
*Delft, December 2019*



# Contents

<b>1</b>	<b>Research Paper</b>	<b>1</b>
1.1	Introduction . . . . .	2
1.2	Method . . . . .	3
1.3	Results . . . . .	7
1.4	Discussion . . . . .	9
1.5	Conclusion . . . . .	11
1.6	Acknowledgement . . . . .	11
1.7	References . . . . .	11
<b>A</b>	<b>Implementation</b>	<b>13</b>
A.1	Haptic Shared Control . . . . .	13
A.2	Lane Change support Algorithm . . . . .	14
A.2.1	Human Compatible Reference . . . . .	14
A.2.2	Lane Change Algorithm vs Bessel filter approach . . . . .	15
A.3	Recommendations . . . . .	19
<b>B</b>	<b>Experiment Forms</b>	<b>21</b>
B.1	Informed Consent . . . . .	21
B.2	Van Der Laan questionnaire. . . . .	21
B.3	Demographics questionnaire . . . . .	21
B.4	Results . . . . .	33
B.4.1	Van Der Laan questionnaire . . . . .	33
B.4.2	Demographics questionnaire . . . . .	35
<b>C</b>	<b>Supplementary Results</b>	<b>37</b>
C.1	Raw Data Plots . . . . .	37
C.2	Additional Results. . . . .	67
<b>D</b>	<b>Planning</b>	<b>71</b>
	<b>Bibliography</b>	<b>73</b>



# 1

Research Paper

# Transitions of control authority between highly automated driving and manual control using Haptic Shared Control

Kevin M. van Dintel, Sebastiaan M. Petermeijer, Edwin. J. H. de Vries, David A. Abbink

**Abstract**—The arrival of highly automated vehicles introduces a new interaction between the vehicle and driver. System limitations during highly automated driving require the driver to be ready to take back control at request. Previous studies on the take-over process concluded that the driver requires a transition period to stabilize vehicle control after resuming manual control. These studies used traded control to instantaneously transfer control back to the driver, causing an abrupt switch in control authority. Therefore, this study explores Haptic Shared Control as a different transition approach. By varying the level of haptic authority, a smooth connection between automation system and driver can be realized. The aim of this study is to investigate if Haptic Shared Control improves the take-over performance compared to the traded control approach. A total of 30 participants drove two trials in a driving simulator, one for each transition approach. Each trial consisted of 10 take-over scenarios divided into two levels of time-criticality. During autonomous driving the participants were engaged in a secondary task. The take-over performance was assessed based on safety performance, lateral vehicle control, controller performance and subjective measures. Results showed a significant decrease in the standard deviation of the lateral position evaluated over the mean trajectory per participant for the Haptic Shared Control approach compared to traded control. Haptic Shared Control also showed a significant decrease for the mean lateral obstacle clearance. The analyses on torque conflicts revealed a significant increase for critical take-over maneuver compared to non-critical take-over maneuvers. This suggests that haptic shared control can assist the driver in stabilizing lateral vehicle control after resuming manual control. On the other hand, the driver is limited in performing a sharp evasive maneuver, and this relationship is discussed. More research is needed on using an adaptable human compatible reference.

**Index Terms**—autonomous driving, control transitions, Haptic Shared Control, driving simulator

## I. INTRODUCTION

**N**OWADAYS, modern on-road vehicles are equipped with one or more advanced driver-assistance systems (ADAS). These systems are designed to assist or take over driving tasks from the driver. The motivation behind ADAS is that they increase traffic safety, traffic efficiency and the ride comfort [1]. In the near future the first highly automated driving (HAD) vehicles are expected on the road [2], [3]. During HAD the vehicle assumes lateral and longitudinal control, and performs the full dynamic driving task (DDT). This enables the driver to go out-of-the-loop and shift their attention to a non-driving related task (NDRT), e.g. reading a book. The new interaction between driver and automation will require frequent back and forth transitioning of control authority. Studies have shown that

drivers engaged in NDRT during HAD suffer from out-of-the-loop performance problems such as loss of situation awareness (SA) [4]. In particular, a system-initiated transition from HAD to manual control, in this study referred to as the take-over maneuver, can cause serious safety implications. Scenarios where system limits are reached vary widely in criticality, ranging from expected highway exits to unexpected accidents happening in front of the vehicle. It is in these situations that the driver relies on the system to supply key information and assistance to ensure a safe and smooth transition of control authority. Therefore, the challenge is to get the driver back-in-the-loop and capable of performing an adequate control input.

In case of a take-over maneuver, the system signals the driver to take back control of the vehicle. The time provided to the driver between the take-over request (TOR) and the system limit is referred to as the time budget (TB) [5]. In [6] it is argued that the driver needs to perform four main actions after the TOR:

- 1) shift visual attention to the road,
- 2) cognitively process and evaluate the traffic situation and select an appropriate action (i.e. braking or steering),
- 3) reposition himself, so that control of the vehicle can be resumed (e.g. hands on steering wheel and feet on pedals),
- 4) implement the selected action via the steering wheel and/or pedals.

Item 1 and 2 form the mental process of the take-over maneuver. Parallel to the mental aspect are items 3 and 4, forming the physical process of the take-over maneuver. Extensive research has been done in driving simulators on the driving behavior during and after the transition, with the main area of focus on item 1,2 and 3, whereas hardly any attention is given to item 4 [5]–[23]. A large fraction of these studies measure the take-over performance in terms of driver reaction time. In other words, how long does the TB need to be to ensure a safe take-over maneuver. An overview is given in [24] and [25]. It is argued that a TB of 7 s is sufficient for a driver to safely resume manual control. [5] found that there is a relation between the provided TB and the reaction time; shorter TB's lead to faster reaction times. When provided with short TB's, the drivers are still capable of reacting in time, but results show impaired driving performance. Research found a decrease in mirror and shoulder checks [5]. In several studies [5], [7], [9], object avoidance was necessary after resuming manual control, the results showed the vehicle overshooting

the target lane in combination with higher measured lateral accelerations, followed by poorly damped stabilization of the lateral vehicle control. [11] argued that it can take up to 40 s for the driver to resume manual control and to stabilize the lateral control in terms of high frequency component of steering (HFS). [10] made similar conclusions and showed that the driver required 6-9 s to stabilize lateral vehicle control in terms of standard deviation of lateral position (SDLP) after a TOR was signaled. These results indicate that it is important to include a transition period in which the driver needs time to stabilize vehicle control and gain SA after resuming manual control. This aspect of the take-over performance is referred to as the take-over quality.

There are two key moments of interaction between driver and automation during the take-over maneuver. The first moment is the TOR, and the second is when the control authority is transferred to the driver. These interaction moments are the focus areas to increase take-over performance. As mentioned, most studies focus on improving the cognitive process by increasing the SA and aid in decision making before transferring the control back to the driver. [17] introduces a human machine interface (HMI) that uses augmented reality with projections in the windscreen to inform the driver about the current driving situation. [6] used haptic stimuli in the seat to provide the driver with directional warnings. These studies use traded control (TC) for the transitions. In this approach all control authority is transferred instantaneous to the driver upon deactivation of the HAD system. However, research shows that differences in driving speed prior to HAD and after HAD, necessitates an adaption period for the driver before returning to previous steering behavior [8]. This, and the impaired driving performance during the required transition period to stabilize vehicle control, imply that the take-over performance can benefit from system assistance at the control input level, concerning item 4. On the basis of these results, this study proposes a new method to transfer control authority back to the driver.

It is envisioned that Haptic Shared Control (HSC) can be implemented to assist the driver in vehicle control during the transition phase. In multiple studies HSC has been implemented in the automotive domain and shows improved results for driving performance in both lateral [26]–[29] and longitudinal [30] direction. Through continuous haptic feedback at the steering wheel, the system and driver are able to communicate and simultaneously perform control actions resulting in enhanced driving performance. An interesting feature of HSC is that it can realize any level of control authority between manual control and full automation by tuning the level of haptic authority (LoHA) [31]. In this way a smooth transfer of control authority can be realized. More weight should be put towards implementing HSC to assist the driver with lateral control, because research has shown that drivers tend to steer first before using the pedals when confronted with system failure [32]. In [33]–[35], ways to use HSC as a transition approach are already being explored and it is found that it can increase the stability of vehicle motion

in terms of SDLP. However, these studies mainly focus on the transition approach in non-critical situation without including other take-over maneuver related issues, such as obstacle avoidance, different levels of criticality or traffic density.

The aim of this research is to extend current knowledge on the take-over maneuver by exploring a transition approach with HSC. A simulator study is conducted in which it is investigated if the introduced approach yields take-over performance benefits in comparison with the TC approach used in literature. It is hypothesized that HSC can assist the driver in stabilizing lateral vehicle control in terms of SDLP and that it can minimize the unwanted carryover effects in terms of safety aspects, such as the higher measured lateral accelerations and the overshooting target lane behavior found by previous studies.

## II. METHOD

### A. Participants

The study counted 33 participants (25 male, 8 female). The experimental data of two participants was omitted from the study, due to a logging error and a misuse of the system. Another experiment had to be ended prematurely due to motion sickness, leading to no usable data. This leaves the data of 30 participants (24 male, 6 female) to be analyzed in this study. The participants were between 22 and 62 years old ( $M=31.9$  years;  $SD=11.2$  years), and were all in possession of a valid driver's license. Their mean driving experience was 13.4 years ( $SD=11.3$  years). Ten participants reported to have no prior driving simulator experience, whereas fifteen participants reported to have driven in a driving simulator five times or more.

### B. Apparatus

1) *Hardware:* This study used an AS2 six degrees of freedom (6DoF) motion-based driving simulator from the company Cruden BV, depicted in figure 1. The 6DoF Hexapod provides vestibular and haptic feedback to the driver. A



Fig. 1. The AS2 6DoF motion-based Cruden driving simulator with the setup used during the experiment.

control loader running at a frequency of 1000 Hz is used to generate the required haptic feedback to the driver through the steering wheel. The simulator is equipped with a conical projection screen which provides a 210 degrees front view of the environment generated by three projectors operating at 120 Hz. Rear view of the environment is realized by three LCD screens mimicking the mirrors (right, center, and left), shown in figure 1. The simulator was equipped with a fully functioning dashboard with working indicators, similar to modern day vehicles. Road and engine noise are played back over the audio system.

2) *ADAS Controls*: To transfer control authority between HAD and manual control the participants could activate the automation system by pressing the ACC-on button on the lever. At this point an icon on the dashboard appeared indicating that the HAD mode is active. At all times, the system could be deactivated using the same button. In case of TC, the system also deactivated if the driver intervened by exerting a torque greater than 2 Nm on the steering wheel or by pressing the brake pedal past its 10% capacity range. During the HSC transition approach, these inputs caused the system to fall back to a cooperative driving mode. The HAD mode could be resumed by pulling the lever towards the steering wheel, or manual control could be realized by pressing the ACC-on button on the lever.

3) *Software*: The simulator runs on Cruden's own Panthera ADAS simulator software. The logged data was collected at a frequency of 1000 Hz. By means of the openDRIVE format from VIREs virtual test drive software, traffic was integrated into the software. A collision was only possible with the guardrail. In case of a collision with another vehicle, the ego vehicle would drive through these objects.

### C. Implementation of haptic shared control

In this study HSC has been implemented using the Four Design Choice Architecture (FDCA), based on previous work [36]. The motivation for this controller is that it uses separate feedback and feedforward control. The separate feedforward control allows for a continuous haptic feedback, to compensate for the moments without a feedback error. When active, this system provides a cooperative state in which the driver and system communicate by exerting forces on the steering wheel.

1) *Four Design Choice Architecture*: The settings of the FDCA controller are based on four design parameters:

- *Human Compatible Reference (HCR)*: An online determined reference trajectory by the system.
- *Level of Haptic Strength (LoHS)*: A percentage of the desired torques based on the desired steering wheel angle to follow the HCR. 0% means no assistance at all, and 100% represents autonomous driving.
- *Level of Haptic Feedback (LoHF)*: The torques by the feedback control to correct for the deviations of the HCR, based on the heading error and lateral error.
- *Level of Haptic Authority (LoHA)*: Virtual springs that can dynamically change the steering stiffness in order to change the level of resistance on the steering wheel.

2) *Human Compatible Reference*: The implementation of the HCR in this study is limited to a straight three lane highway. During lane keeping, the lane center is used as HCR for the controller. However, it is also desired that the system can provide support during a lane change based on the steering input of the driver. The lane change support system is related to the work in [37], and uses the time-to-line crossing (TLC) as a measure to trigger a lane change, and is defined as the time duration available for the driver before any lane boundary crossing [38]. If the TLC drops below a heuristically tuned threshold ( $T_{TLC}$ ), the system initiates support for a lane change. In case of a steering input combined with active indicator lights,  $T_{TLC}$  is set higher, in order to achieve a smooth lane change.

After a lane change support has been triggered, the HCR switches from the current lane center to the next desired lane center. A 4<sup>th</sup> order low-pass Bessel filter is used to filter the step response in the HCR in order to realize a smooth lateral reference trajectory, connecting the two lane centers. The coefficients of the filter polynomials are given in equation 1, with  $\omega_0$  as cut-off frequency.

$$tf_{Bess} = \frac{1}{\frac{s^4}{\omega_0^4} + 3.124 \frac{s^3}{\omega_0^3} + 4.392 \frac{s^2}{\omega_0^2} + 3.201 \frac{s}{\omega_0} + 1} \quad (1)$$

The filter has a continuous output up until the third derivative, even if the input is discontinuous, which makes it very suitable for trajectory planning [36]. Another property of the Bessel filter is that it has a linear phase lag, which is equivalent to a time delay. This makes it possible to predetermine the lane change duration. A one-size-fits-all approach was used with a fixed lane change duration for all supported lane changes. The lane change duration was set to 4 seconds in this study.

### D. Experiment Design

For this study a repeated measures within-subject experiment was designed with two within-subject factors: transition and criticality. Transition was divided into the two transition approaches. Criticality also contained two levels, a time critical scenario and a time non-critical scenario. This gives the 4 levels of independent variables, listed in table I. The critical scenario contained a take-over maneuver with a TB of 5 s, whereas the non-critical scenario provided a TB of 7 s. These TB's were chosen to make the results of this study comparable with previous studies [5], [7], [40], [43], [49], [50].

TABLE I  
LEVELS OF INDEPENDENT VARIABLES

Independent Variables:	Levels:
<i>Transition:</i>	Traded Control (TC)
	Haptic Shared Control (HSC)
<i>Criticality:</i>	Critical (TB = 5 s)
	Non-Critical (TB = 7 s)

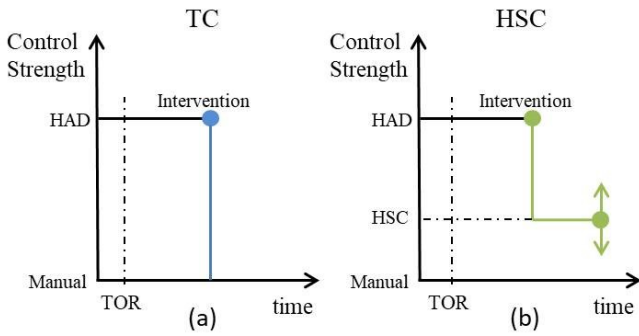


Fig. 2. Schematic illustration, visualizing the tuning of the controller during a take-over maneuver; (a) TC, (b) HSC

1) *Transition approaches*: The transitions in this study are all initiated by the automation system during autonomous driving, while the driver is engaged in a NDRT. During autonomous driving, the system functions as a lane keeping system, that assumes both lateral and longitudinal control at a velocity of 100 km/h. The longitudinal control is based on an adaptive cruise control (ACC) system, and the lateral control is performed by the FDCA controller described in section II-C. The strength of the LoHS are set to 100% and the LoHA is set high to simulate autonomous driving. If a system limit is detected, a multi-modal TOR is signaled to the driver in the form of an auditory beep and a flashing icon on the dashboard. A multi-modal TOR is used in many previous studies, an overview is given in [24], and results in faster reaction times than uni-modal TOR's [39]. The differences between the two approaches to transfer control back to the driver start as soon as the driver intervenes and takes back control. In both cases the longitudinal support is deactivated when the driver intervenes. However, after intervention the tuning of the lateral support is done in two different ways, shown in figure 2.

- *Traded Control*: TC uses a binary approach for the transition, illustrated in figure 2a. After the driver intervenes and deactivates the automation system, all control authority is transferred back to the driver instantaneously. The TC approach is based on the method used in previous studies [5], [8], [9], [11], [12], [14]–[16], [40]–[44].
- *Haptic Shared Control*: After intervention, the control strength of the system is dropped to a cooperative state as described in section II-C. In this state the system acts as a haptic guidance system to assist the driver in vehicle control following a transition. The driver can either continue in this mode, resume HAD, or deactivate the system, as seen in figure 2b.

2) *Driving scenario*: During the experiment, participants drove two experimental trials on a straight endless three lane highway (figure 3). The order of the experimental trials was counterbalanced to reduce order effects. During a single trial

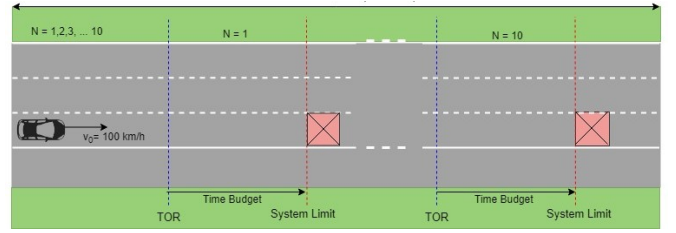


Fig. 3. Schematic visualization of the driving scenarios performed in the experiment. The TB varied randomly per driving scenario, providing either 5 s or 7 s between TOR and system limit.

drivers were supported by the lane keeping assistance with a single transition approach (i.e. TC or HSC), and experienced 10 take-over scenarios. The take-over scenarios involved a stationary vehicle appearing in front of the ego vehicle. The vehicles appeared at a random interval between 1.5 and 2 minutes apart over a distance of 40 km. Other traffic on the road during the experiment included faster vehicles overtaking in the left lane and a vehicle in the middle lane driving at a constant distance in front of the ego vehicle. This created a realistic environment, without interfering with the take-over scenarios. At the same time it was presumed that this would encourage normal driving behavior and that participants would perform safety checks.

3) *Non-Driving Related Task*: In order to simulate driver-out-of-the-loop effects, the participants were asked to perform a secondary task. The task was to play the game Angry Birds on the touch screen monitor mounted on the right next to the driver, which can be seen in figure 1. The motivation for Angry Birds is that it is an interruptible game. This allows the participant to freely switch between manual driving and the secondary task, without it affecting their score in the game.

### E. Procedure

At the start of the experiment, the participants were provided with a document containing the details of the experiment. After reading the document, they were requested to sign an informed consent form. Then the participants were asked to fill out a demographics questionnaire. After taking place in the simulator, the participants were given the time to adjust the seat and mirrors to their liking. Next, three practice sessions were performed. The first practice session was a manual drive during which the participant could familiarize with the driving simulator and get a feeling of the vehicle dynamic response. The second practice session included a demo run with HSC mode active. In this session, the participants could experience driving with HSC and try some assisted lane changes. Finally, the participants were verbally instructed how to engage and disengage the automation system followed by two practice take-over maneuvers, one for each transition approach. Prior to the driving experiment, the participants were instructed that in case of a TOR they had to take back control of the vehicle and avoid an obstacle on the road by making a lane change to the left and then back to the right lane and reengage the automation system once they thought the situation was safe. They were reminded to drive as they normally would

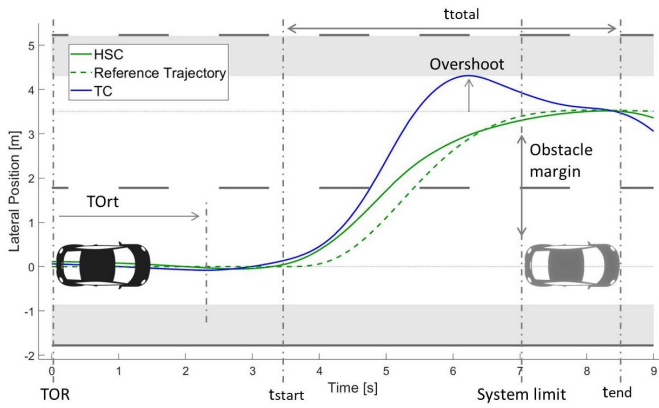


Fig. 4. A schematic overview of a take-over maneuver highlighting the main events and dependent variables. The gray area represents critical boundaries of half a car width wide. Indicating a lane departure if a trajectory enters this region.  $t_{total}$  represents the evaluation period. Note that the vehicles in the figure are not to scale and that this example is based on a non-critical scenario, providing a time budget of 7 s.

on the highway. At the beginning of the driving experiment, the participants spawned in a generic sedan on the hard shoulder of the highway. The participants were instructed to accelerate to 100 km/h, move into the right lane and engage the automation system. Once engaged, the participants were asked to focus on the NDRT on the touch screen mounted next to the driver's seat. After each trial, the participants had a short break, during which they were asked to fill out a Van der Laan questionnaire on usefulness and satisfaction. The total duration of the experiment was approximately one hour.

#### F. Dependent Variables

In this section the objective and subjective measures used to assess the take-over performance are discussed. Certain objective measures in this study are evaluated over a period of time ( $t_{total}$ ) (illustrated in figure 4). The beginning of this period is aligned for both transition approaches at  $t_{start}$ , and is defined as the moment a lane change trigger is detected, which is when TLC falls below the threshold. Although TC does not provide any support, the TLC is continuously updated and can therefore still be used as  $t_{start}$ . The evaluation period ends as soon as the ego vehicle has fully passed the stationary vehicle, referred to as  $t_{end}$ . It is the exact point in time when the rear of the ego vehicle is aligned with the front of the stationary vehicle.

##### 1) Safety Performance:

- **Minimum Time to Collision [s]:** The minimum TTC is evaluated and is used to determine the criticality of the evasive maneuver [7]. In this study stationary objects were placed in front of the ego vehicle. For stationary objects the TTC can be calculated using equation 2:

$$TTC = \frac{dx}{v_{ego}} \quad (2)$$

where  $dx$  is the longitudinal distance between the stationary vehicle and the ego vehicle, and  $v_{ego}$  is the velocity

at which the ego vehicle is traveling.  $TTC_{min}$  is the minimum recorded value until sufficient steering input has caused the ego vehicle's trajectory to be clear of the stationary object, also defined as the collision free point.

- **Take-Over reaction time [s]:** The TORT is used to determine how long it takes for the driver to shift their attention back to the driving task. It is measured as the time between the TOR and the moment when the first control maneuver is executed which is defined as: the first time the steering wheel angle exceeds 2 degrees or the brake pedal exceeds 10% of maximum braking. TORT was originally defined in [5], and has been used as a measure for reaction time in many studies. An overview is given in [24].
- **Lateral Obstacle Clearance [m]:** The lateral distance between the right side of the car and the left side of the obstacle at the moment when the front of the ego vehicle aligns with the rear end of the stationary vehicle.
- **Maximum overshoot [m]:** The maximum measured lateral displacement from the lane center in the target lane in the analyzed period. A negative value indicates that the vehicle has not reached the future lane center.
- **Maximum lateral acceleration [ $m/s^2$ ]:** The maximum measured lateral accelerations during  $t_{total}$

##### 2) Vehicle Control:

- **Standard Deviation Lateral Position\* [m]:** The SDLP\* is used to evaluate the vehicle control stability during the take-over process. SDLP is generally used to determine the standard deviation around the lane center. In this study, the SDLP is defined as the standard deviation of the within-subject mean trajectory evaluated over  $t_{total}$ , and will therefore be referred to as SDLP\*.
- **Steering Wheel Reversal Rate [ $min^{-1}$ ]:** SWRR is used to determine the amount of steering corrections made by the driver during the take-over maneuver in terms of high frequency control activity. It is defined as the number of steering wheel reversals per minute larger than the angular value of 2 degrees. SWRR is determined during  $t_{total}$ , and is a measure of workload [45].

##### 3) Controller performance:

- **Average Torque Conflicts [Nm]:** Torque conflicts arise if the intentions of the driver and that of the human compatible reference do not align. The torque conflicts are measured when the controller and human apply forces on the steering wheel in opposite directions, assessed over  $t_{total}$ . Note that torque conflicts can only occur during cooperative driving and therefore are not present during the TC transition approach.

##### 4) Subjective measures:

- **System Acceptance:** The Van der Laan questionnaire assesses the acceptance of the two transition approaches in two dimensions, on a Satisfaction scale and on an Usefulness scale. The usefulness and the satisfaction are

evaluated based on nine Likert items. This study follows the methodology from [46].

### G. Statistical Analysis

The objective measures were captured in matrices of 4x30. For each level of the 4 independent variables there were 30 mean within-subject observations. Prior to the statistical test, all objective measures were checked for normality using the Sharipo-Wilkes test. In case of violations, the matrix was rank transformed from smallest to largest value ranging from 1 to 120 according to [47]. Sphericity was assumed because both within-subject factors consisted of only two levels [48]. Subsequently, a repeated measures analysis of variance (ANOVA) was run on the results. As a post hoc test a Bonferroni adjustment was made to control for the error rate inflation.

The subjective measure results of the VDL questionnaire were also checked for normality using the Sharipo-Wilkes test, before being assigned to a paired t-test. In case the normality assumption was violated, the non-parametric Friedman's test was performed, for which the assumption of normality is not required.

## III. RESULTS

### A. Data Analyses

In this study a total of 600 take-over maneuvers were analyzed (4 x levels of independent variables, 5 x repetitions, 30 x Participants). The results of the non-critical take-over maneuvers in the TC transition approach experienced 45 false positives out of a total of 150, due to a logging error. The stationary vehicles were placed at a distance of 7 seconds in front of the ego vehicle, however the TOR was triggered after two seconds and therefore provided a TB of 5 seconds instead of the intended 7 seconds. In figure 5, a falsely timed take-over maneuver is highlighted in red for the critical and non-critical scenarios. In the critical scenario, the trajectory

starts at the placement of the stationary vehicle. No input from the driver is observed, indicating that the driver was actively engaged with the NDRT and not aware of the vehicle. After the TOR, the trajectory shows similar behavior to the other critical scenarios. All 45 cases have been analyzed and have been classified as critical take-over maneuvers. During the experiment, five accidents were recorded. In these cases the driver had failed to react in time to the TOR and drove through the stationary vehicle. This involved three critical and one non-critical take-over maneuvers in the TC transition approach, and one in the critical HSC transition approach. For the analyses, these cases have been replaced by the mean of the other within-subject results. The descriptive statistics and the results of the statistical tests are listed in table II. Values for  $p < 0.05$  are considered marginally significant, and values for  $p < 0.01$  are considered highly significant. It was found that all dependent measures, except TORt, encountered normality violations as a result of the Sharipo-Wilkes normality check. The objective measures with violations have been rank transformed accordingly, and the subjective measures with normality violations have been submitted to Friedman's test.

### B. Safety Performance

1) *Minimum Time to Collision*: HSC shows significant higher  $TTC_{min}$  values compared to TC,  $F(1, 29) = 110.2$ ,  $p < 0.01$ . It can be concluded that the trajectory followed by drivers that are assisted by HSC is clear of a collision earlier than the TC transition, indicating safer take-over maneuvers. Similar results for criticality are found. Non-critical scenarios show higher  $TTC_{min}$  values compared to critical scenarios, regardless of the transition approach  $F(1, 29) = 10.6$ ,  $p < 0.01$ . No significant interaction effect is found.

2) *Take-Over reaction time*: The TORt is not significantly dependent on the type of transition. The analysis shows a significant main group effect for the level of criticality,  $F(1, 29) = 99.0$ ,  $p < 0.01$ . The results indicate that the drivers react faster to a TOR in critical scenarios, compared to non-critical scenarios. There is also a significant interaction effect,

TABLE II  
MEANS PER DEPENDENT MEASURE WITH STANDARD DEVIATION IN PARENTHESES ( $N = 30$ ), RESULTS OF REPEATED MEASURES ANOVA( $F_p$ )

Objective Measures	TC		HSC		Statistical Results					
	Critical M(SD)	Non-critical M(SD)	Critical M(SD)	Non-critical M(SD)	Transition		Criticality		T*C	
					F(1,29)=	p-value	F(1,29)=	p-value	F(1,29)=	p-value
TOrt (s)	2.07 (0.39)	2.55 (0.52)	1.98 (0.23)	2.69 (0.55)	0.18	0.675	98.95	0.000	4.67	0.039
$TTC_{min}$ (s)	1.15 (0.31)	1.38 (0.58)	1.63 (0.39)	1.98 (0.57)	110.24	0.000	10.63	0.003	0.07	0.790
Lat. obstacle clearance (m)	1.37 (0.32)	1.55 (0.27)	1.29 (0.22)	1.49 (0.18)	12.10	0.002	27.70	0.000	4.45	0.044
Overshoot (m)	-0.20 (0.28)	-0.08 (0.27)	-0.31 (0.21)	-0.16 (0.18)	19.73	0.000	14.40	0.001	6.69	0.015
Max. Lat. Acceleration ( $m/s^2$ )	5.61 (1.24)	3.98 (1.25)	5.23 (1.38)	3.47 (0.65)	5.61	0.025	122.02	0.000	0.54	0.467
SDLP* (m)	0.21 (0.07)	0.19 (0.10)	0.16 (0.07)	0.18 (0.06)	9.60	0.004	0.21	0.649	3.76	0.062
SWRR ( $min^{-1}$ )	2.26 (1.56)	5.86 (4.30)	3.18 (2.21)	3.67 (2.94)	0.06	0.813	15.81	0.000	12.34	0.001
Torque Conflicts (Nm)	(-)	(-)	0.49 (0.08)	0.38 (0.03)	(-)		94.67	0.000	(-)	
							Usefulness		Satisfaction	
Subjective measures					$\chi^2(1,N=29) =$	p-value	$\chi^2(1,N=29) =$	p-value		
Van Der Laan	0.61 (0.74)	0.61 (0.73)	0.61 (0.82)	0.86 (0.71)	2.79	0.095	0.037	0.847		

**Note:** TC = Traded Control, HSC = Haptic Shared Control. All dependent measures except TORt have been rank transformed because they contained normality violations. The Friedman's test has been used for the subjective measures due to normality violations. Values for  $p < 0.05$  are considered marginally significant, and values for  $p < 0.01$  are considered highly significant.

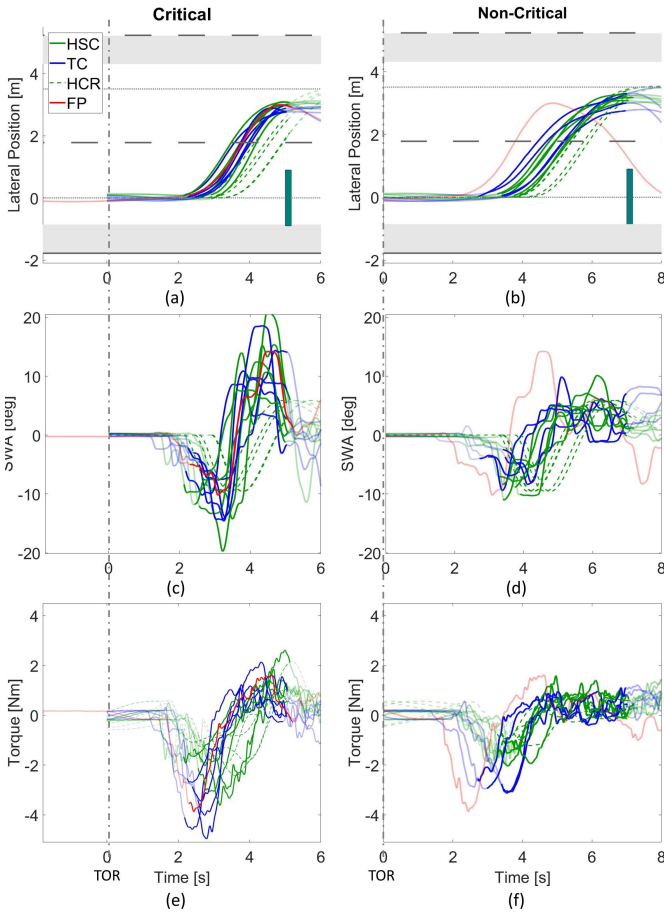


Fig. 5. Raw data time traces of all critical (left) and non-critical (right) take-over maneuvers performed by one participant (Nr. 17) aligned at TOR. Top: lateral position, Middle: steering wheel angle, Bottom: Steering Torques. The highlighted area represents the analyzed period for the dependent variables from  $t_{start}$  to  $t_{end}$ . The false positive TOR during TC in (b) has been analyzed as a critical take-over maneuver, shown in (a). The time trace starts at the placement of the stationary vehicle and shows no driver input until after the TOR. The vertical bar represents the stationary vehicle with only its width to scale.

$F(1, 29) = 4.7, p < 0.05$ . In a critical take-over scenario the TC approach experiences slower take-over reaction times. However, in the non-critical scenarios TC reacts faster to a TOR signal compared to the HSC approach.

3) *Lateral Obstacle Clearance*: In figure 6c and 6d the results of the lateral obstacle clearance are plotted. In both criticality scenarios the means of HSC are significantly lower than the means of TC,  $F(1, 29) = 12.1, p < 0.01$ . In terms of safety performance, this means that HSC leaves a less safe margin between the ego vehicle and the stationary vehicle. The results also show that the lateral obstacle clearance significantly decreased when the criticality increased,  $F(1, 29) = 27.7, p < 0.01$ . For critical scenarios, the lateral obstacle clearance decreased significantly less for HSC compared to TC than for non-critical scenarios,  $F(1, 29) = 4.5, p < 0.05$ . Figure 6c and 6d also show that in nearly all cases the vehicle was on the right side of the target lane center at the moment of passing the stationary vehicle, except for the non-critical TC scenarios. No lane departures have been observed.

4) *Maximum Overshoot*: All mean values are negative, which means that in general the participants undershoot the target lane center regardless of the level of criticality or the transition approach. In critical scenarios, the maximum overshoot is significantly higher compared to the maximum overshoot in non-critical scenarios,  $F(1, 29) = 14.4, p < 0.01$ . The results also show a significant decrease in maximum overshoot for HSC in comparison with TC,  $F(1, 29) = 19.7, p < 0.01$ . The interaction effect indicates that the difference between HSC and TC is significantly less in non-critical scenarios,  $F(1, 29) = 6.7, p < 0.05$ .

5) *Maximum Lateral Acceleration*: The maximum lateral acceleration significantly decreases when the level of criticality decreases,  $F(1, 29) = 122.0, p < 0.01$ . A significant increase in the maximum lateral acceleration is found for TC compared to HSC,  $F(1, 29) = 5.6, p < 0.05$ . The results show no interaction effect between transition and criticality. Therefore,

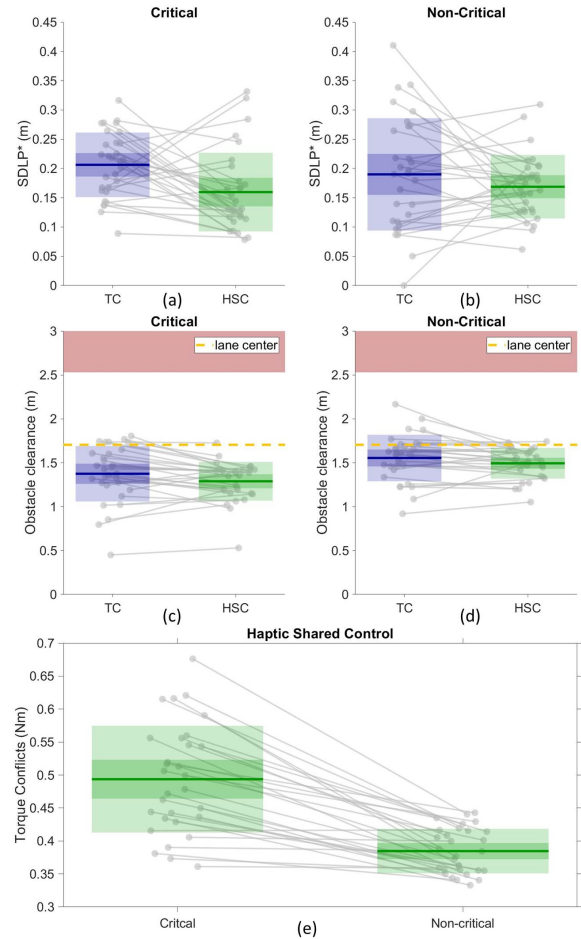


Fig. 6. Results of the critical (left) and non-critical (right) take-over maneuvers of the dependent variables: Top: SDLP\*, Middle: Obstacle clearance, Bottom: Torque conflicts. The mean is illustrated by the horizontal line within the shaded areas. The darker regions represent the standard error of the mean with a 95% confidence interval and the lighter shaded regions highlight the standard deviation. The dots represent each participant in one level of criticality, connected to a dot of the same participant in the other level. In the results of the obstacle clearance the yellow line represents lane center, and the red patch indicates the critical area for a lane departure.

TC has a higher maximum lateral acceleration than HSC regardless of the criticality. Similarly, critical scenarios experience higher lateral accelerations compared to non-critical scenarios, despite the transition approach.

### C. Vehicle Control

1) *SDLP\**: The results of *SDLP\** are shown in figure 6a and 6b. There is a main group effect for transition, showing a lower *SDLP* for HSC compared to TC,  $F(1, 29) = 9.6$ ,  $p < 0.01$ . Criticality does not demonstrate a significant effect on the *SDLP\**. Likewise, no interaction effect is found between transition and criticality on the *SDLP\**. It can be said that during HSC the participants showed higher performance in stabilizing lateral vehicle control, despite the provided TB.

2) *SWRR*: HSC and TC do not differ significant from one another in terms of *SWRR*. When the driver is provided with a TB of 5 seconds, significantly less reversals are measured than when the driver is provided with a TB of 7 seconds,  $F(1, 29) = 15.8$ ,  $p < 0.01$ . This means that the drivers experience less workload during non-critical take-over maneuvers. In critical scenarios, TC has less reversals than HSC. However, in the non-critical scenarios more reversals are measured for TC compared to HSC (interaction effect,  $F(1, 29) = 12.3$ ,  $p < 0.01$ ).

### D. Controller Performance

1) *Torque Conflicts*: The torque conflicts are shown in figure 6e. The results of TC are left out in this analysis, because the system does not provide haptic feedback in these cases. A significant effect was found for HSC based on the criticality of the take-over maneuver,  $F(1, 29) = 94.7$ ,  $p < 0.01$ . When the drivers were supported by HSC after a transition, higher torque conflicts were measured in the critical scenarios.

### E. Subjective Measures

1) *System Acceptance*: The results of the Van der Laan questionnaire are shown in figure 7. Both systems are located in the top right quadrant indicating that the participants accepted both systems. After performing a Friedman's ANOVA test no significant effect was found between the two transition approaches for usefulness or satisfaction,  $\chi^2(1, N=29) = 2.79$   $p = 0.095$  and  $\chi^2(1, N=29) = 0.037$   $p = 0.847$ .

## IV. DISCUSSION

The goal of this study was to investigate the effect of HSC on the take-over performance compared to TC transitions used in literature. In the introduction it was pointed out that previous studies on the take-over maneuver found that increasing the criticality of the scenarios leads to faster reaction times, however the take-over quality deteriorates. Building on this, a driving simulator experiment was conducted evaluating the take-over performance for both transition approaches which included two levels of criticality. Furthermore, it was hypothesized that compared to TC, HSC could yield beneficial effect on the take-over quality curing the required adaption period, following a transition. It was expected that HSC would assist the driver in stabilizing the lateral vehicle control, by minimizing the *SDLP*. It was also anticipated that HSC would minimize the unwanted carryover effect after a transition in terms of maximum accelerations and overshoot and  $TTC_{min}$  values. First, the general results will be discussed to see if similar relations are found in comparison to previous studies. Then, the differences between the two transition approaches will be discussed in detail, followed by an evaluation of the controller performance. Finally, the limitations of this study will be reviewed and how they relate to future work.

### A. General results on the take-over performance

In this study the level of criticality was varied by providing the participants with two different TB's, 5 seconds and 7 seconds [5], [7], [40], [43], [49], [50]. A reason for using different TB's, is that the drivers are encouraged to stay alert during the experiment, since they do not know how much time they will have to react. The mean *TORt*'s found in this study for the critical scenarios are 1.98 s for HSC and 2.07 s for TC, and for the non-critical scenarios 2.55 s for TC and 2.69 s for HSC. The significant decrease in *TORt* for critical scenarios confirms the relation found by [5] that *TORt* decreases when drivers are provided with shorter TB's. The means are also in line with the ranges found in studies with the same TB's and similar *TOR* modalities (e.g. visual and auditory). For a TB of 7 s, [49] found 2.22-3.09 s and [43] found 1.55-2.92 s, and for a TB of 5 s, [5] found 2.06 s and [50] found 1.67-2.22 s.

The results for the critical scenarios show a decrease in the take-over quality in terms of maximum lateral accelerations and overshoot, which show a significant increase when drivers are provided with a TB of 5 s compared to a TB of 7 s. However, the means of the overshoot are negative, indicating that the drivers undershoot the target lane center, which was

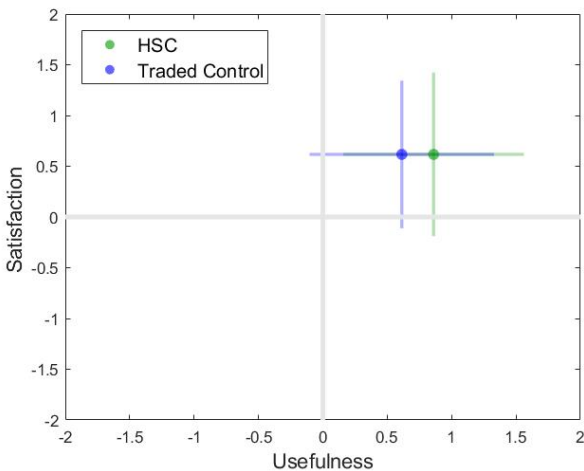


Fig. 7. Results of the Van der Laan questionnaire with the mean satisfaction and usefulness per transition approach represented as a dot. The shaded bars indicate the mean  $\pm$  the standard deviation across all participants.

expected based on the findings of [7] and [5]. An explanation for this could be the difference in traffic situations. In contrast to this study, there was no other traffic on the road in [7], except for a lead vehicle driving in front of the ego vehicle. This might have given the drivers consciously more freedom to use all space when performing an evasive maneuver without the danger of colliding with another road user. In addition, the transition in [7] and [5] happened at a speed of 120 km/h compared to 100 km/h in this study. In both studies the drivers were provided with the same TB's, however the vehicle dynamic response at 120 km/h is different to 100 km/h. At 120 km/h a driver is more likely to overshoot the target lane center when changing lanes quickly. In summation, the general results on the take-over performance found in this study are in line with the conclusions found in literature [5]: "For shorter TB's, faster reaction times are found. However, the take-over quality also decreases."

### B. Haptic Shared Control vs. Traded Control

1) *Safety Performance*: No significant effect was found between the two transition approaches based on the reaction time of the drivers. This was to be expected, since the TOrt is determined around the same time as the transfer of control authority. At this point the two conditions are the same, and therefore the results of the TOrt are not effected by the different transition approaches. In terms of safety performance HSC showed significant better results for minimum TTC and maximum lateral accelerations compared to TC. This means that with HSC the drivers left a safer obstacle free point with respect to the stationary vehicle when changing lanes, and changed lanes with a more controlled speed than the drivers did with TC. This shows that during TC the drivers took longer to fully commit to a lane change, followed by a sharper trajectory than when they were driving in cooperative mode. However, TC showed significant safer results in terms of overshoot and lateral obstacle clearance, leaving more space between the stationary vehicle and ego vehicle, without overshooting the target lane. A possible explanation can be that the supported lane change trajectory is not yet completed when the ego vehicle passes the object, this explanation is also visible in figure 5a and 5b. This is because the HCR has been implemented using a one-size-fits-all approach, always supporting a lane change of 4 s. The mean TOrt for HSC in critical scenarios is 1.98 s, this leaves approximately 3 s before reaching the system limit. As a result of this the haptic guidance system follows an uncompleted lane change trajectory at the moment of passing the stationary vehicle, which might be closer than desired. This probably is the case since the actual driven trajectories do not coincide with the HCR. However, only one collision occurred during HSC, whereas TC witnessed four collisions. This suggests that although the obstacle clearance for HSC is significantly less, it does not guide the driver towards a collision.

2) *Vehicle Control*: The premise of this research was formed based on previous studies concluding that the driving performance after a control transition is impaired in terms of lateral vehicle control. In this study it was found that

HSC significantly decreases the SDLP\* compared to TC. In [35] similar results are found for HSC transitions in terms of SDLP. However, the significant results are compared to a Cut-ADS(Automated Driving System) transition approach, during which the system is switched off with the TOR simultaneously. No significant effect was found in this study when HSC was compared to the TC approach similar to the one discussed in this study. In addition, [35] used a different tuning approach for the HSC. The control strength linearly decreased after steering input from the driver. The results of the tuning method of HSC used in this study indicate that using HSC during a transition of control authority can indeed assist the driver in the lateral vehicle control.

A lower workload demand would be expected in non-critical scenarios compared to the critical scenarios in terms of SWRR. The results show that a significant increase was found for non-critical take-over scenarios. This is related to the fact that  $t_{total}$  was not a fixed time duration. For the non-critical take-over maneuvers the evaluation period was longer than for the critical take-over maneuvers and therefore, more SWRR could be observed. No effect was found between the different transition approaches. However, a significant interaction effect highlights that in non-critical scenarios HSC measures lower SWRR, but in critical scenarios HSC measures higher SWRR compared to TC. This relation could also be explained by the observation that the goals of the HCR and the driver do not align in the critical scenarios, causing the driver to make more steering corrections.

3) *Controller performance*: If a mismatch between the driver's intentions and the system's intentions are present in critical scenarios, more torque conflicts are expected. The results in figure 6e show significant larger torque conflicts in the critical scenarios compared to the non-critical scenarios, this supports the earlier made assumptions that the HCR in the critical scenarios does not align with the driver's goals, explaining the higher torque conflicts. If the driver is fully aware of the situation and implements a correct control input, then the torque conflicts are a disturbance [51]. However, it is important to note that in these critical situation the driver suffers from loss of situation awareness, and can implement a wrong choice of action [4]. In these situations it is essential that the system continuously communicates with with the driver, and perhaps even overrules the driver to prevent an accident [51].

4) *System Acceptance*: The results of the Van der Laan Questionnaire show no statistical significant differences in terms of reported satisfaction and usefulness. Nonetheless, it can be seen in figure 7 that the participants found both systems satisfying and useful. HSC was rated more useful than TC. Both systems were rated equally satisfying. Most of the participant had no previous experience with ADAS such as, ACC and LKA. This made the experience of autonomous driving entirely new to them. Some participants commented that the TB was too short for them to react, and that the sound was annoying. These aspect of the take-over maneuver were the same for both transition approaches. This might have influenced their interpretation on the differences between the two systems, and could explain why the to two systems have

been rated very similar.

### C. Limitations and Future Work

As a result of analyzing the false positives witnessed in the experiment in a different category, the statistical test were performed with data sets with different sample size. This causes a general loss of statistical power [48]. In the false positive cases the drivers did not notice the vehicle being placed in front of them. This highlights the DOL issues. The driver is fully engaged in the NDRT and is not aware of the danger in front of the vehicle. The drivers simply react to the TOR signal, and this points out the importance of clear TOR's. Future research on the take-over maneuver should include the transition approach in the design of HMI systems for the TOR.

In this study a one-size-fits-all implementation has been used for the HCR. Results from a previous study [52] show that this kind of control strategy can cause a mismatch in goals, resulting in torque conflicts based on inter and intra driver variability. The results in this study are in line with these findings. In figure 5 this can be seen. However, the HSC take-over maneuvers showed lower SDLP\* and lower maximum lateral accelerations compared to TC, despite the HCR not always agreeing with the driver. This highlights the potential of HSC as a transition approach. The driver tends to want to make a sharper lane change compared to the HCR. Especially, in the critical take-over scenarios high torque conflicts are measured. To reduce these conflicts, future research should investigate HCR implementations that adapt their trajectory based on the criticality of the take-over maneuver. In addition, the HCR could be made adaptable based on the drivers intentions to compensate for the intra driver variability. For example, by determining the lane change duration based on the driver's inputs at the start of the lane change, similar to the implementation of [37]. In this way the controller performance can be increased so that the driver experiences more assistance from the system, and therefore could increase the take-over performance even further.

### V. CONCLUSION

In this study HSC has successfully been implemented as a transition approach during the take-over maneuver in order to realize a smooth transfer of control authority between highly automated driving and manual control and to act as a driver support system after a transition. By means of a driving simulator experiment, the take-over performance was assessed for two levels of criticality and compared to the take-over performance of TC transition approach. It was hypothesized that the haptic shared control approach would yield beneficial effects on the driver performance after a control transition in terms of stabilizing lateral vehicle control and reduce unwanted carryover effects, compared to the TC approach.

HSC effectively assisted the driver in vehicle control in terms of reduced SDLP\* after regaining manual control compared to TC. HSC also showed enhanced safety performance in terms of significant higher TTCmin and

reduced maximum accelerations. Nonetheless, mean lateral obstacle clearance indicated lower margins for HSC in critical scenarios. In combination with the increased torque conflicts found in these situations, these results suggest that the HCR in these scenarios does not match the desired trajectory of the driver.

To summarize, HSC showed beneficial results as a transition approach during a take-over maneuver in terms of take-over performance compared to TC. However, future research should focus on adaptable human compatible reference trajectories that adapt to the criticality level of the take-over maneuver.

### ACKNOWLEDGMENT

This study is supported by Cruden BV.

### REFERENCES

- [1] M. J. Hanna and S. C. Kimmel, "Current us federal policy framework for self-driving vehicles: Opportunities and challenges," *Computer*, vol. 50, no. 12, pp. 32–40, 2017.
- [2] A. Toffetti, E. S. Wilschut, M. H. Martens, A. Schieben, A. Rambaldini, N. Merat, and F. Flemisch, "Citymobil: Human factor issues regarding highly automated vehicles on elane," *Transportation research record*, vol. 2110, no. 1, pp. 1–8, 2009.
- [3] S. Underwood, "Automated vehicles forecast vehicle symposium opinion survey," in *automated vehicles symposium*, Conference Proceedings, pp. 15–17.
- [4] M. R. Endsley and E. O. Kiris, "The out-of-the-loop performance problem and level of control in automation," *Human factors*, vol. 37, no. 2, pp. 381–394, 1995.
- [5] C. Gold, D. Damböck, L. Lorenz, and K. Bengler, "'take over!' how long does it take to get the driver back into the loop?" *Proceedings of the Human Factors and Ergonomics Society Annual Meeting*, vol. 57, no. 1, pp. 1938–1942, 2013.
- [6] S. M. Petermeijer, J. C. De Winter, and K. J. Bengler, "Vibrotactile displays: A survey with a view on highly automated driving," *IEEE Transactions on Intelligent Transportation Systems*, vol. 17, no. 4, pp. 897–907, 2016.
- [7] R. Happee, C. Gold, J. Radlmayr, S. Hergeth, and K. Bengler, "Take-over performance in evasive manoeuvres," *Accident Analysis & Prevention*, vol. 106, pp. 211–222, 2017.
- [8] H. E. Russell, L. K. Harbott, I. Nisky, S. Pan, A. M. Okamura, and J. C. Gerdes, "Motor learning affects car-to-driver handover in automated vehicles," *trials*, vol. 6, no. 6, p. 6, 2016.
- [9] T. Louw, G. Markkula, E. Boer, R. Madigan, O. Carsten, and N. Merat, "Coming back into the loop: Drivers' perceptual-motor performance in critical events after automated driving," *Accident Analysis & Prevention*, vol. 108, pp. 9–18, 2017.
- [10] E. Dogan, M.-C. Rahal, R. Deborne, P. Delhomme, A. Kemeny, and J. Perrin, "Transition of control in a partially automated vehicle: Effects of anticipation and non-driving-related task involvement," *Transportation Research Part F: Traffic Psychology and Behaviour*, vol. 46, pp. 205–215, 2017.
- [11] N. Merat, A. H. Jamson, F. C. Lai, and O. Carsten, "Highly automated driving, secondary task performance, and driver state," *Human factors*, vol. 54, no. 5, pp. 762–771, 2012.
- [12] C. Gold, M. Körber, C. Hohenberger, D. Lechner, and K. Bengler, "Trust in automation—before and after the experience of take-over scenarios in a highly automated vehicle," *Procedia Manufacturing*, vol. 3, pp. 3025–3032, 2015.
- [13] C. G. Gold, "Modeling of take-over performance in highly automated vehicle guidance," Thesis, 2016.
- [14] K. Zeeb, A. Buchner, and M. Schrauf, "What determines the take-over time? an integrated model approach of driver take-over after automated driving," *Accident Analysis & Prevention*, vol. 78, pp. 212–221, 2015.
- [15] —, "Is take-over time all that matters? the impact of visual-cognitive load on driver take-over quality after conditionally automated driving," *Accident analysis & prevention*, vol. 92, pp. 230–239, 2016.

- [16] K. Zeeb, M. Härtel, A. Buchner, and M. Schrauf, "Why is steering not the same as braking? the impact of non-driving related tasks on lateral and longitudinal driver interventions during conditionally automated driving," *Transportation research part F: traffic psychology and behaviour*, vol. 50, pp. 65–79, 2017.
- [17] A. Eriksson, S. M. Petermeijer, M. Zimmermann, J. C. de Winter, K. J. Bengler, and N. A. Stanton, "Rolling out the red (and green) carpet: supporting driver decision making in automation-to-manual transitions," *IEEE Transactions on Human-Machine Systems*, vol. 49, no. 1, pp. 20–31, 2019.
- [18] M. Körber, C. Gold, D. Lechner, and K. Bengler, "The influence of age on the take-over of vehicle control in highly automated driving," *Transportation research part F: traffic psychology and behaviour*, vol. 39, pp. 19–32, 2016.
- [19] H. Clark and J. Feng, "Age differences in the takeover of vehicle control and engagement in non-driving-related activities in simulated driving with conditional automation," *Accident Analysis & Prevention*, vol. 106, pp. 468–479, 2017.
- [20] A. Feldhütter, C. Gold, S. Schneider, and K. Bengler, *How the duration of automated driving influences take-over performance and gaze behavior*. Springer, 2017, pp. 309–318.
- [21] A. Eriksson and N. A. Stanton, "Driving performance after self-regulated control transitions in highly automated vehicles," *Human factors*, vol. 59, no. 8, pp. 1233–1248, 2017.
- [22] A. P. van den Beukel and M. C. van der Voort, "The influence of time-criticality on situation awareness when retrieving human control after automated driving," in *16th International IEEE Conference on Intelligent Transportation Systems (ITSC 2013)*. IEEE, Conference Proceedings, pp. 2000–2005.
- [23] L. Kalb, L. Streit, and K. Bengler, "Multimodal priming of drivers for a cooperative take-over," in *2018 21st International Conference on Intelligent Transportation Systems (ITSC)*. IEEE, Conference Proceedings, pp. 1029–1034.
- [24] A. Eriksson and N. A. Stanton, "Takeover time in highly automated vehicles: noncritical transitions to and from manual control," *Human factors*, vol. 59, no. 4, pp. 689–705, 2017.
- [25] B. Zhang, J. de Winter, S. Varotto, R. Happee, and M. Martens, "Determinants of take-over time from automated driving: A meta-analysis of 129 studies," *Transportation Research Part F: Traffic Psychology and Behaviour*, vol. 64, pp. 285–307, 2019.
- [26] M. Mulder, D. A. Abbink, and E. R. Boer, "The effect of haptic guidance on curve negotiation behavior of young, experienced drivers," in *Systems, Man and Cybernetics, 2008. SMC 2008. IEEE International Conference on*. IEEE, Conference Proceedings, pp. 804–809.
- [27] —, "Sharing control with haptics: Seamless driver support from manual to automatic control," *Human factors*, vol. 54, no. 5, pp. 786–798, 2012.
- [28] Z. Wang, R. Zheng, T. Kaizuka, K. Shimono, and K. Nakano, "The effect of a haptic guidance steering system on fatigue-related driver behavior," *IEEE Transactions on Human-Machine Systems*, vol. 47, no. 5, pp. 741–748, 2017.
- [29] Z. Wang, R. Zheng, T. Kaizuka, and K. Nakano, "The effect of haptic guidance on driver steering performance during curve negotiation with limited visual feedback," in *2017 IEEE Intelligent Vehicles Symposium (IV)*. IEEE, Conference Proceedings, pp. 600–605.
- [30] M. Mulder, M. Mulder, M. Van Paassen, and D. Abbink, "Haptic gas pedal feedback," *Ergonomics*, vol. 51, no. 11, pp. 1710–1720, 2008.
- [31] D. A. Abbink, M. Mulder, and E. R. Boer, "Haptic shared control: smoothly shifting control authority?" *Cognition, Technology & Work*, vol. 14, no. 1, pp. 19–28, 2012.
- [32] J. Nilsson, N. Strand, P. Falcone, and J. Vinter, "Driver performance in the presence of adaptive cruise control related failures: Implications for safety analysis and fault tolerance," in *2013 43rd Annual IEEE/IFIP Conference on Dependable Systems and Networks Workshop (DSN-W)*. IEEE, Conference Proceedings, pp. 1–10.
- [33] T. Wada, K. Sonoda, T. Okasaka, and T. Saito, "Authority transfer method from automated to manual driving via haptic shared control," in *2016 IEEE International Conference on Systems, Man, and Cybernetics (SMC)*. IEEE, Conference Proceedings, pp. 002 659–002 664.
- [34] T. Wada and R. Kondo, "Shared authority mode: Connecting automated and manual driving for smooth authority transfer," *Proceedings of FAST-zero*, 2017.
- [35] R. Kondo, T. Wada, and K. Sonoda, "Use of haptic shared control in highly automated driving systems?" 09 2019.
- [36] M. M. Van Paassen, R. Boink, D. Abbink, M. Mulder, and M. Mulder, *Four design choices for haptic shared control*, 2017, pp. 237–254.
- [37] K. K. Tsoi, M. Mulder, and D. A. Abbink, "Balancing safety and support: Changing lanes with a haptic lane-keeping support system," in *2010 IEEE international conference on systems, man and cybernetics*. IEEE, Conference Proceedings, pp. 1236–1243.
- [38] S. Mammari, S. Glaser, and M. Netto, "Time to line crossing for lane departure avoidance: A theoretical study and an experimental setting," *IEEE Transactions on Intelligent Transportation Systems*, vol. 7, no. 2, pp. 226–241, 2006.
- [39] J. L. Burke, M. S. Prewett, A. A. Gray, L. Yang, F. R. Stilson, M. D. Coovert, L. R. Elliot, and E. Redden, "Comparing the effects of visual-auditory and visual-tactile feedback on user performance: a meta-analysis," in *Proceedings of the 8th international conference on Multimodal interfaces*. ACM, Conference Proceedings, pp. 108–117.
- [40] L. Lorenz, P. Kerschbaum, and J. Schumann, "Designing take over scenarios for automated driving: How does augmented reality support the driver to get back into the loop?" in *Proceedings of the Human Factors and Ergonomics Society Annual Meeting*, vol. 58. SAGE Publications Sage CA: Los Angeles, CA, Conference Proceedings, pp. 1681–1685.
- [41] N. Merat, A. H. Jamson, F. C. H. Lai, M. Daly, and O. M. J. Carsten, "Transition to manual: Driver behaviour when resuming control from a highly automated vehicle," *Transportation Research Part F: Traffic Psychology and Behaviour*, vol. 27, pp. 274–282, 2014.
- [42] S. Petermeijer, P. Bazilinskyy, K. Bengler, and J. de Winter, "Take-over again: Investigating multimodal and directional cues to get the driver back into the loop," *Applied ergonomics*, vol. 62, pp. 204–215, 2017.
- [43] J. Radlmayr, C. Gold, L. Lorenz, M. Farid, and K. Bengler, "How traffic situations and non-driving related tasks affect the take-over quality in highly automated driving," *Proceedings of the Human Factors and Ergonomics Society Annual Meeting*, vol. 58, no. 1, pp. 2063–2067.
- [44] M. Walch, K. Lange, M. Baumann, and M. Weber, "Autonomous driving: Investigating the feasibility of car-driver handover assistance," in *Proceedings of the 7th International Conference on Automotive User Interfaces and Interactive Vehicular Applications*. ACM, Conference Proceedings, pp. 11–18.
- [45] W. A. Macdonald and E. R. Hoffmann, "Review of relationships between steering wheel reversal rate and driving task demand," *Human Factors*, vol. 22, no. 6, pp. 733–739, 1980.
- [46] J. D. Van Der Laan, A. Heino, and D. De Waard, "A simple procedure for the assessment of acceptance of advanced transport telematics," *Transportation Research Part C: Emerging Technologies*, vol. 5, no. 1, pp. 1–10, 1997.
- [47] W. J. Conover and R. L. Iman, "Rank transformations as a bridge between parametric and nonparametric statistics," *The American Statistician*, vol. 35, no. 3, pp. 124–129, 1981. [Online]. Available: [www.jstor.org/stable/2683975](http://www.jstor.org/stable/2683975)
- [48] A. Field, *Discovering statistics using IBM SPSS statistics*. sage, 2013.
- [49] P. Kerschbaum, L. Lorenz, and K. Bengler, "A transforming steering wheel for highly automated cars," in *2015 IEEE Intelligent Vehicles Symposium (IV)*. IEEE, Conference Proceedings, pp. 1287–1292.
- [50] C. Gold, L. Lorenz, and K. Bengler, "Influence of automated brake application on take-over situations in highly automated driving scenarios," in *Proceedings of the FISITA 2014 World Automotive Congress*, Conference Proceedings.
- [51] M. Itoh, F. Flemisch, and D. Abbink, "A hierarchical framework to analyze shared control conflicts between human and machine," *IFAC-PapersOnLine*, vol. 49, no. 19, pp. 96–101, 2016.
- [52] R. Boink, M. M. van Paassen, M. Mulder, and D. A. Abbink, "Understanding and reducing conflicts between driver and haptic shared control," in *2014 IEEE International Conference on Systems, Man, and Cybernetics (SMC)*. IEEE, Conference Proceedings, pp. 1510–1515.

# A

## Implementation

During this study two control authority transition approaches were compared: Traded Control (TC) and Haptic Shared Control (HSC). The implementation of the two systems has been done in Matlab&Simulink. Both approaches needed to be able to drive autonomously in a lane on a straight highway. The longitudinal control for this was based on an existing Adaptive Cruise Control (ACC) system provided by Cruden BV, and assumed 100km/h. The lateral control for the lane keeping system and the HSC system were both provided by a Four Design Choice Architecture controller (FDCA) [4]. A FDCA controller was provided by the TU Delft. This controller has been made compatible with Cruden's driving simulator. A lane change algorithm has been added to this system in order to provide continuous feedback during highway driving. Three Simulink models have been created during this master thesis; Haptic Shared Control DEMO file, Traded Control Transition file and HSC transition file. The demo file allowed the drivers to practice driving with haptic shared control. If the support system is active, the system assumes a cooperative driving mode, known as HSC. In this mode the system provides support during lane keeping, and also supports lane changes to the right and left. The TC file was used during the TC trials and the HSC file was used during the HSC trials. The implementation of the systems will be discussed in this chapter.

### A.1. Haptic Shared Control

The motivation for the FDCA controller is that it uses separate feedback and feedforward control. The separate feedforward control allows for a continuous haptic feedback, to compensate for the moments without a feedback error. When active, this system provides a cooperative state in which the driver and system communicate by exerting forces on the steering wheel. The settings of the FDCA controller are based on four design parameters, a schematic overview is given in figure A.1

- *Human Compatible Reference (HCR)*: An online determined reference trajectory by the system.
- *Level of Haptic Strength (LoHS)*: A percentage of the desired torques based on the desired steering wheel angle to follow the HCR. 0% means no assistance at all, and 100% represents autonomous driving.
- *Level of Haptic Feedback (LoHF)*: The torques by the feedback control to correct for the deviations of the HCR, based on the heading error and lateral error.
- *Level of Haptic Authority (LoHA)*: Virtual springs that can dynamically change the steering stiffness in order to change the level of resistance on the steering wheel.

In figure A.1 a schematic overview is given of the FDCA controller highlighting the main components of the system. In the Vehicle & Steering dynamics block, the input torques of the driver and the controller on the steering wheel are translated to a steering angle by means of the steering dynamics, shown in equation A.1

$$\sum T = J\ddot{\theta} + B\dot{\theta} + K\theta \quad (\text{A.1})$$

here  $T$  is the total sum of the torques acting on the steering wheel, provided by the human and the FDCA controller.  $\theta$  is the steering wheel angle,  $\dot{\theta}$  and  $\ddot{\theta}$  are the first and second derivative of the steering angle with

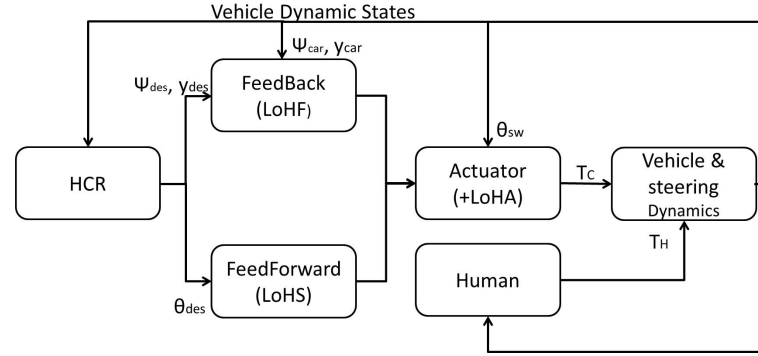


Figure (A.1) Schematic overview of the FDCA controller used in this study;  $\Psi_{des}, y_{des}$  and  $\theta_{des}$  are the desired heading trajectory, the desired lateral position and the desired steering wheel angle based on the HCR.  $\Psi_{car}, y_{car}$  and  $\theta_{sw}$  are the actual heading trajectory, lateral position and the steering wheel angle.  $T_C$  and  $T_H$  are the controller torques and the force exerted by the human on the steering wheel.

respect to time and represent the steering angular velocity and the steering angular acceleration.  $J$  is the total inertia of the steering column,  $B$  represents the damping of the system and  $K$  stands for the stiffness of the steering system. The control loader realizes the determined steering wheel angle resulting in the new vehicle states, which are send back to the driver and the controller. Based on the new states, both entities generate a new input. By means of this control loop the driver and automations system continuously communicate with each other.

The inputs of the FDCA controller are evaluated based on a HCR, which will be discussed later in this chapter. The inputs are  $\Psi_{des}, y_{des}$  and  $\theta_{des}$ , and are divided over a feedback block and a feedforward block. The feedback block determines a steering angle needed to compensate for the lateral and heading error. The feedforward block sends through the steering angle to follow the desired reference trajectory. Both angles are send to the actuator block, where an extra stiffness is added to the system in terms of the LoHA. This stiffness determines the haptic strength. By tuning the LoHS, LoHF and the LoHA extra weight can be added to each aspect of the system. These steering angles are then translated to a total torque of the system by means of the inverse of the steering dynamics (equation A.1)[5]. This torque represent the torque of the FDCA controller and interacts with the driver on the steering wheel.

## A.2. Lane Change support Algorithm

For this study, it was desired that the HSC system provides continuous feedback to the driver based on their inputs. In a straight endless highway environment the driver can either keep lane, or change lanes. Therefore, a system has been designed that assists the driver in lane keeping and monitors the their inputs, and when triggered, supports a lane change. The lane change algorithm used in this study is based on the work of K.K. Tsoi in [3]. A lane change can be triggered if the time to line crossing (TLC) falls below a heuristically tuned threshold. The TLC is the time duration available for the driver before any lane boundary crossing [2]. In this study the threshold was set to 4s, and if an indicator light was active the threshold was set to 12s to ensure a smooth lane change. During straight highway driving the reference trajectory for the HSC system is lane center of that lane. If a lane change is triggered, the lane change flag ( $LC_{flag}$ ) in Simulink is set to 1 (left) or -1 (right). At this point the reference trajectory switches from lane center to a predetermined lane change trajectory, that connects the current lane center with the next desired lane center. If the vehicle comes within the vicinity of the desired lane center,  $LC_{flag}$  changes back to 0, and the lane ID is updated so that the desired lane center becomes the current lane center. At this point the lane change has been completed and the system functions again as a lane keeping support system.

### A.2.1. Human Compatible Reference

The human compatible reference(HCR) is the reference trajectory which the controller follows. During lane keeping the HCR is simply the lane center. If a lane change is triggered the desired reference trajectory jumps from the current lane center to the next. This discontinuity in the reference trajectory is undesired. Therefore, a lane change trajectory is needed that smoothly connects both lane centers.

### A.2.2. Lane Change Algorithm vs Bessel filter approach

In [3] the HCR for a lane change, is a function of time described as equation A.2. This function is derived from a sinusoidal pattern of the lateral acceleration profile which is added to the current lane center to connect both lane centers.

$$y(t) = \frac{-d}{2\pi} \sin\left(\frac{2\pi \cdot t}{T_{lcm}}\right) + \frac{d}{T_{lcm}} \cdot t \quad (\text{A.2})$$

In A.2  $d$  stands for the distance between the current lane center and the future lane center,  $t$  is the elapsed time starting when  $LC_{flag}$  is triggered.  $T_{lcm}$  represents the total lane change duration. By means of equation A.2 both lane centers are smoothly connected. However, it is also desirable that the lane change can be interrupted before the future lane center has been reached, e.g. if the driver changes their mind. This was also often the case for the evasive maneuvers during the experiment, the participants did not complete a lane change before steering back to the right lane. In [3] it is described that if the lane change is interrupted ( $LC_{flag}$  switches back to 0 before the lane ID has been updated, because the driver has overruled the control inputs),  $y(t)$  is decreased in time and thereby supports the driver back to lane center.

This raises some issues when using the FDCA controller. The approach to reverse time so equation A.2 supports the driver back to lane center causes a discontinuity in the HCR to arise. This problem is visualized in figure A.2.

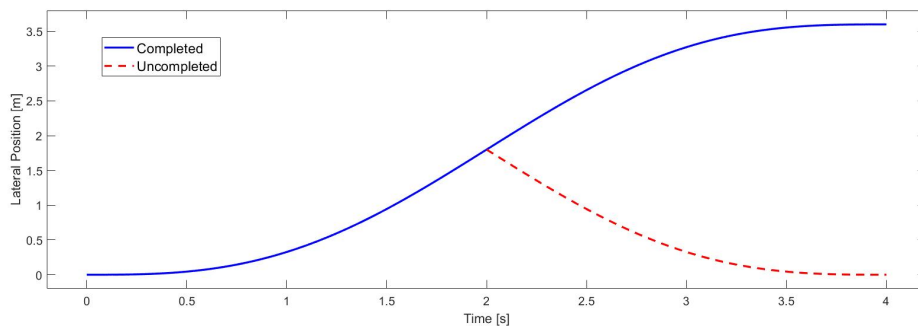


Figure (A.2) Visualization of the interrupted lane change issues. The blue line represents the HCR for a lane change using equation A.2 and a road with  $d = 3.6m$  and  $T_{lcm} = 4s$ . The red dotted line represents the HCR that will be supported if the lane change maneuver is interrupted half way through, highlighting a discontinuity in the trajectory.

The inputs of the FDCA controller are the heading error ( $\Psi_e$ ) and the lateral error ( $y_e$ ) for the feedback controller, and the desired steering wheel angle ( $\theta_{des}$ ) for the feedforward control. These inputs are derived from the HCR. As a result, all the desired inputs of the FDCA have discontinuities in the signals and therefore causes the system to become unstable. Note that this was not an issue in [3], because the study used a different control strategy based on a look-a-head controller. This approach relies on the ( $\Psi_e$ ), ( $y_e$ ) as inputs. By means of the look-a-head strategy the discontinuity can be filtered out. However, with the FDCA control strategy this is not the case. Therefore, two approaches were investigated to solve the issues.

1. *Cross-Fade*: The first approach was to linear cross-fade the HCR of a completed lane change into the HCR of an uncompleted lane change back to lane center at the moment that the lane change was interrupted, shown in equation A.3.

$$HCR(t) = T_C(t) \cdot n(t) + T_{UC}(t) \cdot (1 - n(t)) \quad (\text{A.3})$$

Where  $T_C$  is the trajectory for a completed lane change,  $T_{UC}$  represents the interrupted lane change trajectory and  $n$  linearly decreases from 1 to 0 as a function of time. In this way the discontinuity at the moment of interruption is filtered out of the trajectory.

2. *4<sup>th</sup> order Bessel filter*: The second method used a completely different approach, and did not use equation A.2 to smoothly connect the current lane center with the future lane center. At the moment that  $TLC < threshold$  and a lane change is triggered, the desired HCR switches from the current lane center to the future desired lane center. To smoothly connect the two lane centers, a 4<sup>th</sup> order Bessel filter

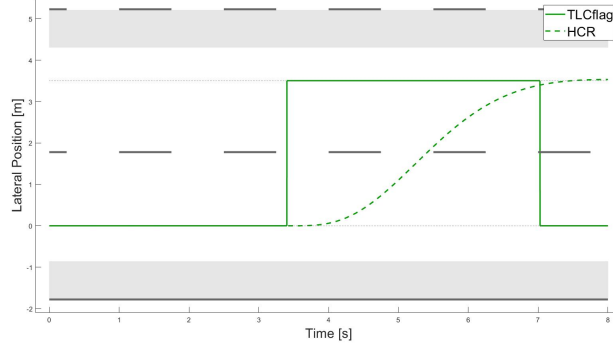


Figure (A.3) Visualization of the Bessel filter approach. If a lane change has been triggered ( $TLC < threshold$ ), the Bessel filter smoothly filters the step input to create a smooth lane change trajectory. **Note:**  $TLC_{flag}$  has been scaled to exactly fit the desired lateral displacement for clarity.

is used to filter the step input [1]. In figure A.3 this approach is visualized. The coefficients of the filter polynomials are given in the transfer function A.4.

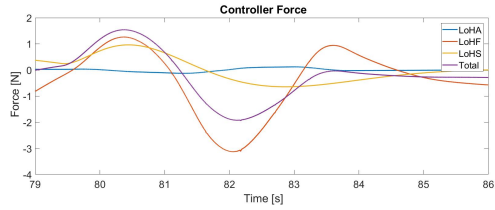
$$tf_{Bess} = \frac{1}{\omega_0^4 \frac{s^4}{\omega_0^4} + 3.124 \frac{s^3}{\omega_0^3} + 4.392 \frac{s^2}{\omega_0^2} + 3.201 \frac{s}{\omega_0} + 1} \quad (A.4)$$

Here  $\omega_0$  is the cut-off frequency. The advantage of using this Bessel filter is that it has a continuous output up until the third derivative (heading, yaw rate and jerk), even if the input is discontinuous. This solves the problem of the discontinuous inputs for the FDCA controller. The filter has a linear phase lag, which is the same as a time delay. It is therefore possible to predetermine a fixed lane change duration, based on the cut-off frequency. Similar to  $T_{lcm}$  used in the approach in [3].

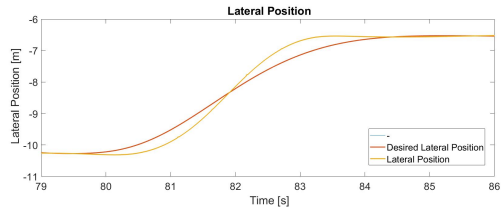
The two approaches to have been implemented in order to test which one was best suitable for the FDCA controller. In figure A.4 the raw data plots of the two approaches are shown for a completed lane change that has not been interrupted, and in figure A.5 the same raw data is shown for a lane change that has been broken off half way through the maneuver. In figure A.4 it can be seen that the HCR for the Lane change algorithm follows a very symmetric path. The Bessel filter turns in slightly sharper compared to the second steering action. Another property of the Bessel filter is that the trajectory has some overshoot. However, for a lane change maneuver this is negligible, as shown in figure A.4.

In figure A.5 it can be seen that the lane change algorithm approach still contains a small discontinuity in the reference after a cross-fade. It can also be seen that the small discontinuity in the lateral reference trajectory (A.5d) has large impact on the desired heading and desired steering wheel angle, which are the inputs of the FDCA controller. In A.5b the output forces of the FDCA control are shown. In this figure the discontinuities are clearly visible and are also clearly noticeable for by the driver and can cause the driver to lose control of the vehicle. On the left hand side of figure A.5 the Bessel filter approach shows a continuous output for all FDCA controller inputs. Therefore, the Bessel filter approach has been used as the lane change support system in this study.

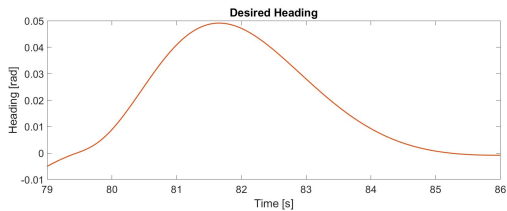
**Bessel Filter Approach**  
*Completed lane change*



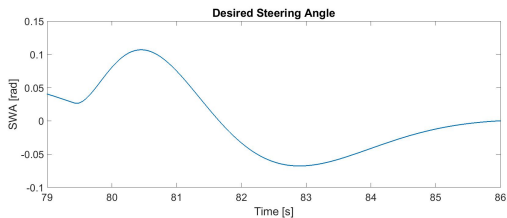
(a) Forces exerted on the steering wheel by the controller



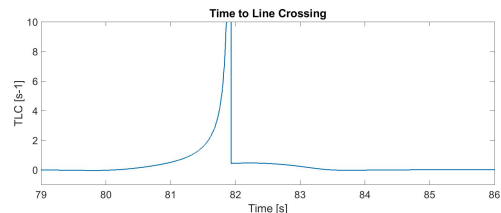
(c) The lateral trajectory



(e) The heading trajectory

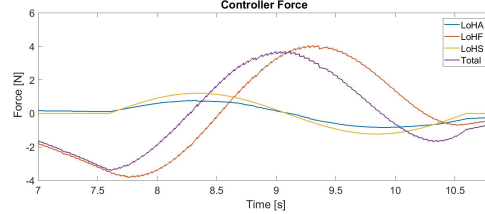


(g) The desired steering angle

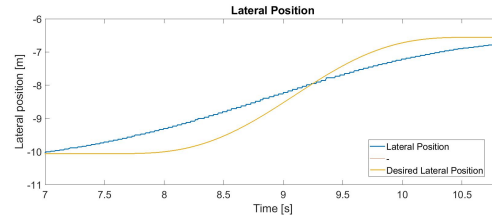


(i) The inverse time to line crossing

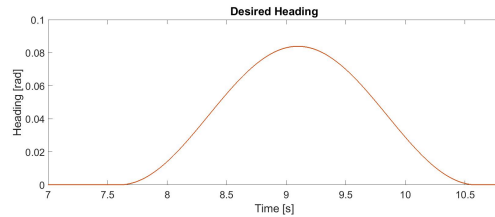
**K.K. Tsoi Algorithm**  
*Completed lane change*



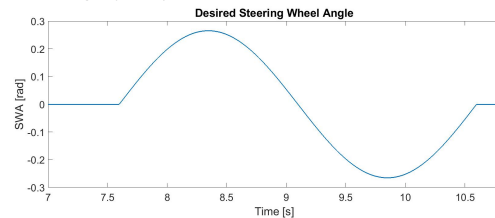
(b) Forces exerted on the steering wheel by the controller



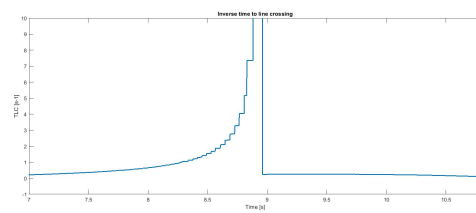
(d) The lateral trajectory



(f) The heading trajectory



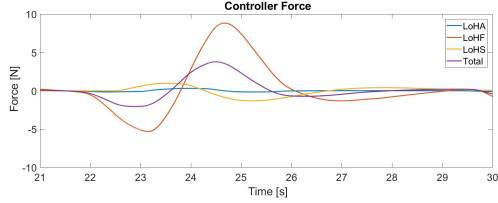
(h) The desired steering angle



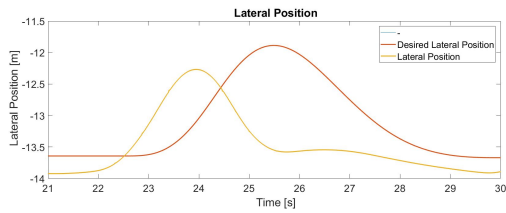
(j) The inverse time to line crossing

Figure (A.4) A comparison of the raw data plots of the Bessel filter approach (left) against the lane change algorithm used in [3] (right) for a completed lane change. **Note:** These trajectories have been driven on a desktop simulation, using the mouse to steer. Therefore, no actual force feedback was experienced during the simulation. The reference trajectory of the Bessel filter approach does not start at 0, since it immediately follows a previous lane change maneuver.

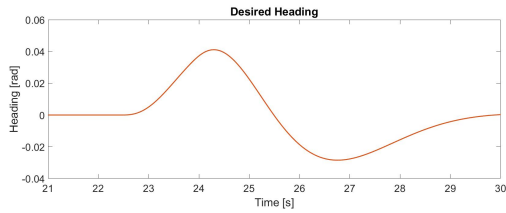
**Bessel Filter Approach**  
*Uncompleted lane change*



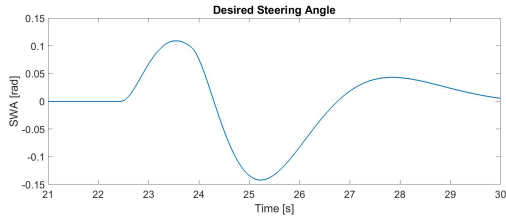
(a) Forces exerted on the steering wheel by the controller



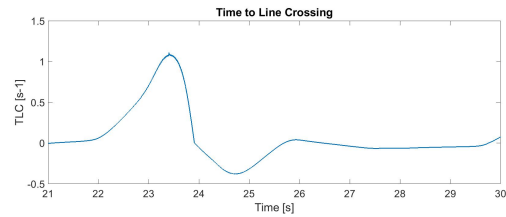
(c) The lateral trajectory



(e) The heading trajectory

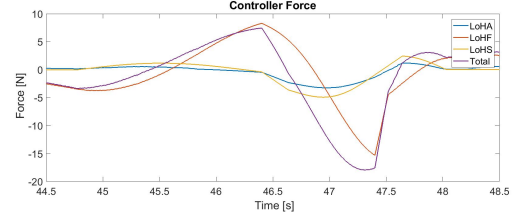


(g) The desired steering angle

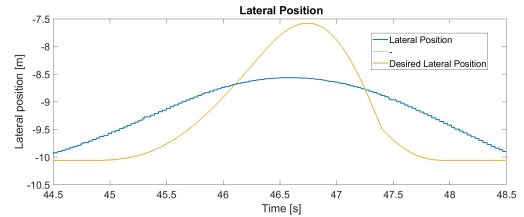


(i) The inverse time to line crossing

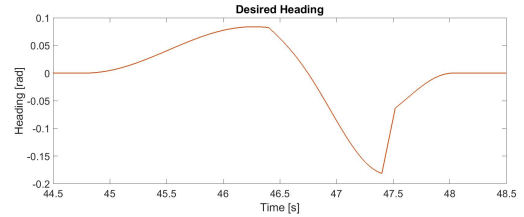
**K.K. Tsoi Algorithm**  
*Uncompleted lane change*



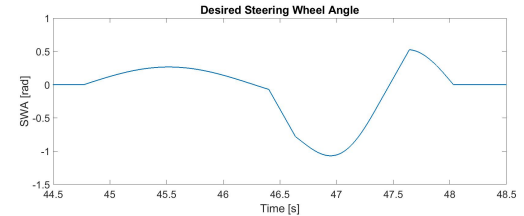
(b) Forces exerted on the steering wheel by the controller



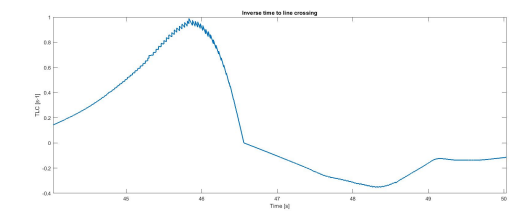
(d) The lateral trajectory



(f) The heading trajectory



(h) The desired steering angle



(j) The inverse time to line crossing

Figure (A.5) A comparison of the raw data plots of the Bessel filter approach (left) against the lane change algorithm used in [3] (right) for a completed lane change. **Note:** These trajectories have been driven on a desktop simulation, using the mouse to steer. Therefore, no actual force feedback was experienced during the simulation.

### A.3. Recommendations

One of the recommendations for future research discussed in the paper, was to use a different approach to the one-size-fits-all implementation of the HCR. It was suggested to make the HCR adaptable to the level of criticality and adaptable to the inputs of the driver. There are many studies focusing on this topic, and how to make the HCR align with the intentions of the driver. In [3] a method is described, this example will be used here to elaborate on how it can be applied to the Bessel filter approach in order to make it adaptable. In equation A.2, the lane change trajectory is defined for the lane change algorithm used in [3] containing  $T_{lcm}$  which defines the lane change duration. To make the system adaptable,  $T_{lcm}$  needs to be determined for each different lane change maneuver at the start. This can be done using equation A.5.

$$T_{lcm} = \frac{e_{lat_{cf}}}{V_{lat}}, \quad T_{min} < T_{lcm} < T_{max} \tag{A.5}$$

Here,  $e_{lat_{cf}}$  is the lateral distance between the center of gravity (CoG) of the car and the future lane center.  $V_{lat}$  is the lateral velocity of the vehicle.  $T_{min}$  and  $T_{max}$  are the bounds for a minimum and maximum lane change duration. By evaluating equation A.5 at the moment a lane change is trigger, the length of the lane change trajectory can be varied according to the vehicle states:  $e_{lat_{cf}}$  and  $V_{lat}$ .

This method can also be implemented for the Bessel filter approach using the same equation A.5. Since the Bessel filter has a linear phase lag,  $T_{lcm}$  can be used to determine the cut-off frequency for the transfer function in A.4 using:  $\omega_0 = 2 \cdot \pi / T_{lcm}$ .  $\omega_0$  is used to calculate all transfer function inputs. In this way the lane change duration can be varied according to the vehicle states at the start of a lane change maneuver. However, the standard transfer function block in Simulink does not allow changes to be made to the inputs, while running a simulation. Therefore, the transfer function should be build up out of integrator blocks, shown in figure A.6. In this way the initial conditions can be updated during a simulation. A control logic is needed to activate the Bessel filter at the start of lane change maneuver with the according initial conditions, and needs to be reset every time a lane change has been completed. This is one possible approach to extend the lane change algorithm used in this study, by making it adaptable.

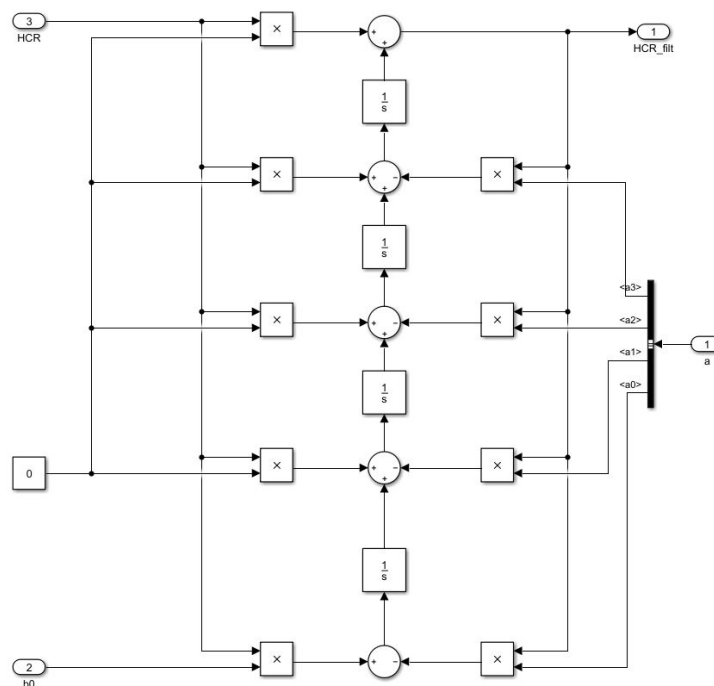


Figure (A.6) Simulink model of the 4<sup>th</sup> order Bessel filter;  $HCR$  = the step input signal from current lane center to future lane center.  $HCR_{filt}$  = the filtered step input signal.  $b_0$  = the inputs for the numerator from equation A.4.  $a$  = the inputs for the denominator from equation A.4



# B

## Experiment Forms

**B.1. Informed Consent**

**B.2. Van Der Laan questionnaire**

**B.3. Demographics questionnaire**

## 1 Research Group

### 1.1 Researchers in charge of the project

Kevin van Dintel <sup>1</sup>	MSc. Student	Delft University of Technology
Edwin de Vries <sup>2</sup>	Senior Vehicle Dynamics Engineer	Cruden B.V.
Bastiaan Petermeijer <sup>1</sup>	Post-doctoral Researcher	Delft University of Technology
David Abbink <sup>1</sup>	Full Professor	Delft University of Technology

### 1.2 Organizations

1. Faculty of Mechanical, Maritime and Materials Engineering, Delft University of Technology, Delft, the Netherlands
2. Cruden B.V., Amsterdam, the Netherlands

## 2 This document

This Informed Consent Form has two parts:

- **Information Sheet**, pages 1 - 6
- **Certificate of Consent**, page 7

Before agreeing to participate in this study, you are asked to read this document carefully. The Information Sheet describes the purpose, procedures, and risks of this study. After reading the Information Sheet, we will be happy to explain any points that seem unclear, or sections that you do not understand. You should feel comfortable to speak to any of the researchers involved to answer any questions you may have at any time. After you have read this Information Sheet and we have answered all of your questions or discussed any concerns, you can decide if you would like to be involved. At the end of this document, we would like to ask you to sign a written Certificate of Consent to confirm your agreement to participate. Your signature is required for participation.

You will be given a copy of the full Informed Consent Form.

## 3 Purpose of the research

In the near future the first vehicles that can engage in a Highly Automated Driving (HAD) mode will be allowed on the road. The HAD system takes over the entire driving task of the driver. During this mode the driver can engage in a different activity, for example reading a book. The HAD system is designed to operate within a specified design domain. In case a scenario outside the design domain occurs, the HAD system will request the driver to take back control of the vehicle. The challenge will be to regain the driver's attention and to get the driver back in control of the vehicle before accidents happen. The purpose of this study is to investigate the effect of

Haptic Shared Control as a support system during the take over process. This knowledge may be useful for the design of safe and smooth HAD systems in the near future.

---

## 4 Participation

### 4.1 Location of the experiment

Participation will involve completing one in-person sessions on different days at Cruden B.V. Global Headquarters, Pedro de Medinalaan 25, 1086 XP Amsterdam, the Netherlands.

### 4.2 Eligibility criteria

You are invited to participate in this project if:

- You are 18 years or older.
- You have a car driving license.
- You have normal or corrected-to-normal vision (i.e. glasses or contact lenses).
- You have not experienced severe (simulator) motion sickness in the past.
- You do not have heart, back or neck issues.
- You have not been diagnosed with epilepsy.
- You are not pregnant.
- You have not recently had surgery.
- You are not physically disabled.
- You are not under the influence of drugs, alcohol or prescription substances that may compromise the comfort when operating a motion-based driving simulator.

The researchers reserve the right at any time to refuse or excuse (from an in-progress session) any participant who does not meet/no longer meets the study requirements or who are behaving in an unnecessarily unsafe manner.

### 4.3 Voluntary participation and right to refuse or withdraw

Your participation in this project is completely voluntary. We welcome you to contact us to ask any questions and to discuss your possible involvement in the project, but it is your choice whether to participate or not. If you do agree to participate you have the right to withdraw from the project at any moment without comment or penalty.

## 5 Procedure

The research consists of 1 driving simulator experiment. The experiment will retrieve take over process data with the aim of analysing human driving behaviour. The driving data will be logged by the driving simulator.

## 5.1 Experiment

You will be asked to perform two driving sessions (2x15 min) in a highway setting. Data from this experiment will be used to analyze the take over process from HAD to manual control. The simulated vehicle is a generic sedan car, equipped with a dashboard containing a speedometer, as well as two side view mirrors and one rear view mirror. The simulated vehicle has three driving modes: Highly automated driving (HAD), Haptic Shared Control and manual control. During manual control the vehicle is controlled in the same way as a normal car: steering wheel, turn signals, pedals. In HAD mode the vehicle does all the driving for you, allowing you to sit back and engage in another task. Haptic shared control is a system that allows the driver and the automation system to drive together and interact by applying forces on the steering wheel.

## 5.2 Prior to the simulator sessions

Prior to the simulator sessions, the informed consent form will be sent to you. When you visit the simulator sessions, the study details will be explained to you, an informed consent form will be signed, and a demographics questionnaire will be completed.

Next, a safety instruction will be given on operating the driving simulator.

## 5.3 Practice simulator session

The experiment will start with three short practice runs. The first run will include manual driving to familiarize yourself with the simulator and the virtual environment. You are encouraged to drive both fast and slow to get a feeling of the dynamics of the vehicle. For the second run you will be explained how to use the haptic shared control. Then it will be tested to get a feel of the system. Finally in the third test run a few practice take over procedures will be done.

## 5.4 Simulator session instructions

### 5.4.1 Driving

During the experiment, you are asked to drive as you normally would and to respect the traffic regulations. Drivers will drive in the right lane, unless avoiding other vehicles. The experiment will take place on a three-lane highway. Between the sessions, there will be a short break.

### 5.4.2 Scenario

The experiment will be conducted on a three lane endless highway, illustrated in figure 1. At the start the ego vehicle will spawn on the hard shoulder. You are then instructed to accelerate to 100 km/h, move into the right lane and activate the automation system. Once engaged, the system assumes lateral and longitudinal control, with a constant vehicle speed at 100 km/h. Over a period of approximately 18 minutes, ten defect vehicles will randomly appear in the in the right lane. If this is the case, the vehicle will signal you to take back control of the vehicle in the form of an auditory beep combined with a flashing icon on the dashboard. When you have resumed manual control of the vehicle, avoid the obstacle in current lane. Note that there may be other road users, therefore check carefully check the environment before steering as you normally would. After each take-over your are requested to move back into the right lane and activate the automation. While the automation system is active, you can perform a secondary task (the game: Angry Birds) on the touchscreen in the simulator.

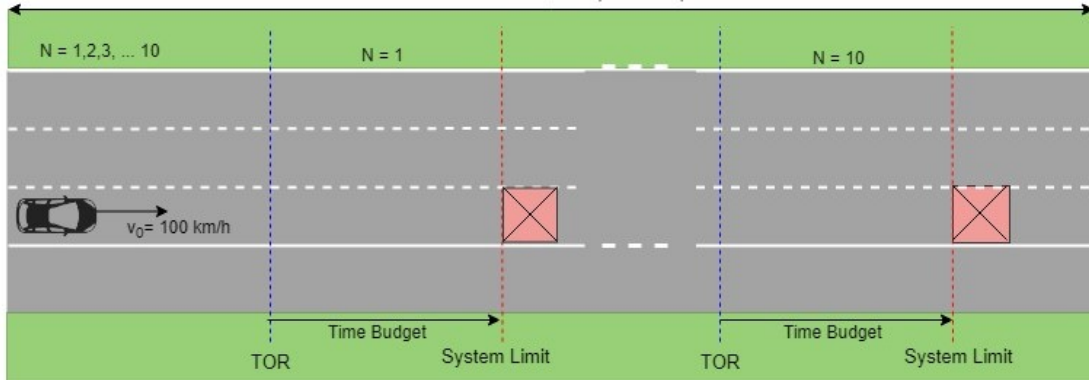


Figure 1: Experiment scenario

### 5.5 Duration and time commitment

The experiment will take approximately 60 minutes and involves signing a consent form, practice simulator sessions, testing simulator sessions, breaks and completing questionnaires.

## 6 Expected benefits

This study provides basic scientific information in terms of driving performance during the take over process. As such, it is not expected that the project directly benefits you. However, your participation in this study will add to our understanding of advanced driver assistance systems and the interaction with drivers. In this way your participation will assist in developing new approaches to improve driver safety and comfort.

## 7 Risks associated with participation

Participants may experience simulator motion sickness. In case a participant experiences such sickness, the experiment can be stopped at any time. An emergency switch is available to the operator which will shut of the simulation immediately. Participants are instructed to wear their seatbelt during the entire simulation. The seatbelt can be unbuckled when the simulation has stopped and the operator has given permission to do so. Unbuckling of the seatbelt during simulation will shut down the simulation.

Taking place on the simulator requires you to climb up a small staircase, which might result in an accidental fall. The participant may only enter the simulator when the simulator is shut-down, to avoid tripping due to motion of the simulator. During the experiment, an operator ensures safe conduct of operation of the driving simulator. If the operator notices unsafe or unwanted behavior of the simulator or participant, the experiment may be terminated prematurely.

Losing control of the vehicle can result in a collision with the guard rail or other objects. The experience of a crash can be emotionally and physically demanding, as the motion base and visual screens simulate these collisions. Finally, other vehicles are non-solid objects, so a participant

can drive through them. Riding through a non-solid object can be an emotionally uncomfortable experience.

If for any reason you wish to onboard the experiment, it can be stopped at all times.

---

## 8 Privacy and confidentiality

All comments and responses are anonymous and will be treated confidentially. The names of individual persons are not required in any of the responses. Publications or presentations of the results will not include any information that could identify you.

Any data collected as part of this project will be stored securely as per TU Delft's Research Data Management policy. Only the researchers involved in the project will have access to this information. Please note that non-identifiable data from this project may be used as comparative data in future projects or stored on an open access database for secondary analysis.

---

## 9 Sharing of results

Results of the study might be presented in scientific and driving simulator seminars and conferences, and published as PhD theses and articles in scientific journals. Data might also be used in related studies on driver behavior, training, training in simulators, design of vehicle safety systems, and human-machine interface design for vehicles.

---

## 10 Responsibility

The researchers, funding bodies or institutions involved do not bear any responsibility for possible inconveniences or damages during travel to or from the location of the experimental activity.

---

## 11 Questions/further information about the project

If you wish to ask questions about the project or require further information, please contact one of the researchers below:

<b>Researcher</b>	<b>E-mail</b>	<b>Phone</b>
Kevin van Dintel	K.M.vandintel@student.tudelft.nl	+31(0)6 2169 3305
Edwin de Vries	E.devries@cruden.com	
David Abbink	D.A.Abbink@tudelft.nl	
Bastiaan Petermeijer	S.M.Petermeijer@tudelft.nl	

---

## 12 Ethical approval and complaints regarding the conduct of the project

This study has been approved by the Human Research Ethics Committee (HREC). If needed, verification of approval can be obtained either by writing to P.O. Box 5015, 2600 GA Delft, The Netherlands or by sending an email to [HREC@tudelft.nl](mailto:HREC@tudelft.nl). If you do have any concerns or complaints about the ethical conduct of the project you may contact the HREC on the above mentioned addresses. The HREC is not connected with the research project and can facilitate a resolution to your concern in an impartial manner. Name of the experiment according to the Ethics Approval Application: *Transition of control authority between Highly Automated Driving and manual control*.

## Consent Form for:

Transition of control authority between Highly Automated Driving and manual control

### Please tick the appropriate boxes

**Taking part in the study** **YES** **NO**

I have read and understood the study information dated [Thursday 5<sup>th</sup> September, 2019], or it has been read to me. I have been able to ask questions about the study and my questions have been answered to my satisfaction

I consent voluntarily to be a participant in this study and understand that I can refuse to answer questions and I can withdraw from the study at any time, without having to give a reason.

I understand that taking part in the study involves the logging of driving data. This study also involves the participant completing questionnaires.

**Risks associated with participating in the study**

I understand that taking part in the study involves the following risks: motion sickness due to movement of the simulator. Physical and emotional discomfort due to the possibility of experiencing a collision scenario.

**Use of the information in the study**

I understand that information I provide will be used for presentation in scientific and driving simulator seminars and conferences and published as Master's theses, PhD theses and articles in scientific journals.

I understand that personal information collected about me that can identify me, such as [e.g. my name or where I live], will not be shared beyond the study team.

**Future use and reuse of the information by others**

I give permission for the driving simulator data that I provide to be archived in TU Delft repository so it can be used for future research and learning

---

Name of participant

---

Signature

---

Date

I have accurately read out the information sheet to the potential participant and, to the best of my ability, ensured that the participant understands to what they are freely consenting.

Kevin van Dintel

---

Name of researcher

---

Signature

---

Date

# VAN DER LAAN QUESTIONNAIRE

I find the system (please tick a box on every line):

1	Useful	_ _ _ _ _	Useless
2	Pleasant	_ _ _ _ _	Unpleasant
3	Bad	_ _ _ _ _	Good
4	Nice	_ _ _ _ _	Annoying
5	Effective	_ _ _ _ _	Superfluous
6	Irritating	_ _ _ _ _	Likeable
7	Assisting	_ _ _ _ _	Worthless
8	Undesirable	_ _ _ _ _	Desirable
9	Raising Alertness	_ _ _ _ _	Sleep inducing

Comments on the experiment and system:

.....

.....

.....

.....

.....

.....

.....

To be filled out by the researcher:

Participant nr:	Condition nr:	Date:

## Simulator study personal details

Please make sure to fill out this form before driving experiment

### 1. Age

---

### 2. Gender

Markeer slechts één ovaal.

- Male  
 Female  
 Prefer not to say

### 3. At what age did you obtain your driving license?

---

### 4. On Average, how often did you drive a car in the last 12 months?

Markeer slechts één ovaal.

- Daily  
 4-6 times per week  
 1-3 times per week  
 Between one a week and once a month  
 Less than once a month  
 Never  
 Prefer not to say

### 5. How many kilometers did you drive in the last 12 months?

Markeer slechts één ovaal.

- 0 km  
 1 - 1.000 km  
 1.001 - 5.000 km  
 5.001 - 10.000 km  
 10.001 - 20.000 km  
 20.001 - 50.000 km  
 50.001 - 100.000 km  
 over 100.000 km  
 Prefer not to say

### 6. Some cars are equipped with Adaptive Cruise Control (ACC), how often did you drive with ACC in the past 12 months?

Markeer slechts één ovaal.

- Daily  
 4-6 times per week  
 1-3 times per week  
 Between one a week and once a month  
 Less than once a month  
 Never  
 I don't know what Adaptive Cruise Control is  
 Prefer not to say

### 7. Some cars are equipped with Lane Keeping Assist (LKA), how often did you drive with LKA in the past 12 months?

Markeer slechts één ovaal.

- Daily  
 4-6 times per week  
 1-3 times per week  
 Between one a week and once a month  
 Less than once a month  
 Never  
 I don't know what Lane Keeping Assist is  
 Prefer not to say

8. How many accidents were you involved in when driving a car in the last three years?

*Markeer slechts één ovaal.*

- 0
- 1
- 3
- 4
- 5 or more
- Prefer not to say

9. How many times have you driven in a driving simulator?

*Markeer slechts één ovaal.*

- 0
- 1
- 2
- 3
- 4
- 5 or more
- Prefer not to say

10. How many times have you driven THIS driving simulator?

*Markeer slechts één ovaal.*

- 0
- 1
- 2
- 3
- 4
- 5 or more
- Prefer not to say

## B.4. Results

### B.4.1. Van Der Laan questionnaire

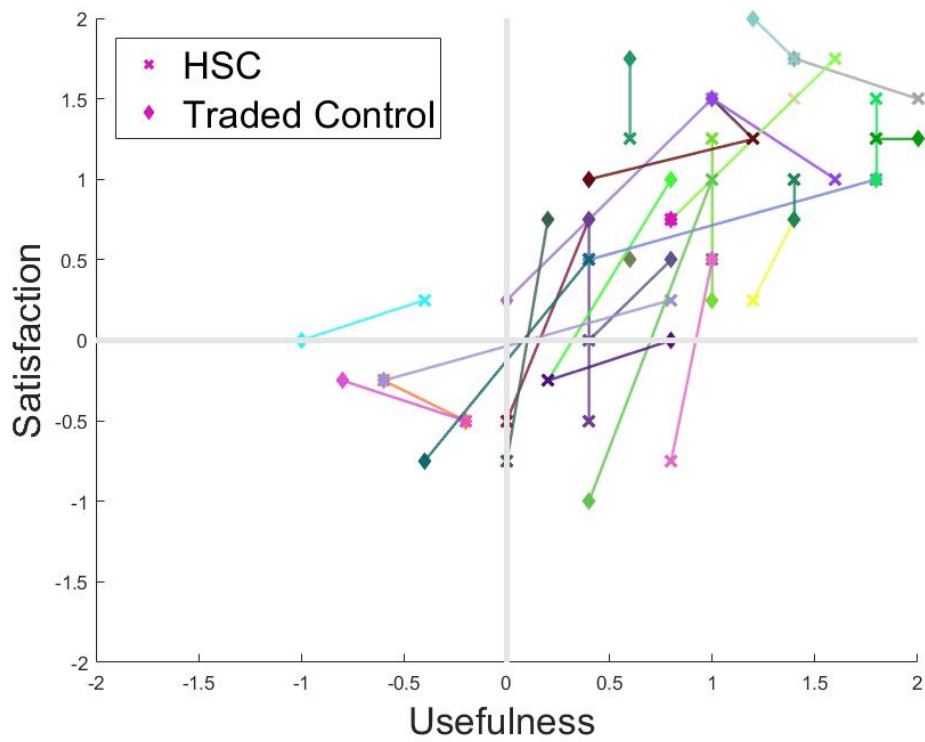


Figure (B.1) Results of the Van der Laan questionnaire per participant. The diamond represents the score for the TC transition and the cross represents the score for HSC transitions. The line connects the scores for HSC and TC per participant.

Participant	Traded Control									Haptic Shared Control								
	TC1	TC2	TC3	TC4	TC5	TC6	TC7	TC8	TC9	HSC1	HSC2	HSC3	HSC4	HSC5	HSC6	HSC7	HSC8	HSC9
1	1	1	1	1	1	0	1	0	-1	1	1	2	2	1	0	1	0	0
2	2	2	0	1	1	2	2	1	0	1	1	1	1	2	1	2	1	0
3	0	-1	0	-1	0	0	1	0	-2	-1	-1	-1	-1	0	0	1	0	-2
4	2	2	1	2	1	2	0	1	-1	1	2	1	2	1	2	2	0	-2
5	1	1	0	1	1	0	1	1	-1	1	-1	-1	-1	1	-1	0	-1	-1
6	1	1	1	0	1	1	2	1	2	1	-1	1	-1	2	-1	1	1	1
7	2	2	1	1	2	2	1	2	1	2	1	2	1	2	1	2	2	2
8	1	-1	1	1	-1	0	1	1	-2	2	1	2	1	1	2	2	2	-2
9	1	0	1	0	1	1	1	0	1	1	1	1	2	1	2	1	1	1
10	2	1	1	1	1	2	0	2	1	2	1	1	0	2	0	1	1	2
11	-2	0	1	2	2	2	2	-1	1	2	2	1	1	2	1	1	1	1
12	1	1	0	0	1	1	1	0	1	0	0	-1	1	0	0	1	0	2
13	-1	1	0	-1	-1	0	-1	0	-2	0	1	0	0	0	0	0	0	-2
14	0	1	2	2	2	1	-1	-1	-1	0	-1	2	-1	2	-2	0	-1	-2
15	2	-1	-1	2	2	1	1	2	0	-1	-1	0	0	1	-1	0	0	1
16	1	1	0	0	0	1	-1	0	2	2	1	2	1	2	1	2	0	1
17	-1	0	0	0	0	-1	-1	0	-1	1	0	0	-1	1	0	0	0	2
18	1	0	1	1	1	1	2	1	-1	2	2	2	1	2	2	2	1	0
19	0	-1	0	-1	0	-1	0	-1	2	2	1	0	0	1	1	2	1	0
20	-1	-1	0	0	-2	0	-2	0	1	-1	0	0	-1	-1	-1	0	0	1
21	1	0	1	1	2	0	1	-1	-1	1	0	0	1	1	-1	-1	-1	0
22	0	1	1	1	0	1	0	1	1	2	1	1	1	1	1	2	2	0
23	2	2	1	2	1	2	1	2	1	2	2	1	1	2	2	2	1	0
24	-1	-1	-1	0	1	-1	0	-1	-1	1	-1	0	0	1	1	1	1	-1
25	0	1	0	1	0	1	0	0	1	0	-1	-1	-2	0	-1	-1	-1	2
26	2	1	1	0	1	0	2	2	1	2	1	1	0	1	0	2	2	1
27	2	1	2	1	1	1	2	1	2	2	1	2	1	2	1	1	2	2
28	1	1	1	1	1	0	1	0	1	1	-1	0	-2	0	-2	1	0	2
29	2	2	2	1	2	0	2	2	2	2	1	2	1	1	2	2	1	2
30	1	1	1	0	1	1	1	1	0	1	0	1	0	1	1	1	1	0

Table (B.1) Results of the Van der Laan Questionnaire containing the ratings of the 9 Likert items for each transition approach per participant.

**B.4.2. Demographics questionnaire**

Participant	Age	Gender	Driving Experience	Q4	Q5	Q6	Q7	Q8	Q9	Q10
1	28	F	10	A	F	E	F	B	F	F
2	25	M	7	D	B	F	F	A	A	A
3	39	F	21	B	E	D	E	A	F	F
4	25	M	5	D	D	F	F	A	A	A
5	31	M	13	A	F	E	E	A	F	A
6	41	M	21	A	F	F	F	A	F	F
7	25	M	7	D	D	F	E	A	F	A
8	27	M	9	D	C	F	F	A	F	F
9	26	M	8	D	C	F	F	A	A	A
10	25	F	7	D	C	E	F	A	A	A
11	25	F	7	D	B	F	G	A	A	A
12	29	M	11	C	E	F	F	A	F	A
13	29	M	11	A	F	E	E	B	F	E
14	25	M	7	A	E	F	F	A	A	A
15	31	M	13	C	C	F	F	A	F	F
16	22	M	3	C	C	E	F	A	B	A
17	29	M	11	D	E	E	F	A	F	F
18	26	M	8	C	D	F	F	A	A	A
19	24	M	7	B	D	F	F	A	F	F
20	24	M	0	C	C	F	F	A	F	F
21	51	M	32	B	E	F	E	A	F	A
22	60	M	42	A	F	A	B	A	A	A
23	26	M	8	D	D	F	F	B	B	A
24	30	M	10	D	C	D	F	A	F	F
25	39	M	21	C	C	F	F	B	F	F
26	56	F	37	B	D	F	F	A	A	A
27	62	F	44	B	D	E	E	A	A	A
28	28	M	10	D	C	F	F	A	B	A
29	24	M	4	D	D	E	F	A	B	A
30	25	M	7	C	D	E	E	A	B	A

Table (B.2) Results of the demographics Questionnaire



# C

## Supplementary Results

### C.1. Raw Data Plots

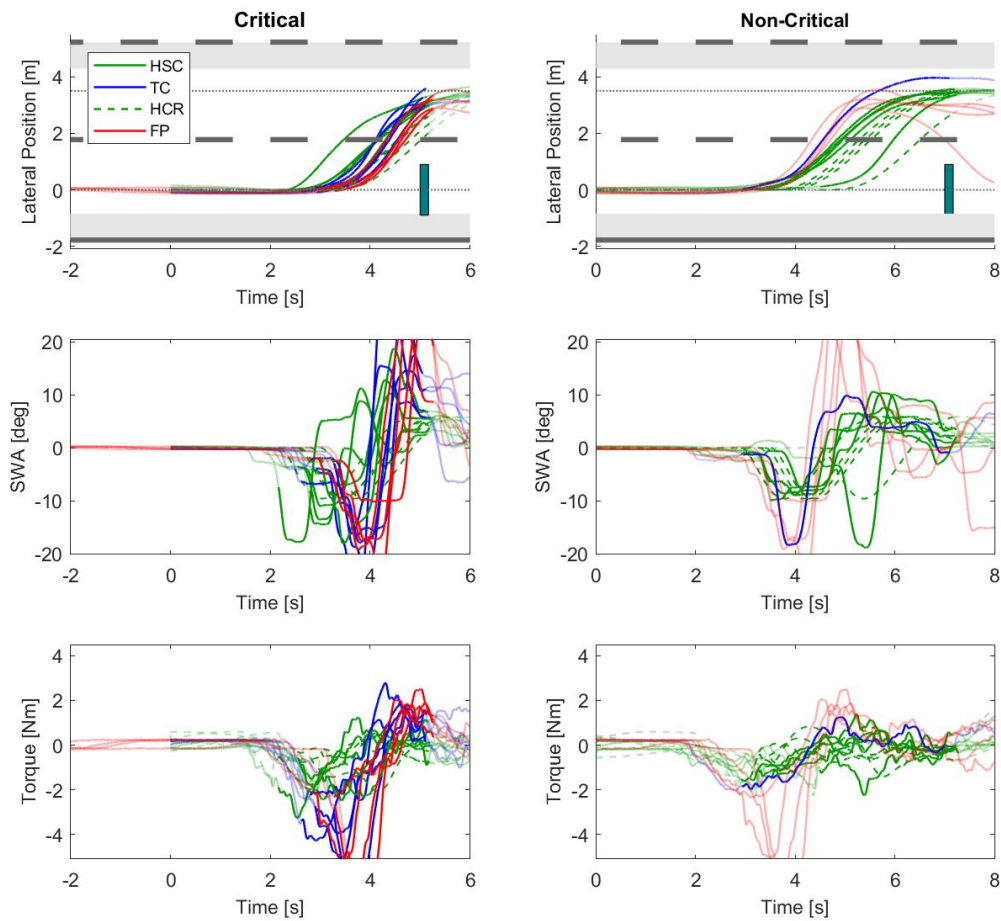


Figure (C.1) Raw data time traces of all critical (left) and non-critical (right) take-over maneuvers performed by one participant (Nr. 1) aligned at TOR. Top: lateral position, Middle: steering wheel angle, Bottom: Steering Torques. The highlighted area represents the analyzed period for the dependent variables from  $t_{start}$  to  $t_{end}$ . The falsely timed TOR during TC in (b) has been analyzed as a critical take-over maneuver, shown in (a). The time trace starts at the placement of the defect vehicle and shows no driver input until after the TOR. The vertical bar represents the defect vehicle with only its width to scale.

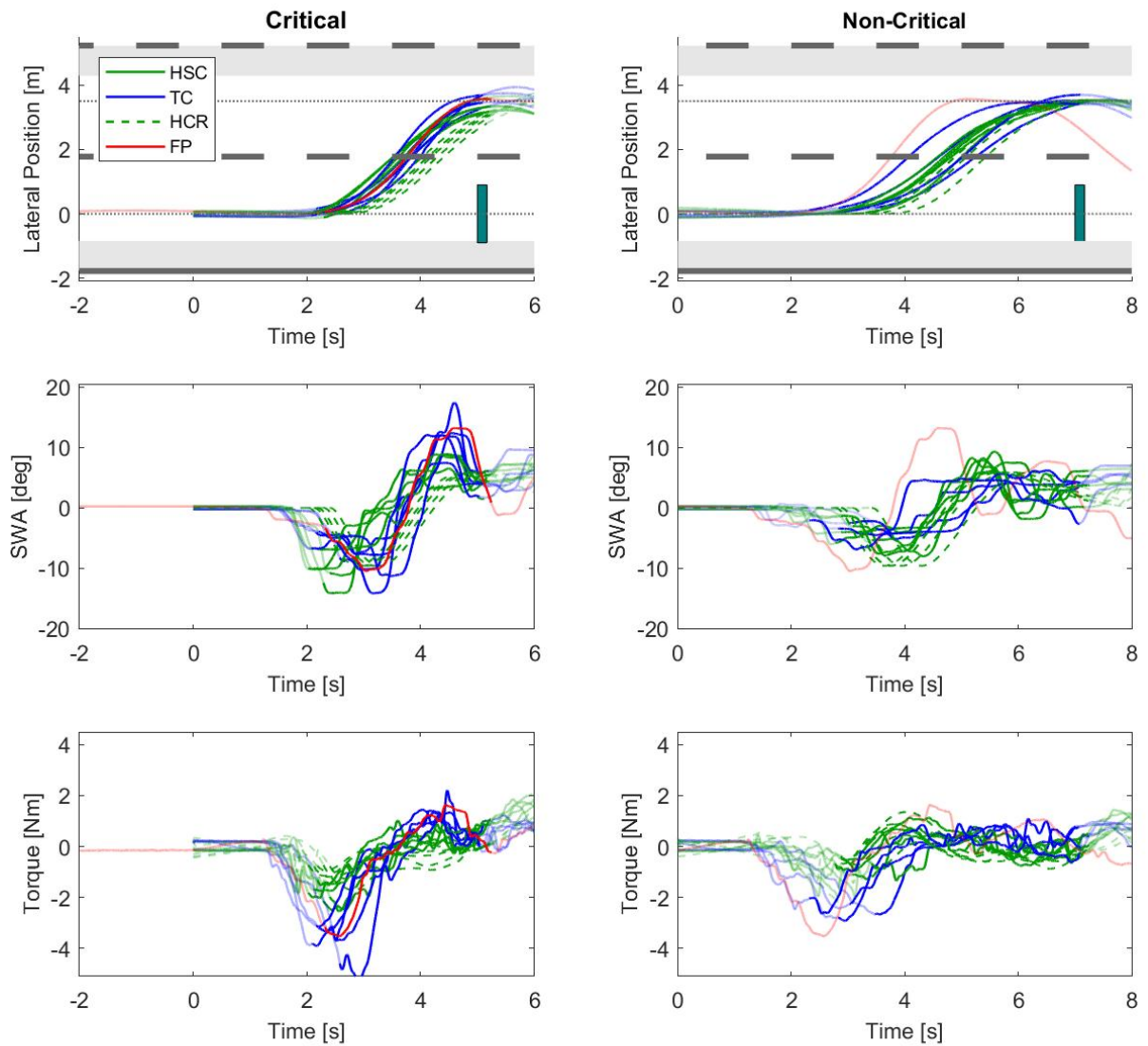


Figure (C.2) Raw data time traces of all critical (left) and non-critical (right) take-over maneuvers performed by one participant (Nr. 2) aligned at TOR. Top: lateral position, Middle: steering wheel angle, Bottom: Steering Torques. The highlighted area represents the analyzed period for the dependent variables from  $t_{start}$  to  $t_{end}$ . The falsely timed TOR during TC in (b) has been analyzed as a critical take-over maneuver, shown in (a). The time trace starts at the placement of the defect vehicle and shows no driver input until after the TOR. The vertical bar represents the defect vehicle with only its width to scale.

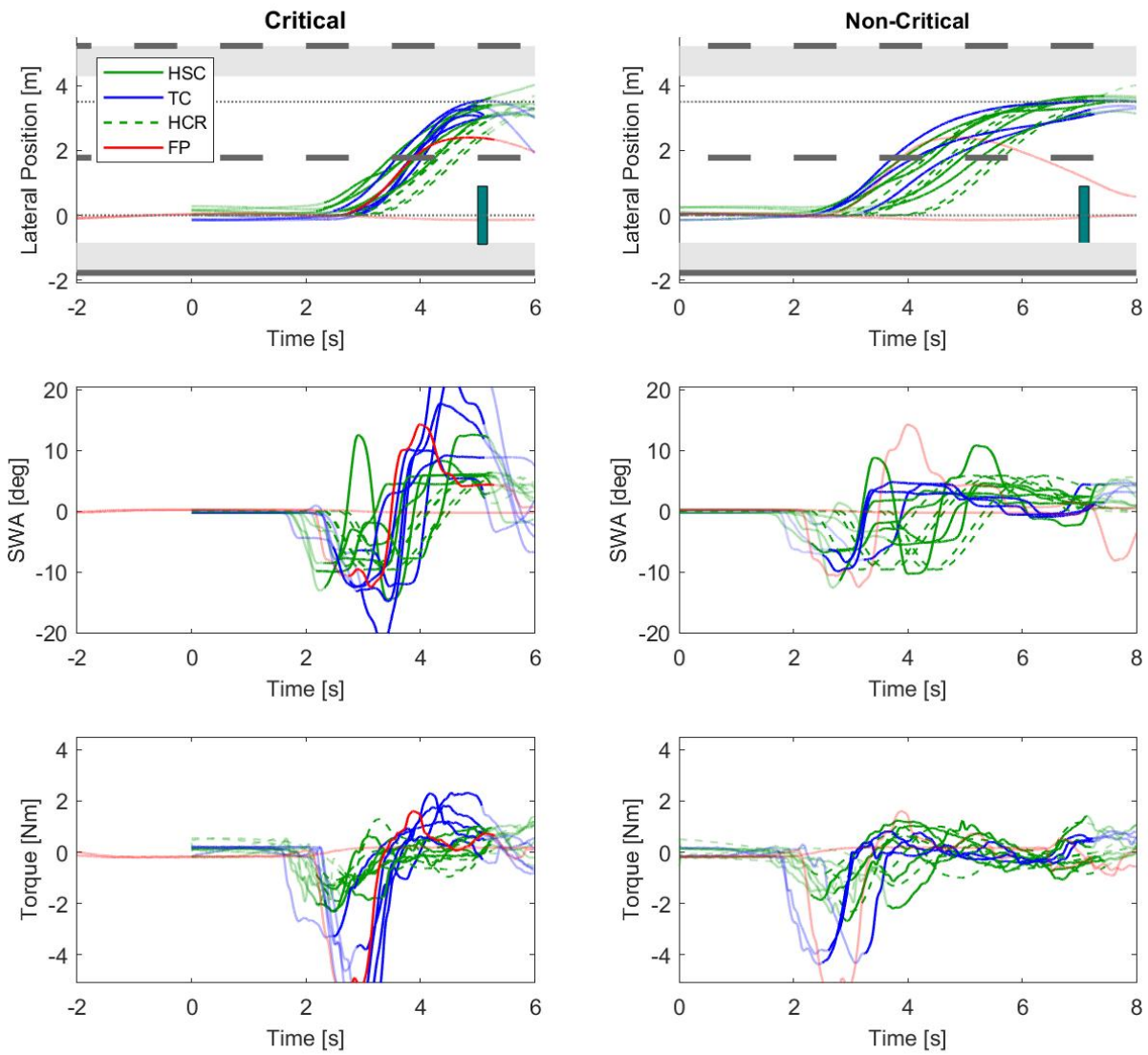


Figure (C.3) Raw data time traces of all critical (left) and non-critical (right) take-over maneuvers performed by one participant (Nr. 3) aligned at TOR. Top: lateral position, Middle: steering wheel angle, Bottom: Steering Torques. The highlighted area represents the analyzed period for the dependent variables from  $t_{start}$  to  $t_{end}$ . The falsely timed TOR during TC in (b) has been analyzed as a critical take-over maneuver, shown in (a). The time trace starts at the placement of the defect vehicle and shows no driver input until after the TOR. The vertical bar represents the defect vehicle with only its width to scale.

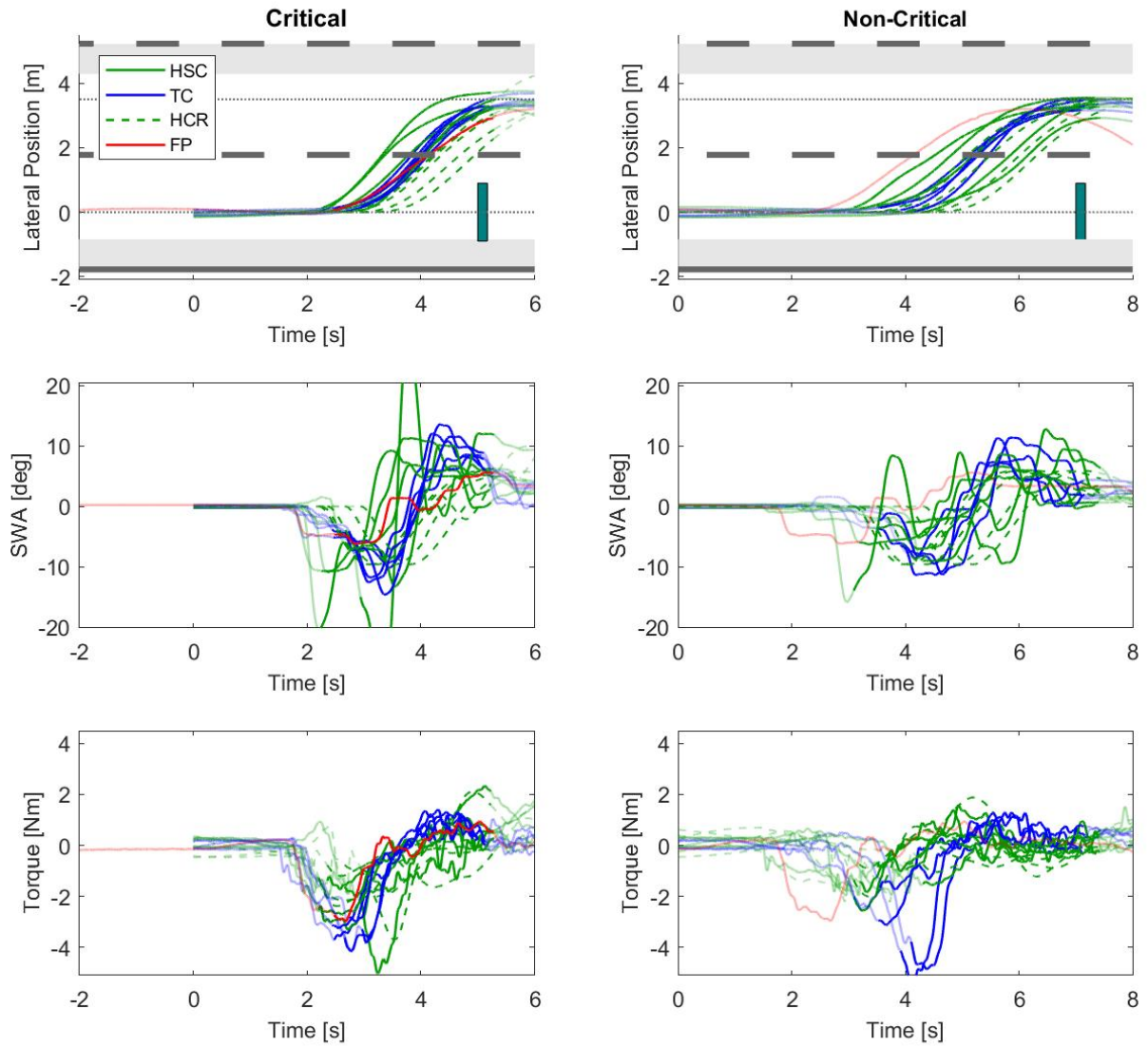


Figure (C.4) Raw data time traces of all critical (left) and non-critical (right) take-over maneuvers performed by one participant (Nr. 4) aligned at TOR. Top: lateral position, Middle: steering wheel angle, Bottom: Steering Torques. The highlighted area represents the analyzed period for the dependent variables from  $t_{start}$  to  $t_{end}$ . The falsely timed TOR during TC in (b) has been analyzed as a critical take-over maneuver, shown in (a). The time trace starts at the placement of the defect vehicle and shows no driver input until after the TOR. The vertical bar represents the defect vehicle with only its width to scale.

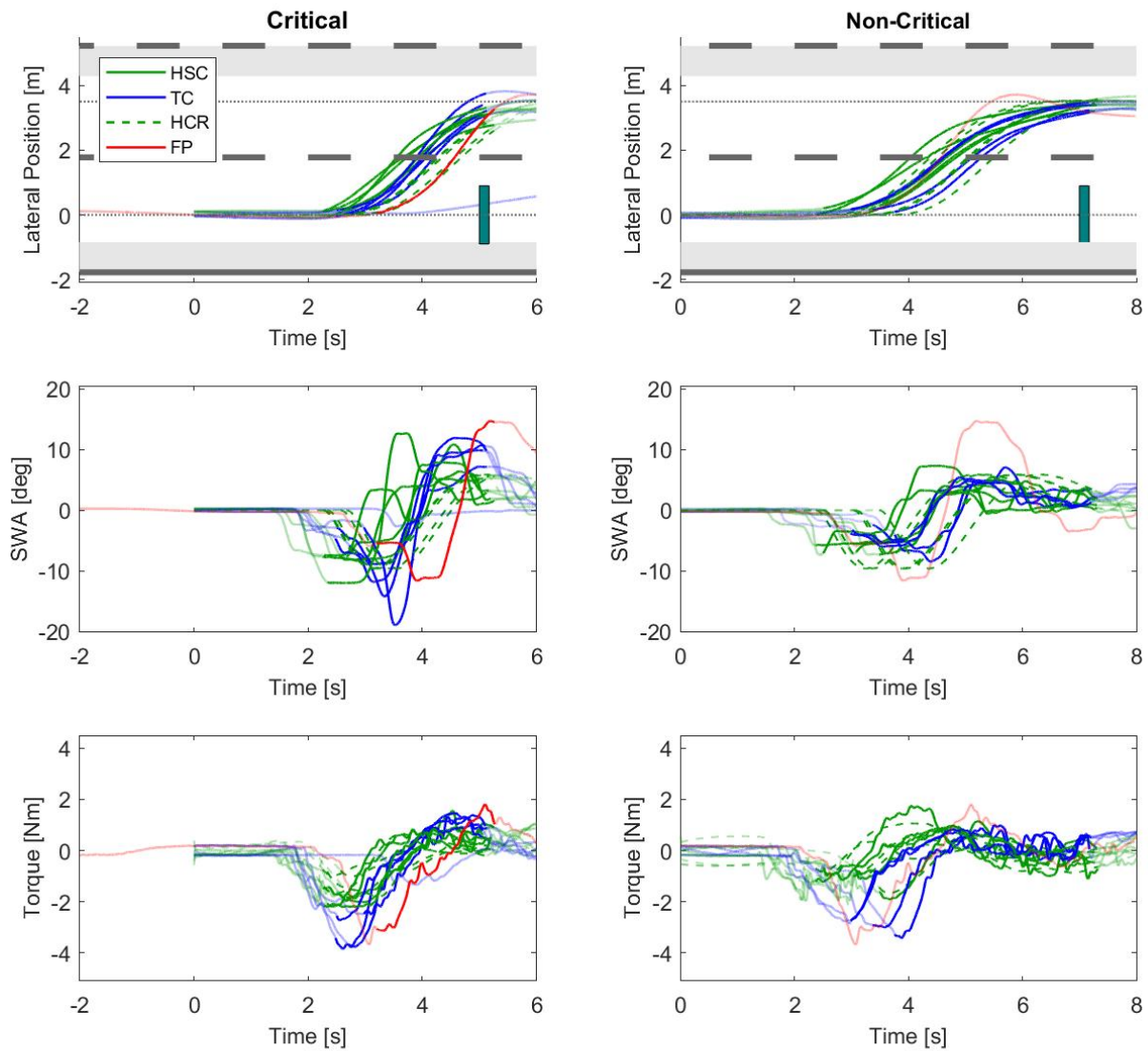


Figure (C.5) Raw data time traces of all critical (left) and non-critical (right) take-over maneuvers performed by one participant (Nr. 5) aligned at TOR. Top: lateral position, Middle: steering wheel angle, Bottom: Steering Torques. The highlighted area represents the analyzed period for the dependent variables from  $t_{start}$  to  $t_{end}$ . The falsely timed TOR during TC in (b) has been analyzed as a critical take-over maneuver, shown in (a). The time trace starts at the placement of the defect vehicle and shows no driver input until after the TOR. The vertical bar represents the defect vehicle with only its width to scale.

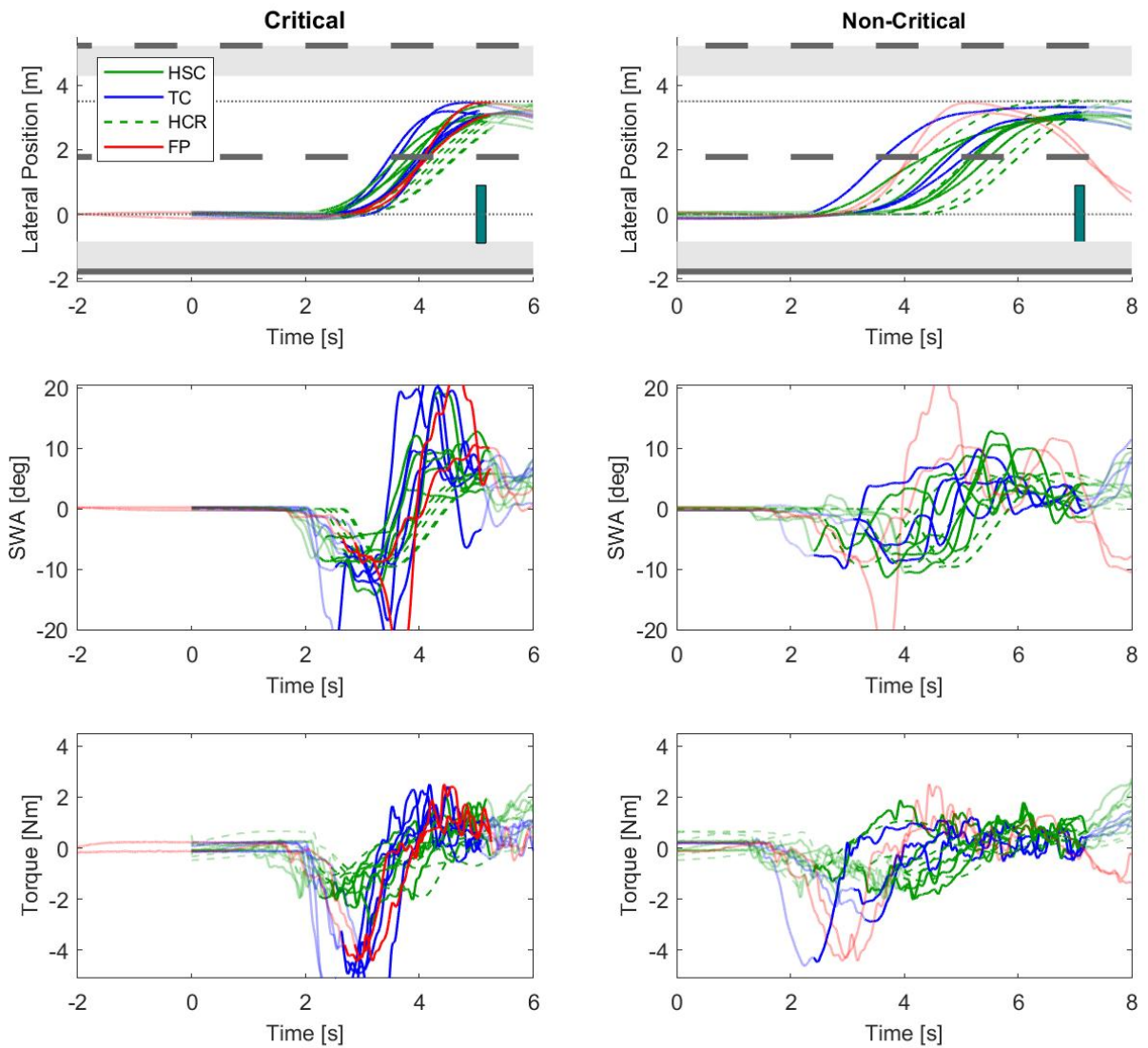


Figure (C.6) Raw data time traces of all critical (left) and non-critical (right) take-over maneuvers performed by one participant (Nr. 6) aligned at TOR. Top: lateral position, Middle: steering wheel angle, Bottom: Steering Torques. The highlighted area represents the analyzed period for the dependent variables from  $t_{start}$  to  $t_{end}$ . The falsely timed TOR during TC in (b) has been analyzed as a critical take-over maneuver, shown in (a). The time trace starts at the placement of the defect vehicle and shows no driver input until after the TOR. The vertical bar represents the defect vehicle with only its width to scale.

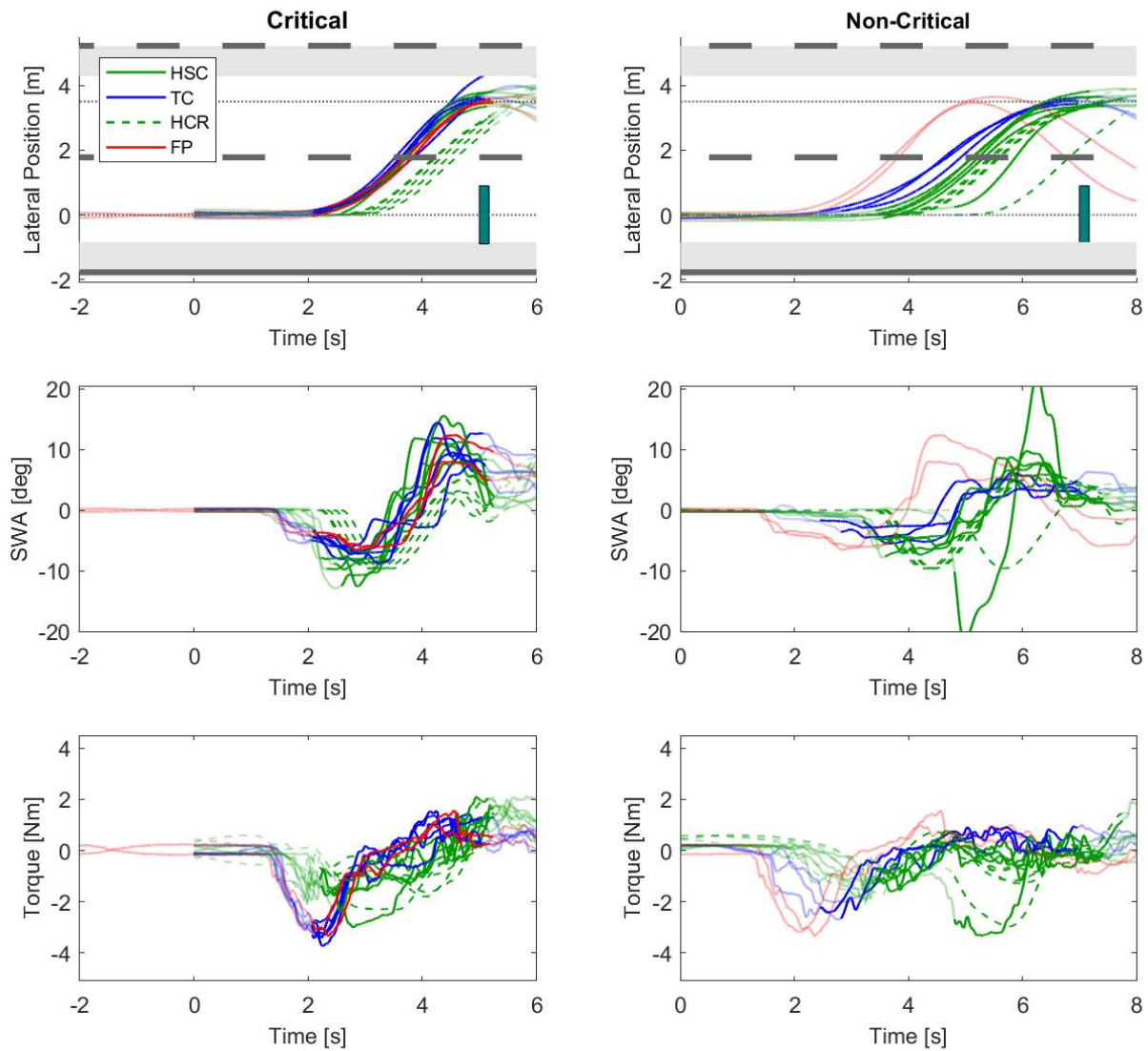


Figure (C.7) Raw data time traces of all critical (left) and non-critical (right) take-over maneuvers performed by one participant (Nr. 7) aligned at TOR. Top: lateral position, Middle: steering wheel angle, Bottom: Steering Torques. The highlighted area represents the analyzed period for the dependent variables from  $t_{start}$  to  $t_{end}$ . The falsely timed TOR during TC in (b) has been analyzed as a critical take-over maneuver, shown in (a). The time trace starts at the placement of the defect vehicle and shows no driver input until after the TOR. The vertical bar represents the defect vehicle with only its width to scale.

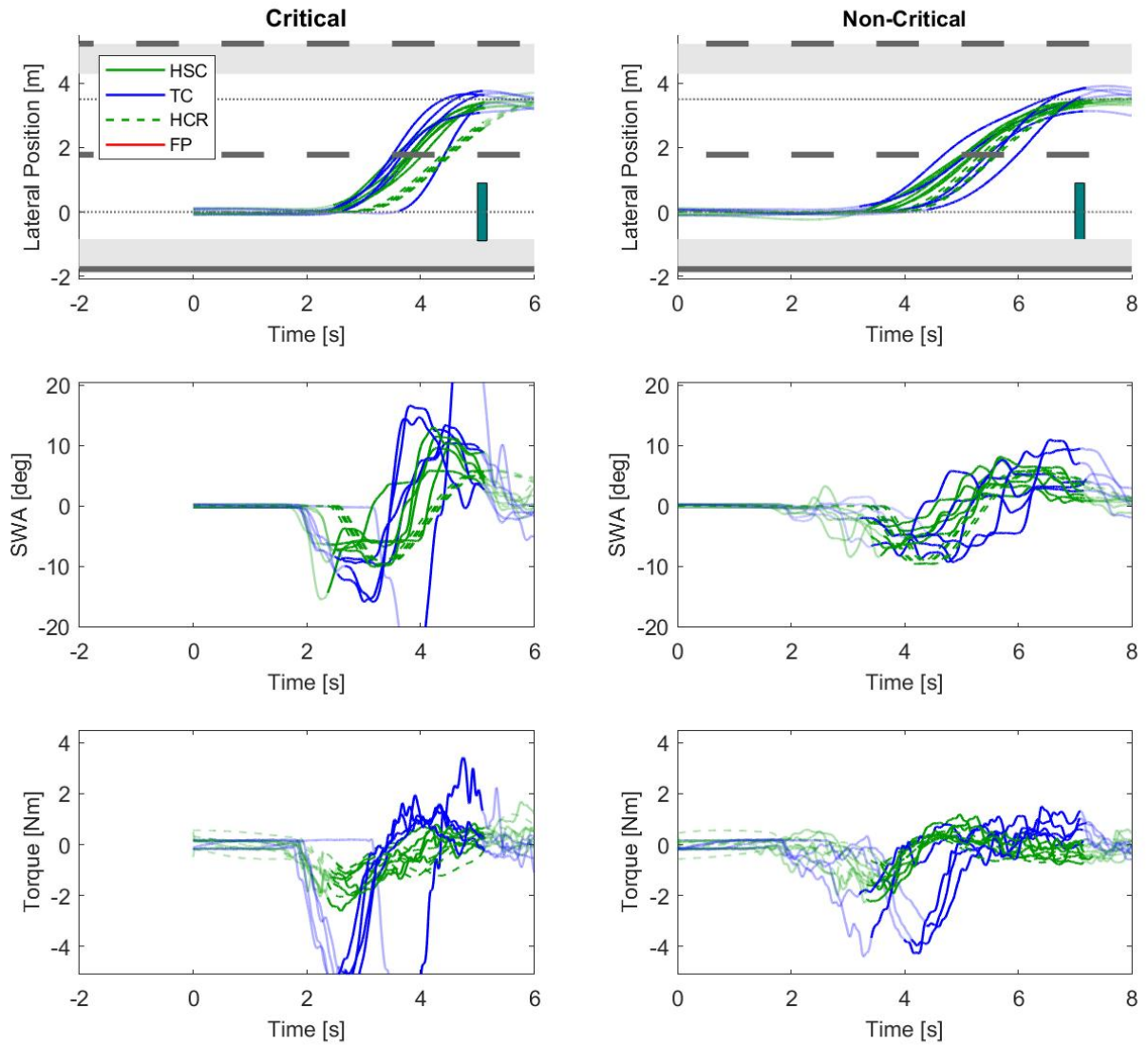


Figure (C.8) Raw data time traces of all critical (left) and non-critical (right) take-over maneuvers performed by one participant (Nr. 8) aligned at TOR. Top: lateral position, Middle: steering wheel angle, Bottom: Steering Torques. The highlighted area represents the analyzed period for the dependent variables from  $t_{start}$  to  $t_{end}$ . The falsely timed TOR during TC in (b) has been analyzed as a critical take-over maneuver, shown in (a). The time trace starts at the placement of the defect vehicle and shows no driver input until after the TOR. The vertical bar represents the defect vehicle with only its width to scale.

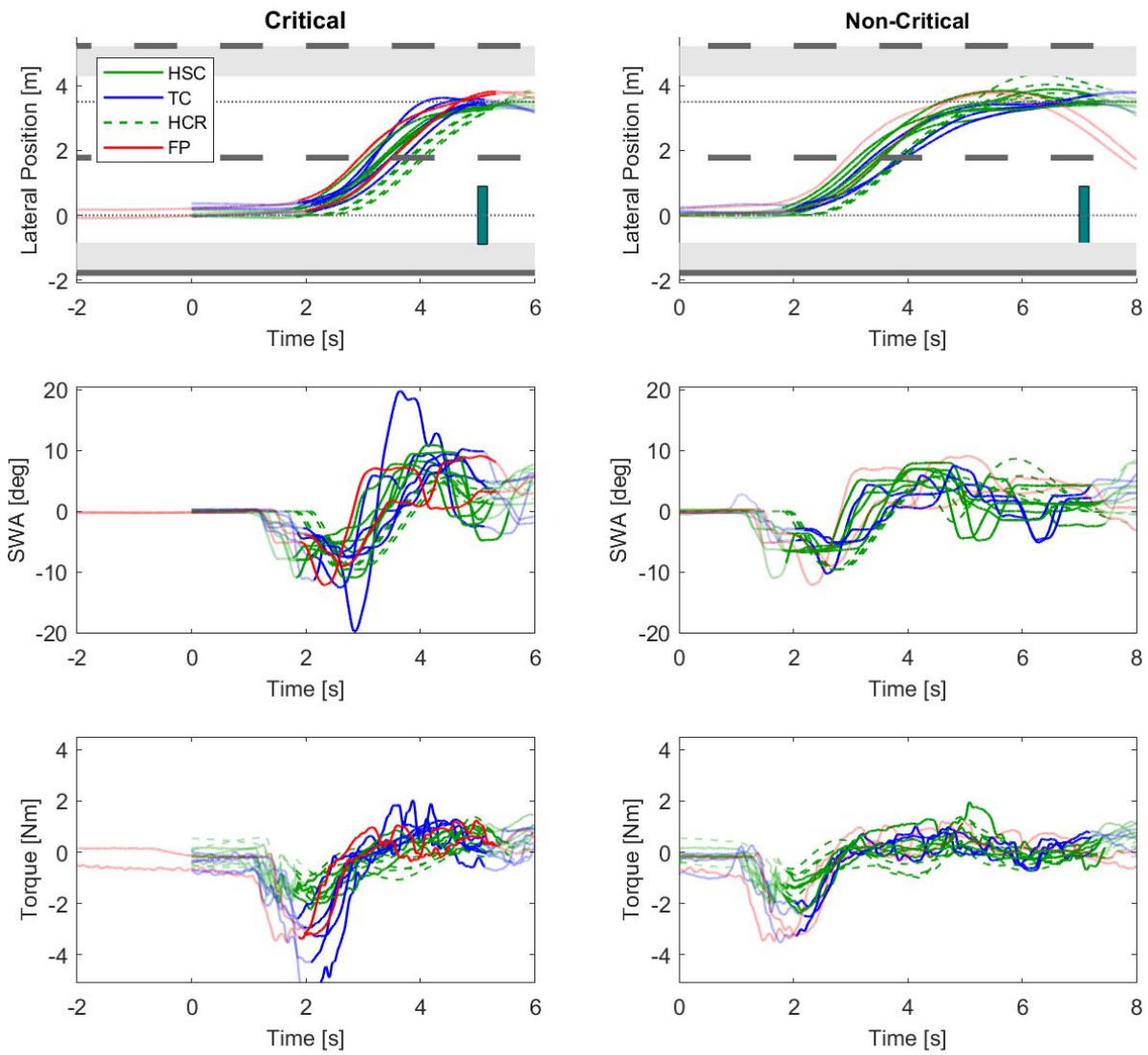


Figure (C.9) Raw data time traces of all critical (left) and non-critical (right) take-over maneuvers performed by one participant (Nr. 9) aligned at TOR. Top: lateral position, Middle: steering wheel angle, Bottom: Steering Torques. The highlighted area represents the analyzed period for the dependent variables from  $t_{start}$  to  $t_{end}$ . The falsely timed TOR during TC in (b) has been analyzed as a critical take-over maneuver, shown in (a). The time trace starts at the placement of the defect vehicle and shows no driver input until after the TOR. The vertical bar represents the defect vehicle with only its width to scale.

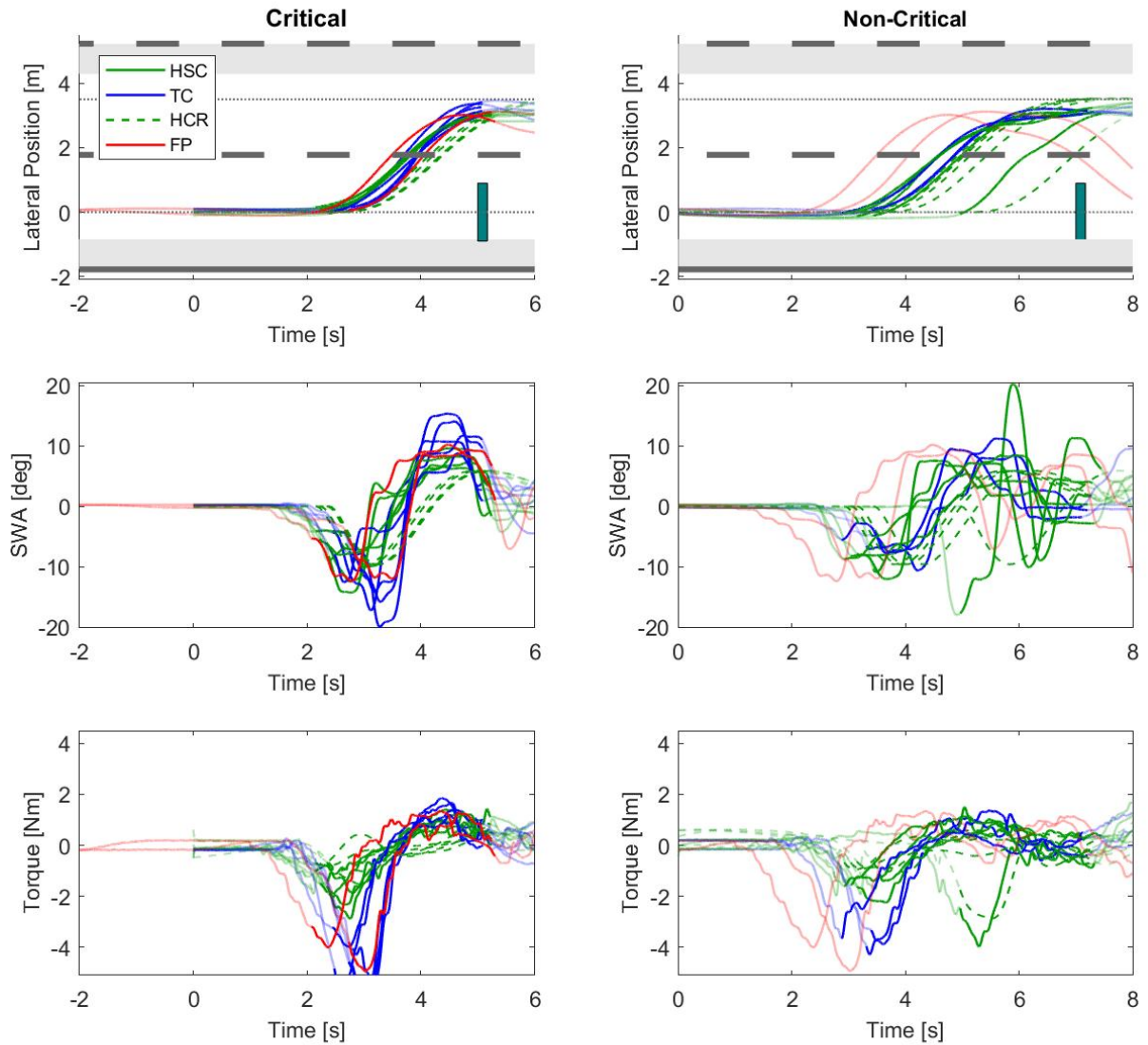


Figure (C.10) Raw data time traces of all critical (left) and non-critical (right) take-over maneuvers performed by one participant (Nr. 10) aligned at TOR. Top: lateral position, Middle: steering wheel angle, Bottom: Steering Torques. The highlighted area represents the analyzed period for the dependent variables from  $t_{start}$  to  $t_{end}$ . The falsely timed TOR during TC in (b) has been analyzed as a critical take-over maneuver, shown in (a). The time trace starts at the placement of the defect vehicle and shows no driver input until after the TOR. The vertical bar represents the defect vehicle with only its width to scale.

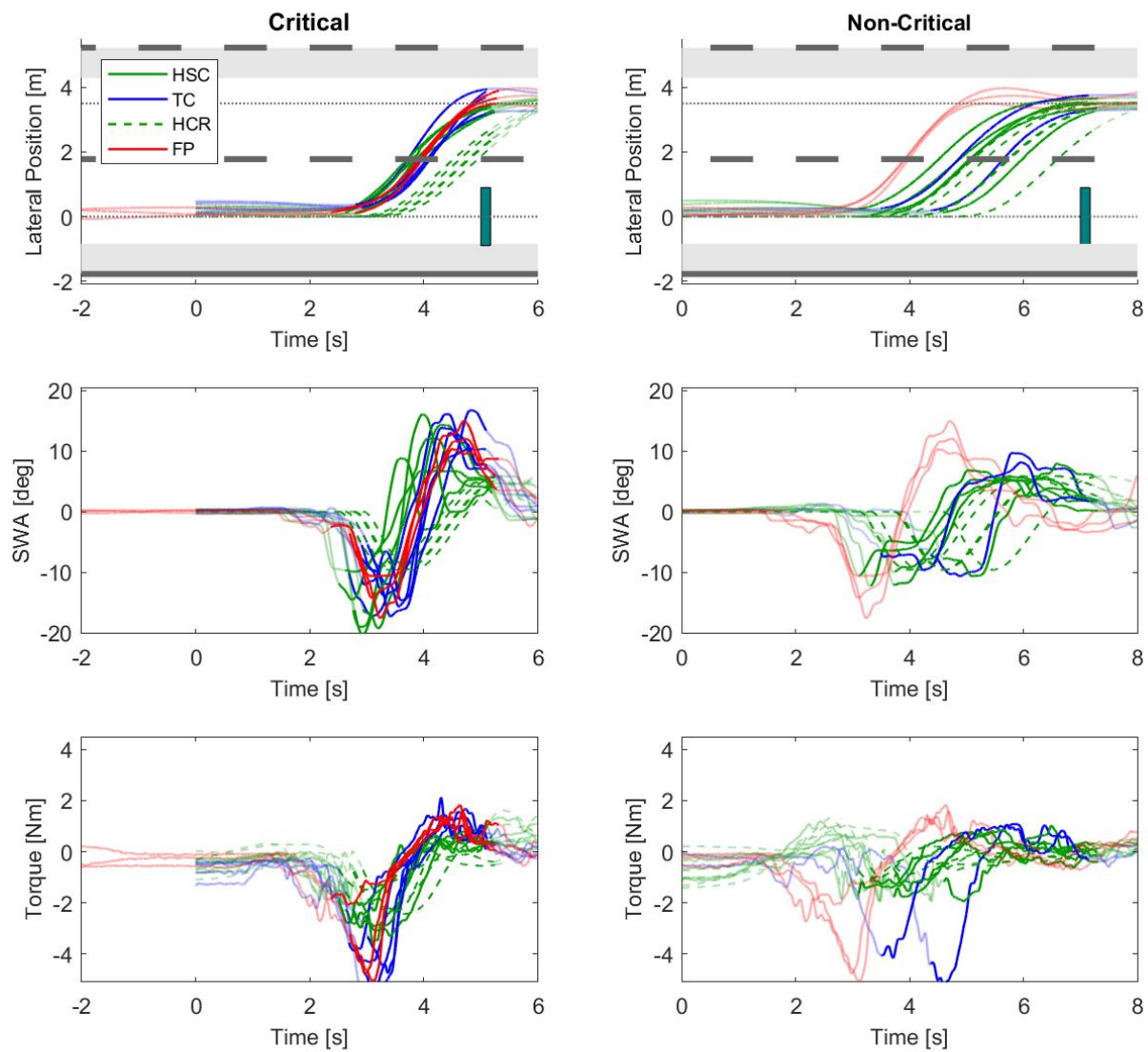


Figure (C.11) Raw data time traces of all critical (left) and non-critical (right) take-over maneuvers performed by one participant (Nr. 11) aligned at TOR. Top: lateral position, Middle: steering wheel angle, Bottom: Steering Torques. The highlighted area represents the analyzed period for the dependent variables from  $t_{start}$  to  $t_{end}$ . The falsely timed TOR during TC in (b) has been analyzed as a critical take-over maneuver, shown in (a). The time trace starts at the placement of the defect vehicle and shows no driver input until after the TOR. The vertical bar represents the defect vehicle with only its width to scale.

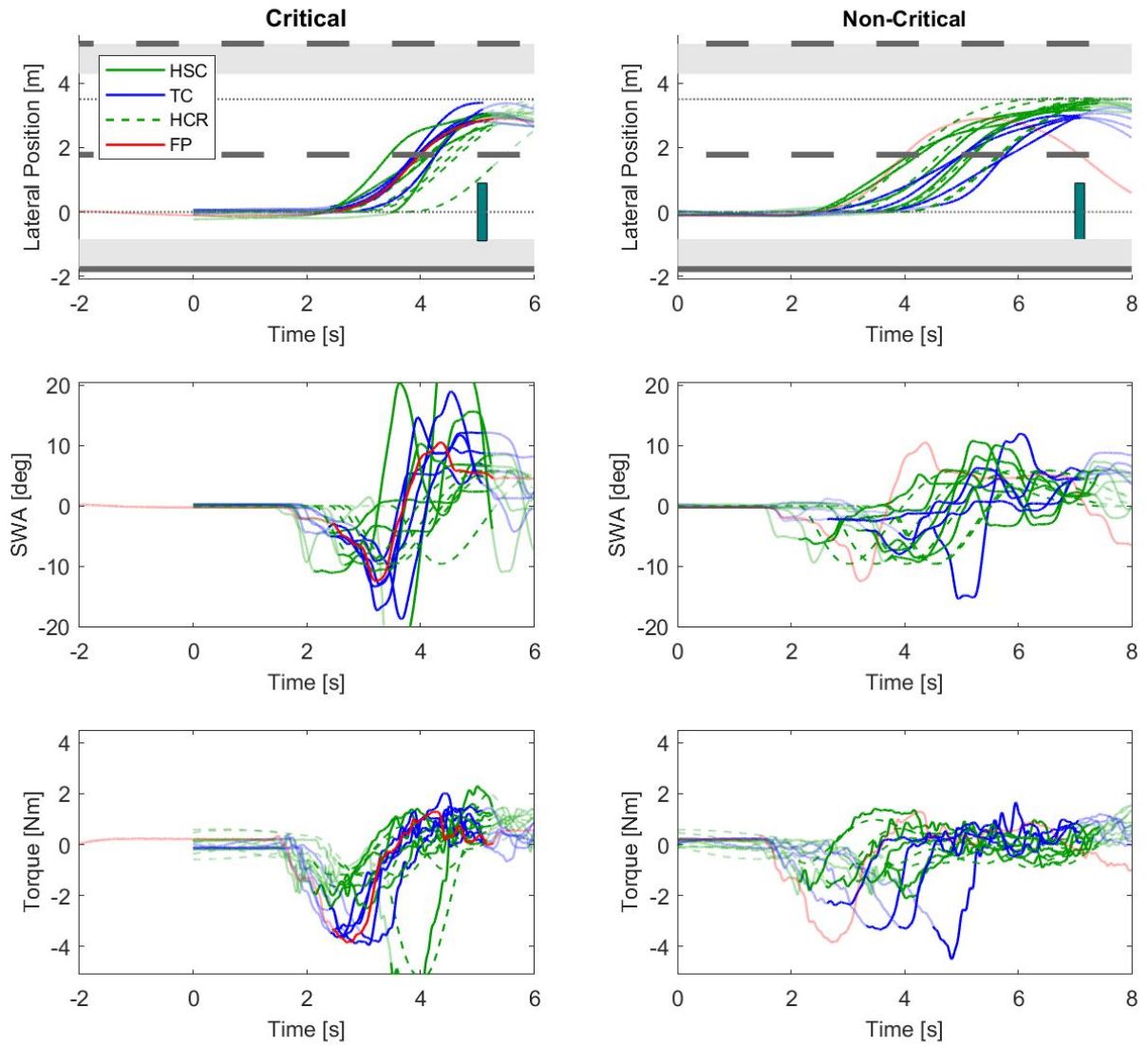


Figure (C.12) Raw data time traces of all critical (left) and non-critical (right) take-over maneuvers performed by one participant (Nr. 12) aligned at TOR. Top: lateral position, Middle: steering wheel angle, Bottom: Steering Torques. The highlighted area represents the analyzed period for the dependent variables from  $t_{start}$  to  $t_{end}$ . The falsely timed TOR during TC in (b) has been analyzed as a critical take-over maneuver, shown in (a). The time trace starts at the placement of the defect vehicle and shows no driver input until after the TOR. The vertical bar represents the defect vehicle with only its width to scale.

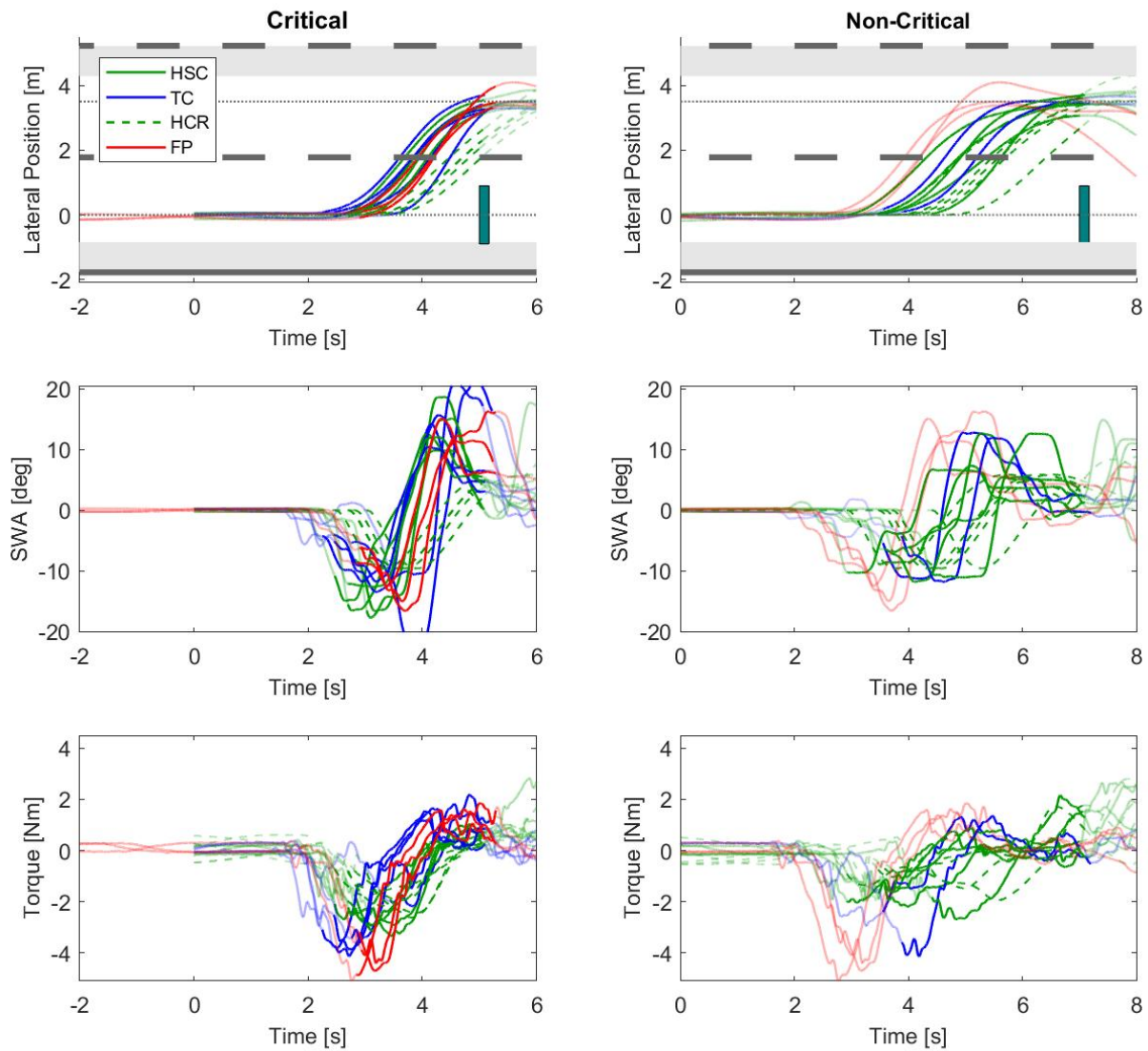


Figure (C.13) Raw data time traces of all critical (left) and non-critical (right) take-over maneuvers performed by one participant (Nr. 13) aligned at TOR. Top: lateral position, Middle: steering wheel angle, Bottom: Steering Torques. The highlighted area represents the analyzed period for the dependent variables from  $t_{start}$  to  $t_{end}$ . The falsely timed TOR during TC in (b) has been analyzed as a critical take-over maneuver, shown in (a). The time trace starts at the placement of the defect vehicle and shows no driver input until after the TOR. The vertical bar represents the defect vehicle with only its width to scale.

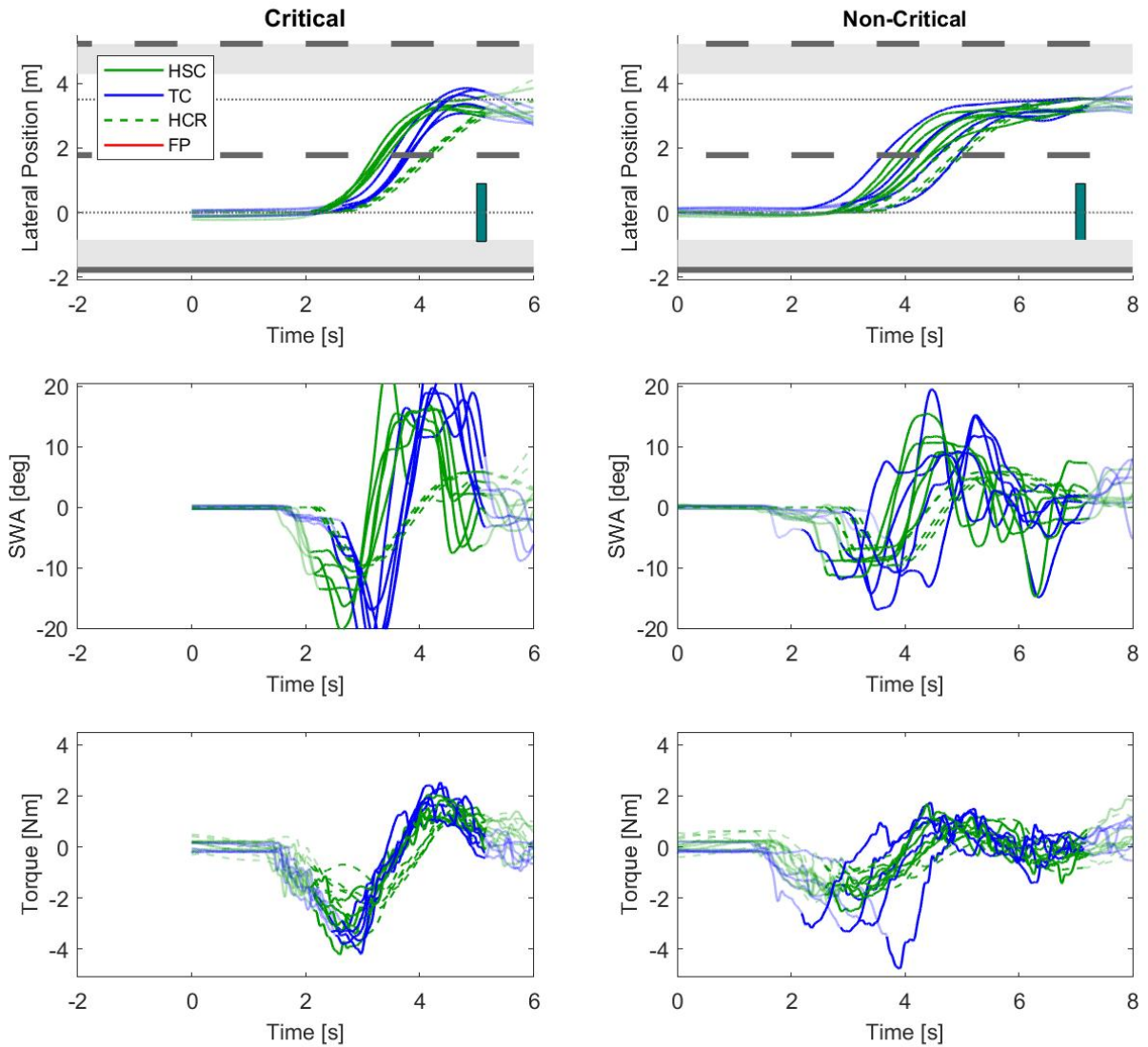


Figure (C.14) Raw data time traces of all critical (left) and non-critical (right) take-over maneuvers performed by one participant (Nr. 14) aligned at TOR. Top: lateral position, Middle: steering wheel angle, Bottom: Steering Torques. The highlighted area represents the analyzed period for the dependent variables from  $t_{start}$  to  $t_{end}$ . The falsely timed TOR during TC in (b) has been analyzed as a critical take-over maneuver, shown in (a). The time trace starts at the placement of the defect vehicle and shows no driver input until after the TOR. The vertical bar represents the defect vehicle with only its width to scale.

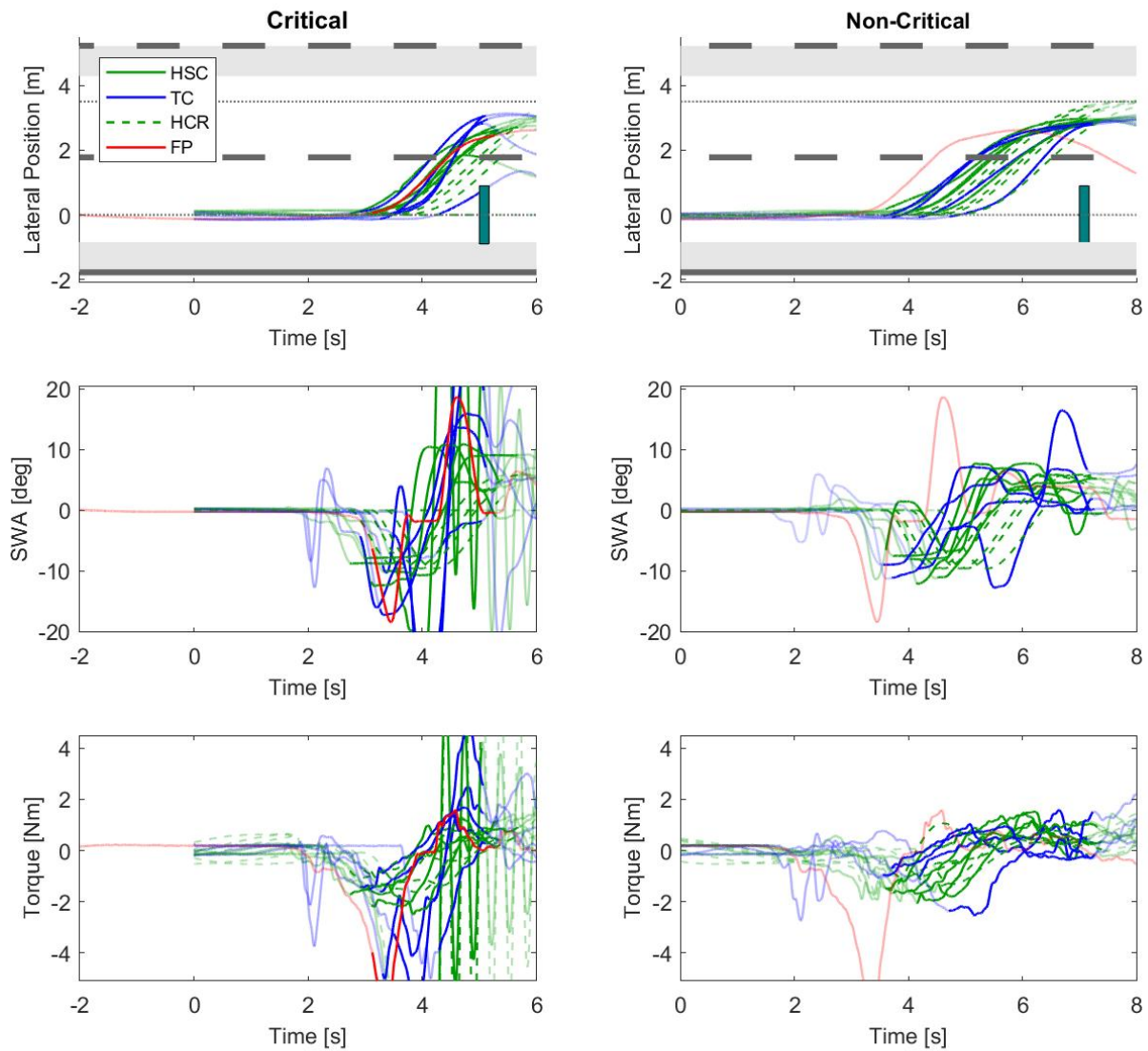


Figure (C.15) Raw data time traces of all critical (left) and non-critical (right) take-over maneuvers performed by one participant (Nr. 15) aligned at TOR. Top: lateral position, Middle: steering wheel angle, Bottom: Steering Torques. The highlighted area represents the analyzed period for the dependent variables from  $t_{start}$  to  $t_{end}$ . The falsely timed TOR during TC in (b) has been analyzed as a critical take-over maneuver, shown in (a). The time trace starts at the placement of the defect vehicle and shows no driver input until after the TOR. The vertical bar represents the defect vehicle with only its width to scale.

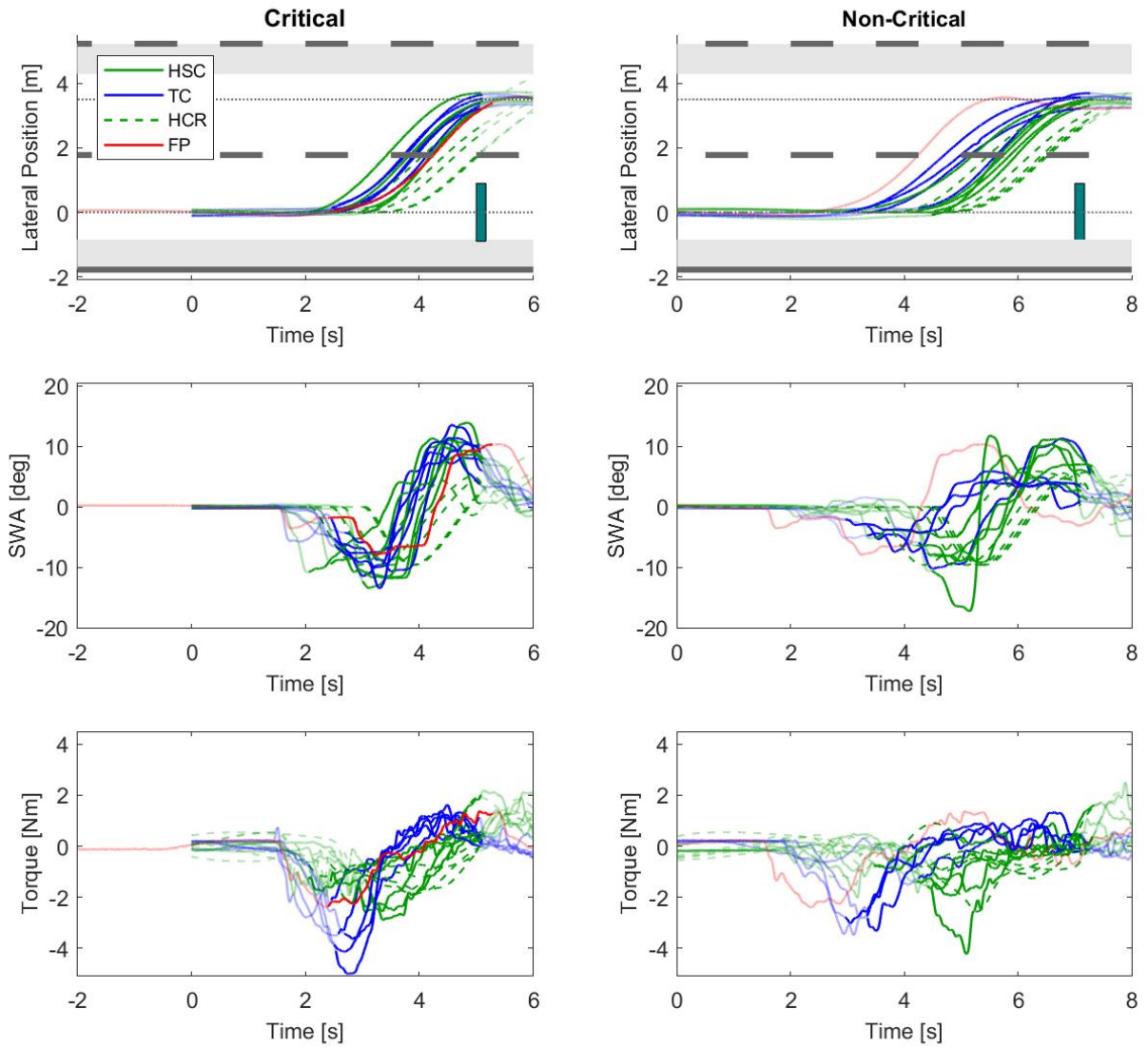


Figure (C.16) Raw data time traces of all critical (left) and non-critical (right) take-over maneuvers performed by one participant (Nr. 16) aligned at TOR. Top: lateral position, Middle: steering wheel angle, Bottom: Steering Torques. The highlighted area represents the analyzed period for the dependent variables from  $t_{start}$  to  $t_{end}$ . The falsely timed TOR during TC in (b) has been analyzed as a critical take-over maneuver, shown in (a). The time trace starts at the placement of the defect vehicle and shows no driver input until after the TOR. The vertical bar represents the defect vehicle with only its width to scale.

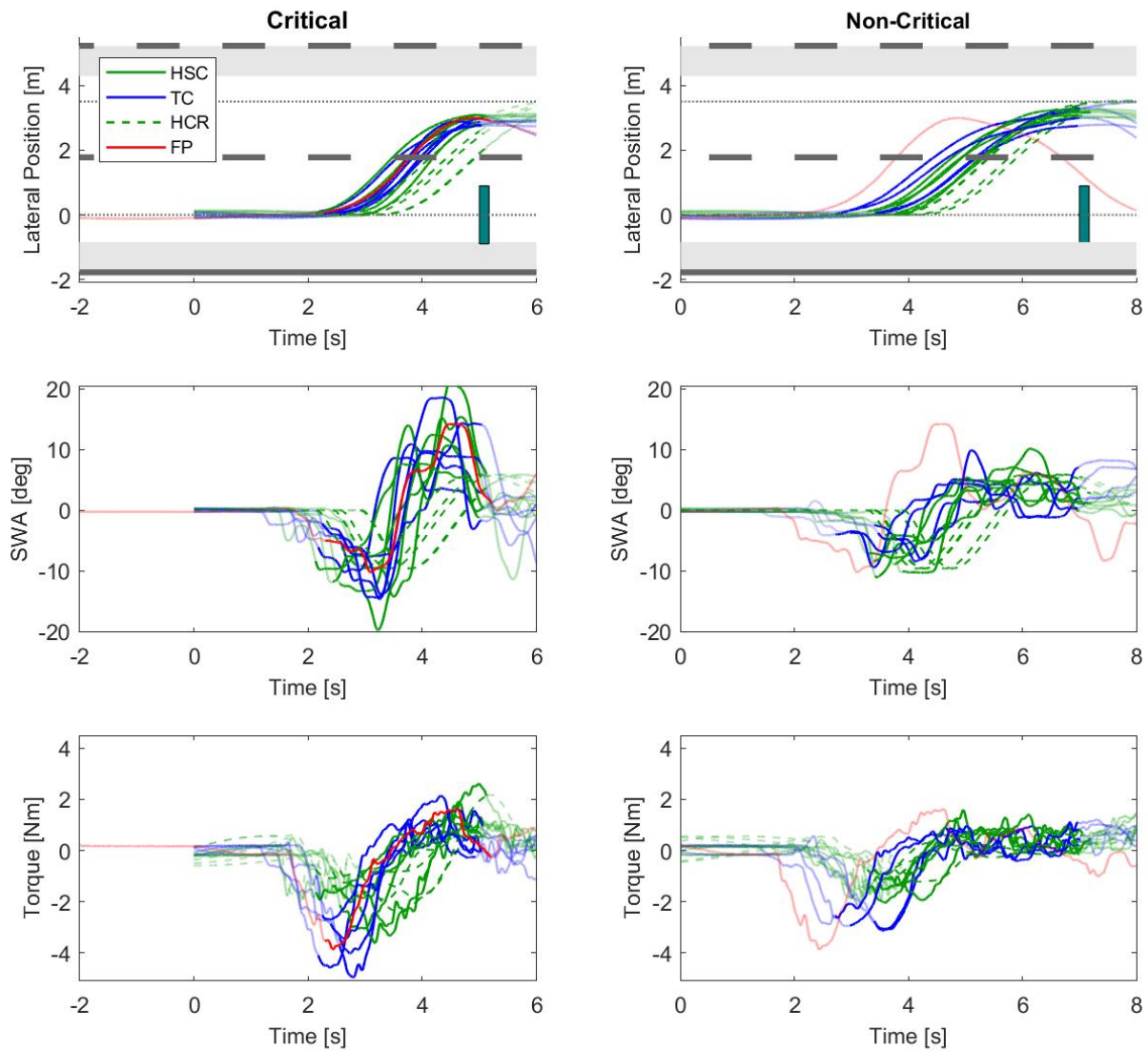


Figure (C.17) Raw data time traces of all critical (left) and non-critical (right) take-over maneuvers performed by one participant (Nr. 17) aligned at TOR. Top: lateral position, Middle: steering wheel angle, Bottom: Steering Torques. The highlighted area represents the analyzed period for the dependent variables from  $t_{start}$  to  $t_{end}$ . The falsely timed TOR during TC in (b) has been analyzed as a critical take-over maneuver, shown in (a). The time trace starts at the placement of the defect vehicle and shows no driver input until after the TOR. The vertical bar represents the defect vehicle with only its width to scale.

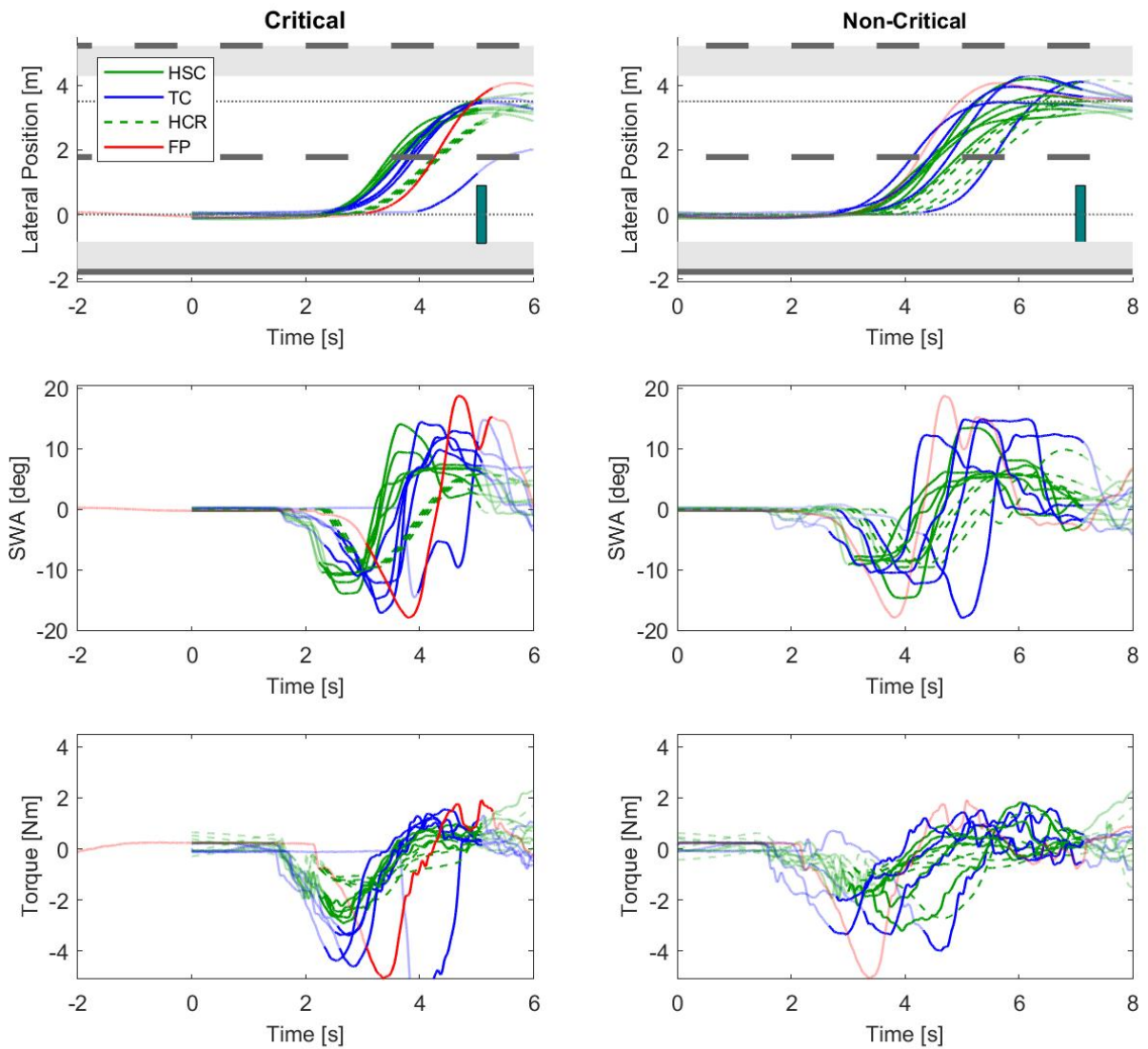


Figure (C.18) Raw data time traces of all critical (left) and non-critical (right) take-over maneuvers performed by one participant (Nr. 18) aligned at TOR. Top: lateral position, Middle: steering wheel angle, Bottom: Steering Torques. The highlighted area represents the analyzed period for the dependent variables from  $t_{start}$  to  $t_{end}$ . The falsely timed TOR during TC in (b) has been analyzed as a critical take-over maneuver, shown in (a). The time trace starts at the placement of the defect vehicle and shows no driver input until after the TOR. The vertical bar represents the defect vehicle with only its width to scale.

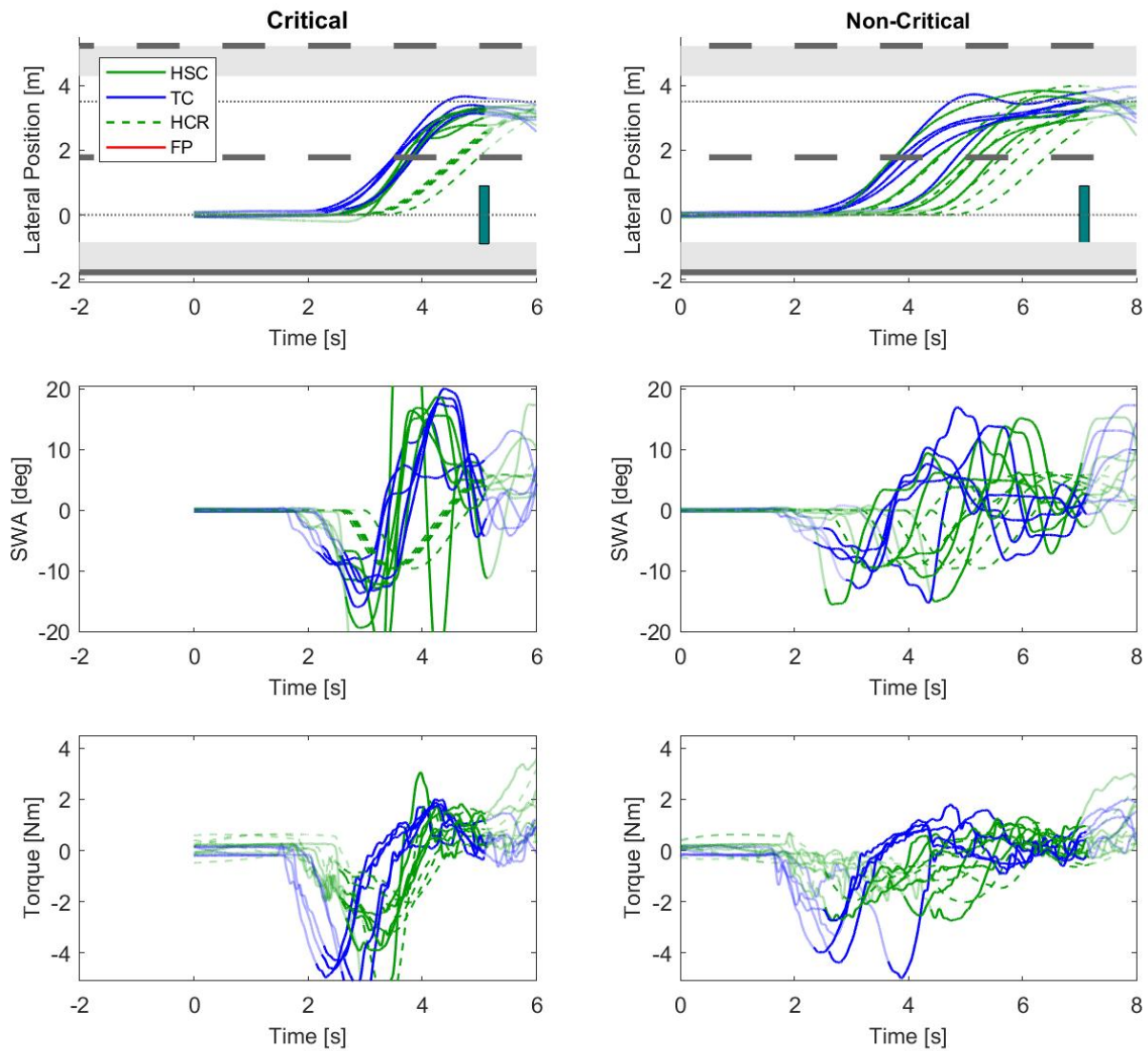


Figure (C.19) Raw data time traces of all critical (left) and non-critical (right) take-over maneuvers performed by one participant (Nr. 19) aligned at TOR. Top: lateral position, Middle: steering wheel angle, Bottom: Steering Torques. The highlighted area represents the analyzed period for the dependent variables from  $t_{start}$  to  $t_{end}$ . The falsely timed TOR during TC in (b) has been analyzed as a critical take-over maneuver, shown in (a). The time trace starts at the placement of the defect vehicle and shows no driver input until after the TOR. The vertical bar represents the defect vehicle with only its width to scale.

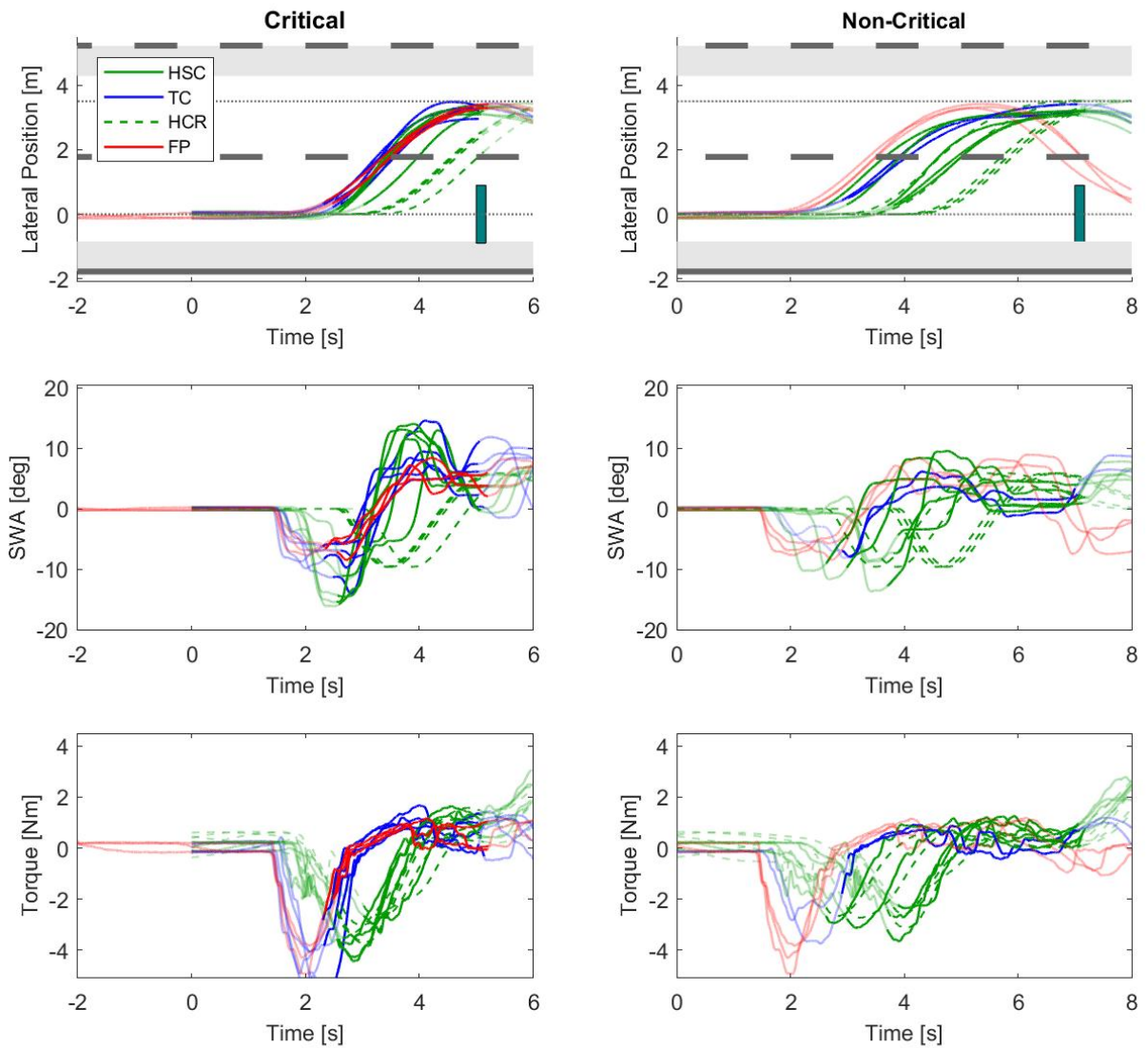


Figure (C.20) Raw data time traces of all critical (left) and non-critical (right) take-over maneuvers performed by one participant (Nr. 20) aligned at TOR. Top: lateral position, Middle: steering wheel angle, Bottom: Steering Torques. The highlighted area represents the analyzed period for the dependent variables from  $t_{start}$  to  $t_{end}$ . The falsely timed TOR during TC in (b) has been analyzed as a critical take-over maneuver, shown in (a). The time trace starts at the placement of the defect vehicle and shows no driver input until after the TOR. The vertical bar represents the defect vehicle with only its width to scale.

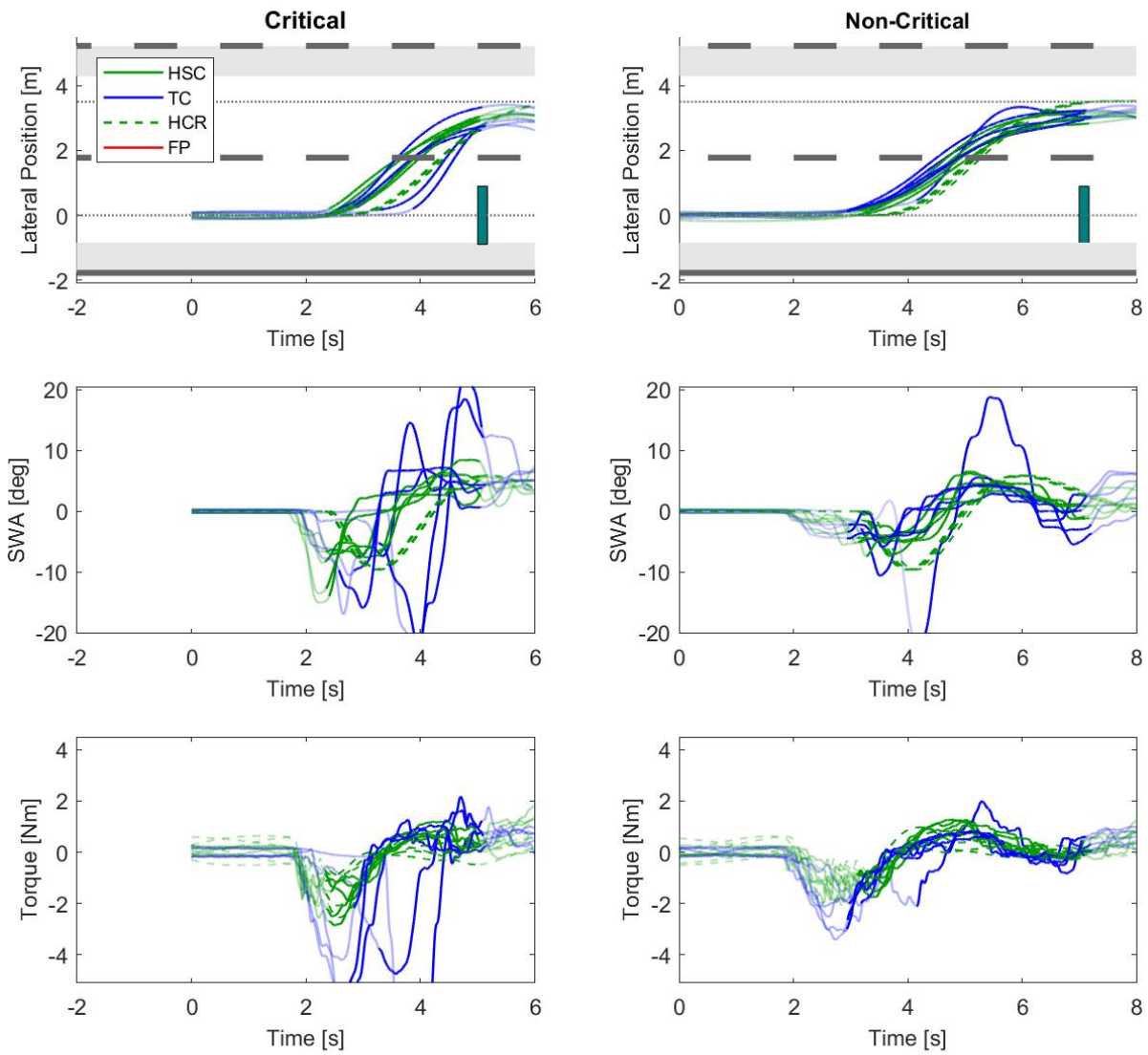


Figure (C.21) Raw data time traces of all critical (left) and non-critical (right) take-over maneuvers performed by one participant (Nr. 21) aligned at TOR. Top: lateral position, Middle: steering wheel angle, Bottom: Steering Torques. The highlighted area represents the analyzed period for the dependent variables from  $t_{start}$  to  $t_{end}$ . The falsely timed TOR during TC in (b) has been analyzed as a critical take-over maneuver, shown in (a). The time trace starts at the placement of the defect vehicle and shows no driver input until after the TOR. The vertical bar represents the defect vehicle with only its width to scale.

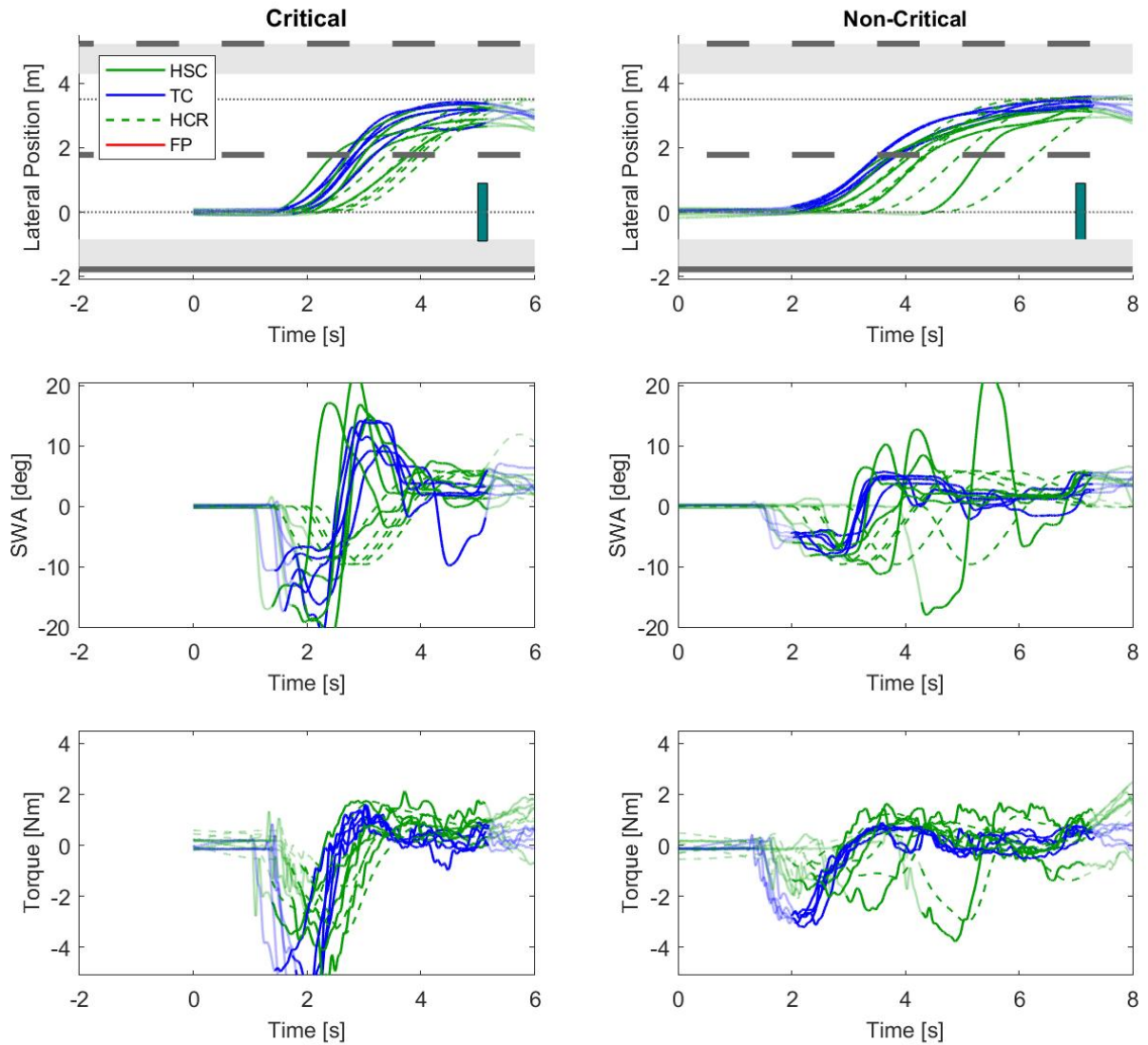


Figure (C.22) Raw data time traces of all critical (left) and non-critical (right) take-over maneuvers performed by one participant (Nr. 22) aligned at TOR. Top: lateral position, Middle: steering wheel angle, Bottom: Steering Torques. The highlighted area represents the analyzed period for the dependent variables from  $t_{start}$  to  $t_{end}$ . The falsely timed TOR during TC in (b) has been analyzed as a critical take-over maneuver, shown in (a). The time trace starts at the placement of the defect vehicle and shows no driver input until after the TOR. The vertical bar represents the defect vehicle with only its width to scale.

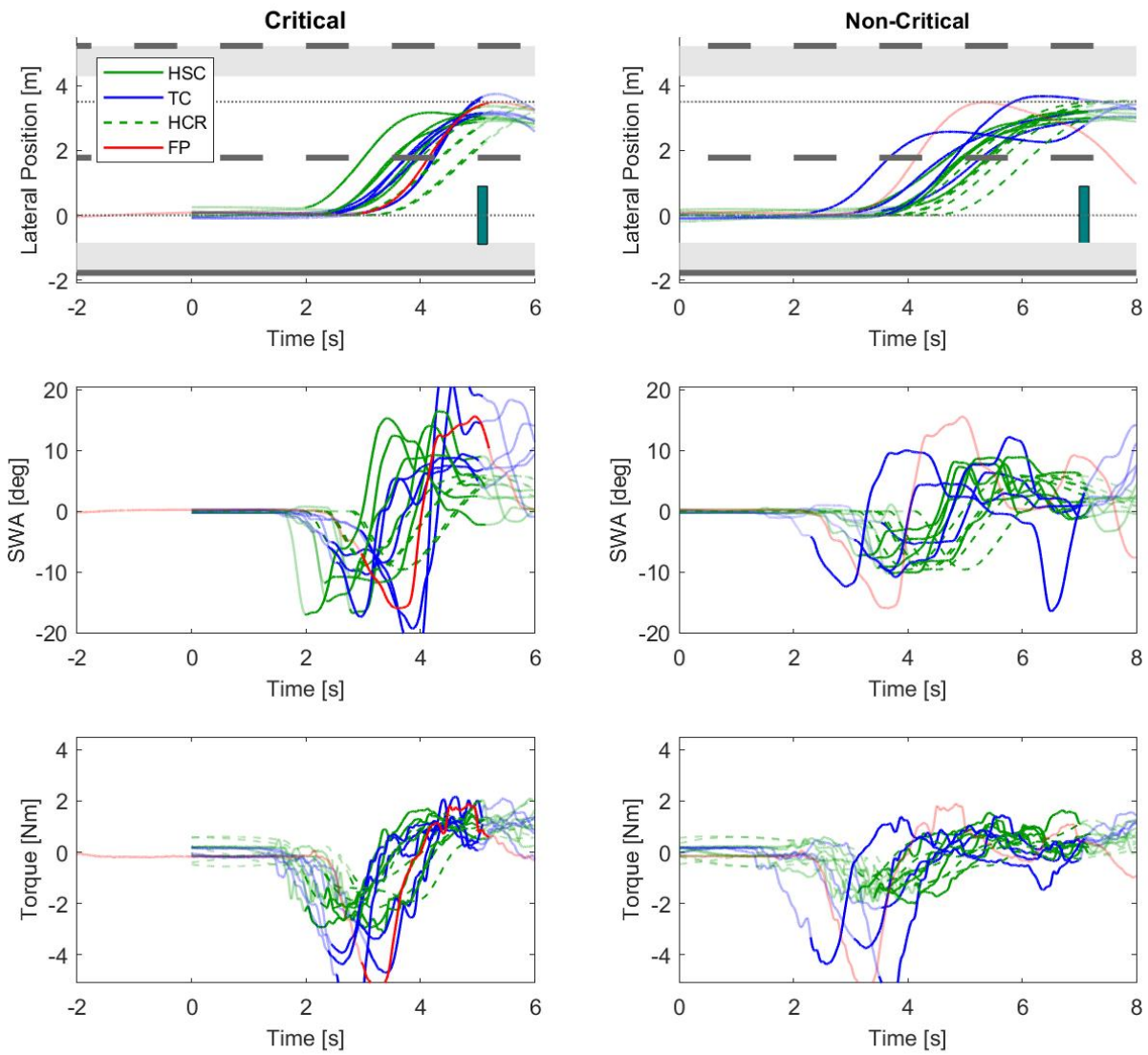


Figure (C.23) Raw data time traces of all critical (left) and non-critical (right) take-over maneuvers performed by one participant (Nr. 23) aligned at TOR. Top: lateral position, Middle: steering wheel angle, Bottom: Steering Torques. The highlighted area represents the analyzed period for the dependent variables from  $t_{start}$  to  $t_{end}$ . The falsely timed TOR during TC in (b) has been analyzed as a critical take-over maneuver, shown in (a). The time trace starts at the placement of the defect vehicle and shows no driver input until after the TOR. The vertical bar represents the defect vehicle with only its width to scale.

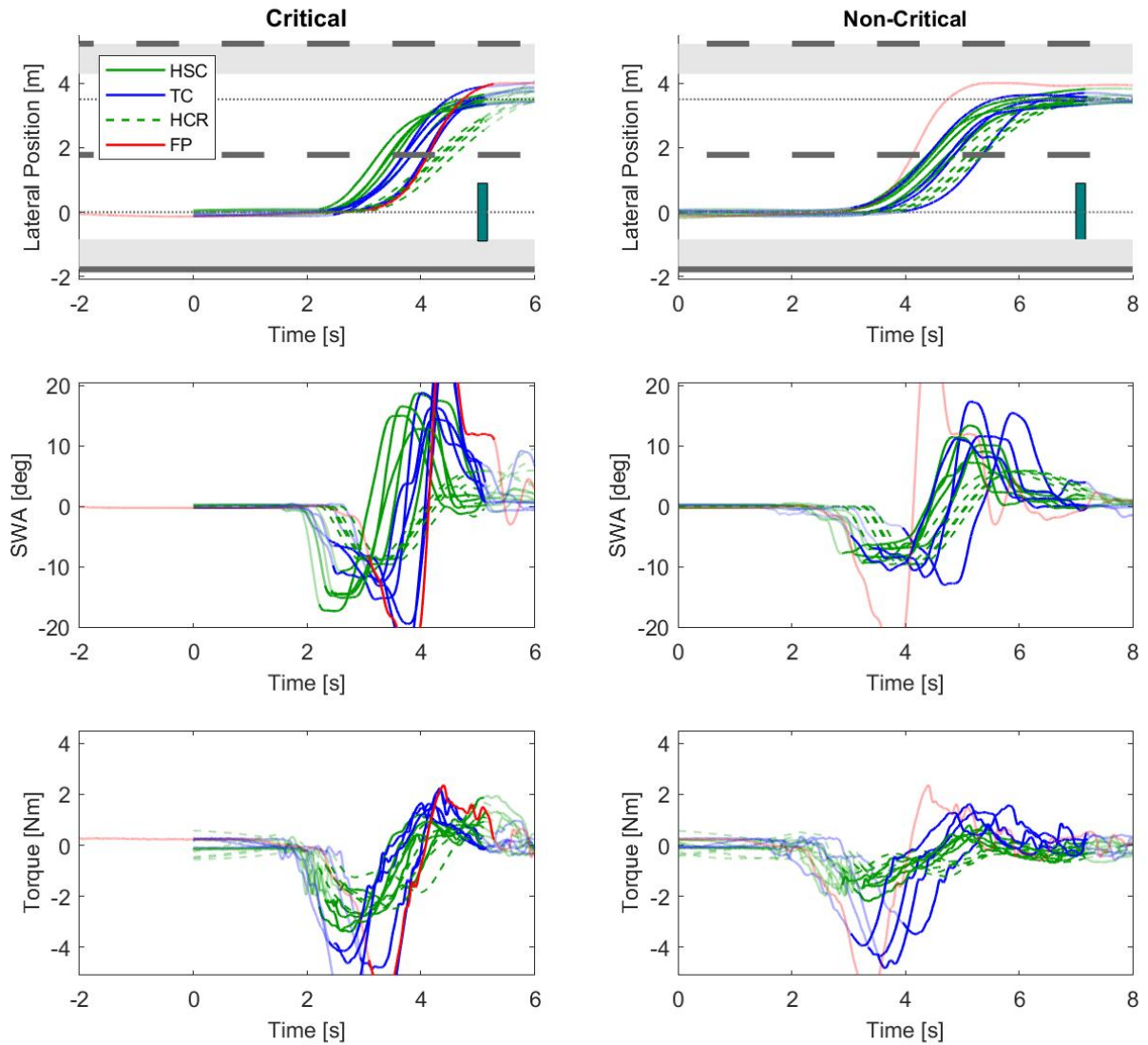


Figure (C.24) Raw data time traces of all critical (left) and non-critical (right) take-over maneuvers performed by one participant (Nr. 24) aligned at TOR. Top: lateral position, Middle: steering wheel angle, Bottom: Steering Torques. The highlighted area represents the analyzed period for the dependent variables from  $t_{start}$  to  $t_{end}$ . The falsely timed TOR during TC in (b) has been analyzed as a critical take-over maneuver, shown in (a). The time trace starts at the placement of the defect vehicle and shows no driver input until after the TOR. The vertical bar represents the defect vehicle with only its width to scale.

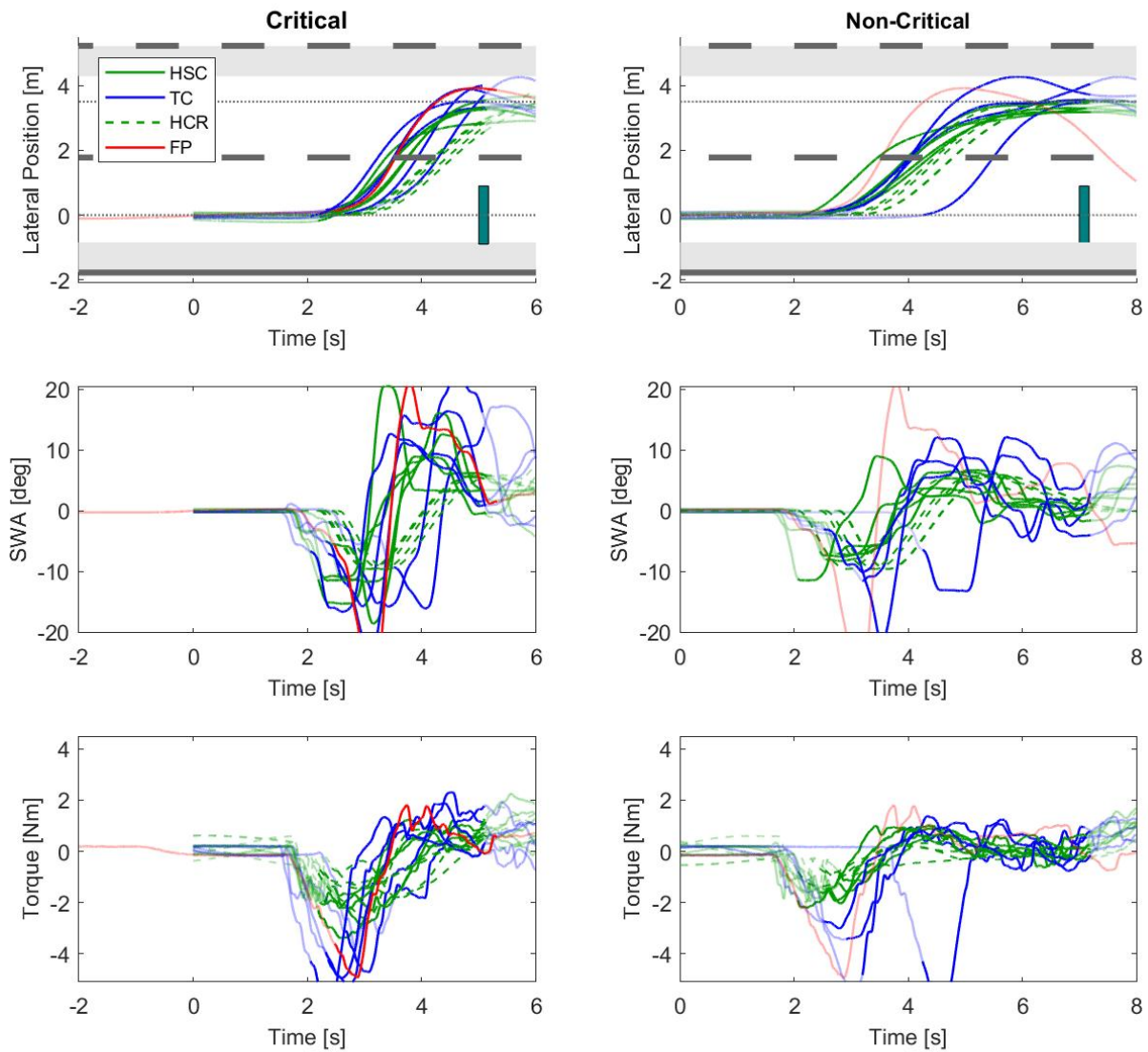


Figure (C.25) Raw data time traces of all critical (left) and non-critical (right) take-over maneuvers performed by one participant (Nr. 25) aligned at TOR. Top: lateral position, Middle: steering wheel angle, Bottom: Steering Torques. The highlighted area represents the analyzed period for the dependent variables from  $t_{start}$  to  $t_{end}$ . The falsely timed TOR during TC in (b) has been analyzed as a critical take-over maneuver, shown in (a). The time trace starts at the placement of the defect vehicle and shows no driver input until after the TOR. The vertical bar represents the defect vehicle with only its width to scale.

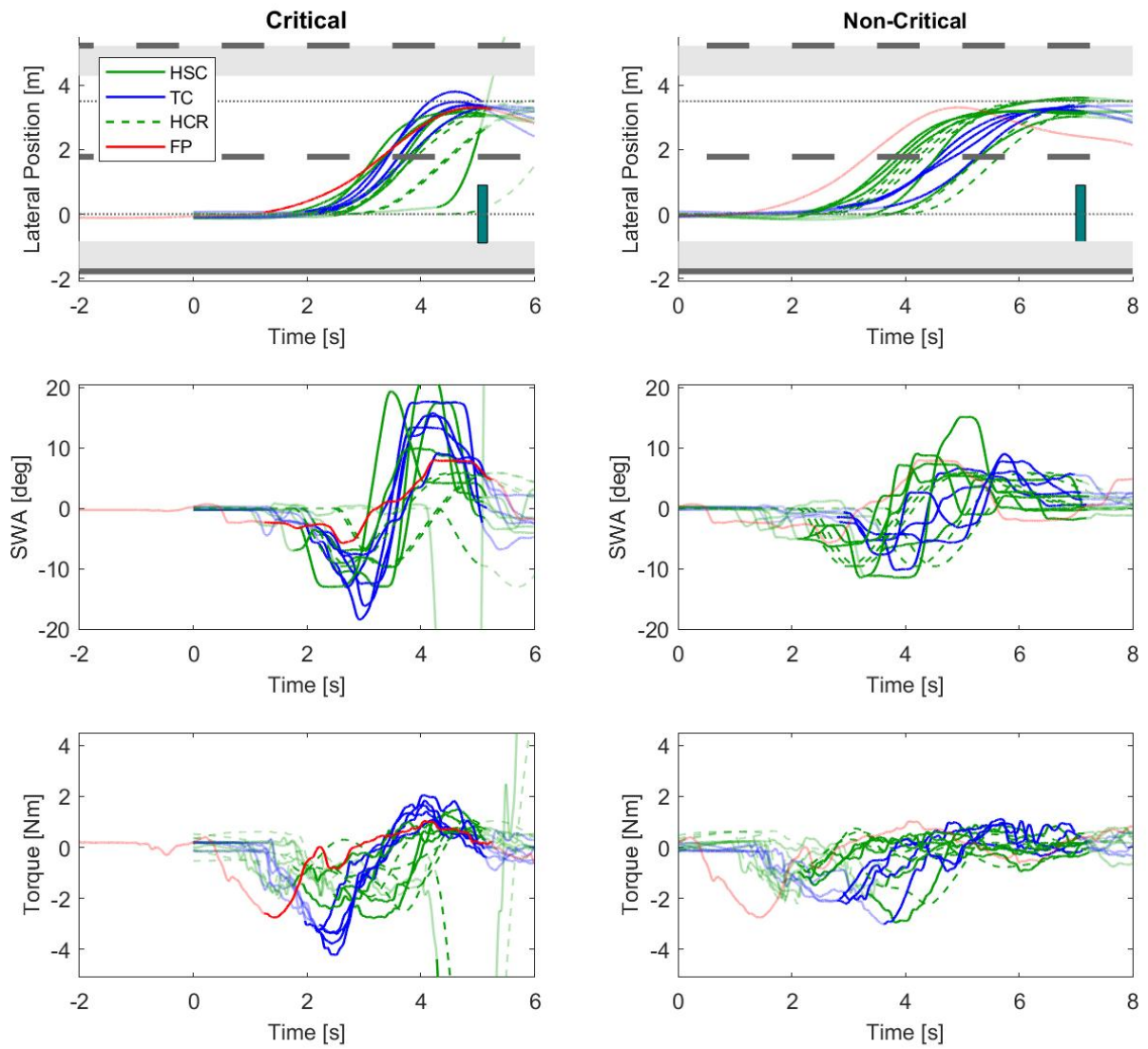


Figure (C.26) Raw data time traces of all critical (left) and non-critical (right) take-over maneuvers performed by one participant (Nr. 26) aligned at TOR. Top: lateral position, Middle: steering wheel angle, Bottom: Steering Torques. The highlighted area represents the analyzed period for the dependent variables from  $t_{start}$  to  $t_{end}$ . The falsely timed TOR during TC in (b) has been analyzed as a critical take-over maneuver, shown in (a). The time trace starts at the placement of the defect vehicle and shows no driver input until after the TOR. The vertical bar represents the defect vehicle with only its width to scale.

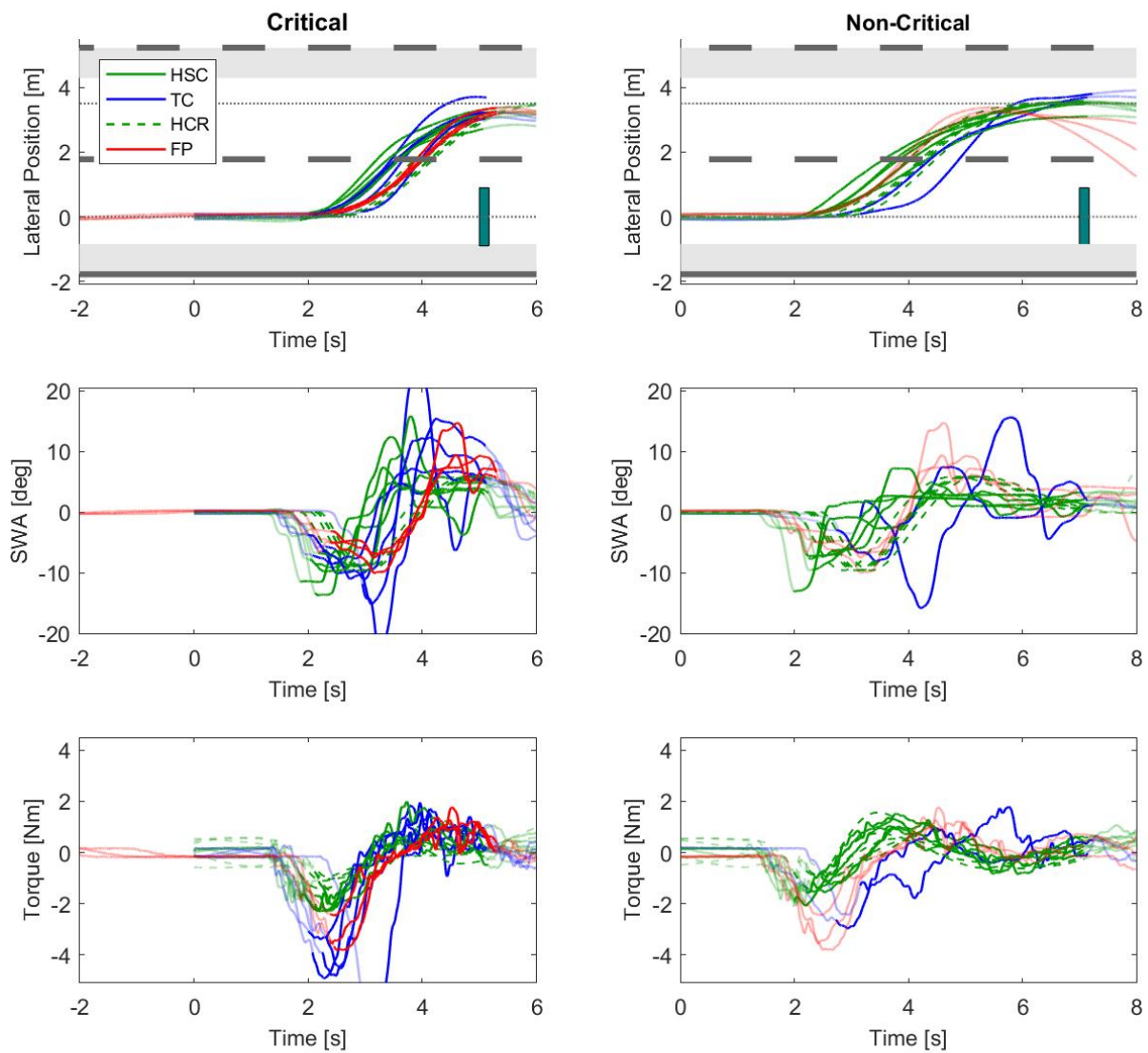


Figure (C.27) Raw data time traces of all critical (left) and non-critical (right) take-over maneuvers performed by one participant (Nr. 27) aligned at TOR. Top: lateral position, Middle: steering wheel angle, Bottom: Steering Torques. The highlighted area represents the analyzed period for the dependent variables from  $t_{start}$  to  $t_{end}$ . The falsely timed TOR during TC in (b) has been analyzed as a critical take-over maneuver, shown in (a). The time trace starts at the placement of the defect vehicle and shows no driver input until after the TOR. The vertical bar represents the defect vehicle with only its width to scale.

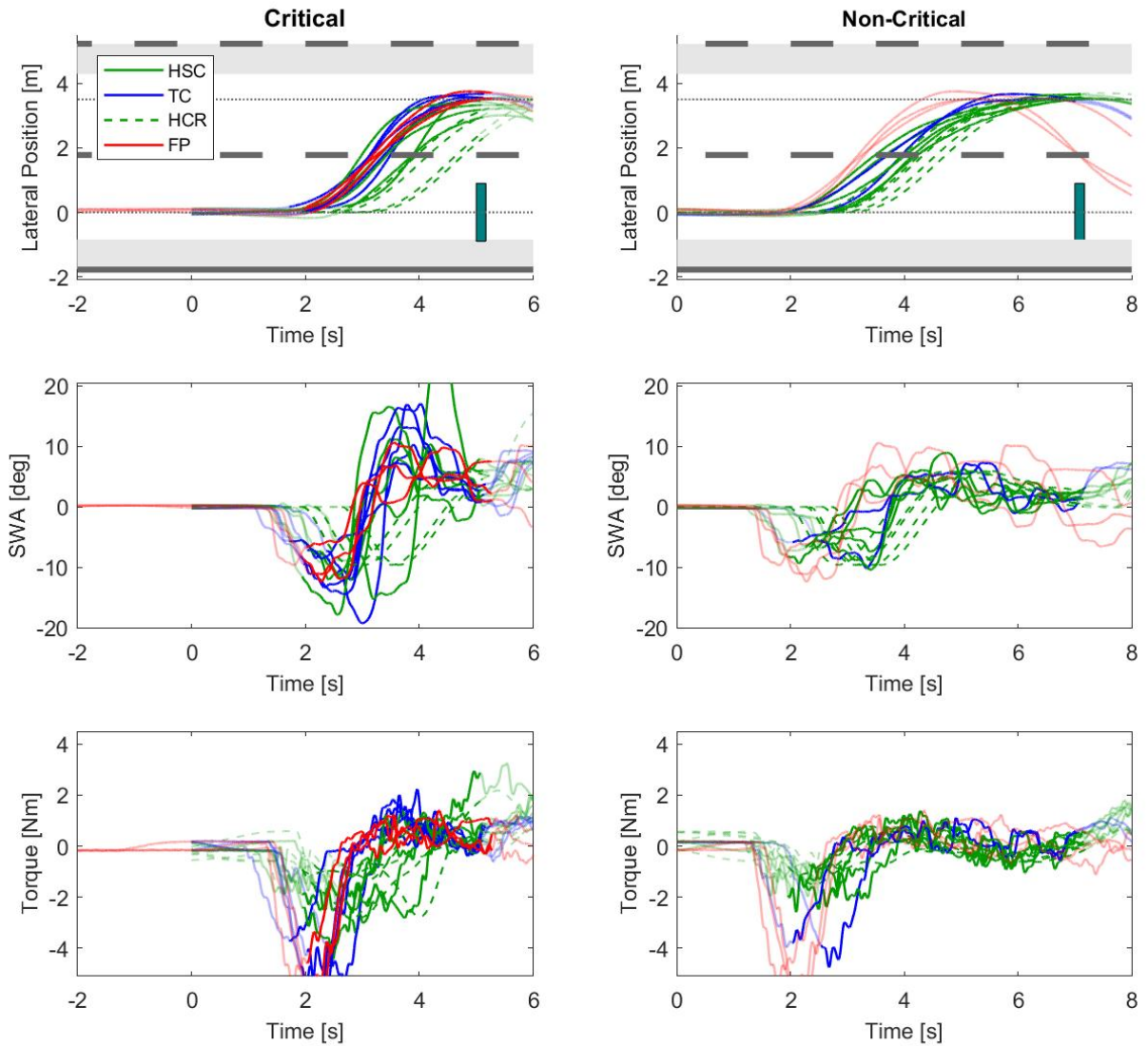


Figure (C.28) Raw data time traces of all critical (left) and non-critical (right) take-over maneuvers performed by one participant (Nr. 28) aligned at TOR. Top: lateral position, Middle: steering wheel angle, Bottom: Steering Torques. The highlighted area represents the analyzed period for the dependent variables from  $t_{start}$  to  $t_{end}$ . The falsely timed TOR during TC in (b) has been analyzed as a critical take-over maneuver, shown in (a). The time trace starts at the placement of the defect vehicle and shows no driver input until after the TOR. The vertical bar represents the defect vehicle with only its width to scale.

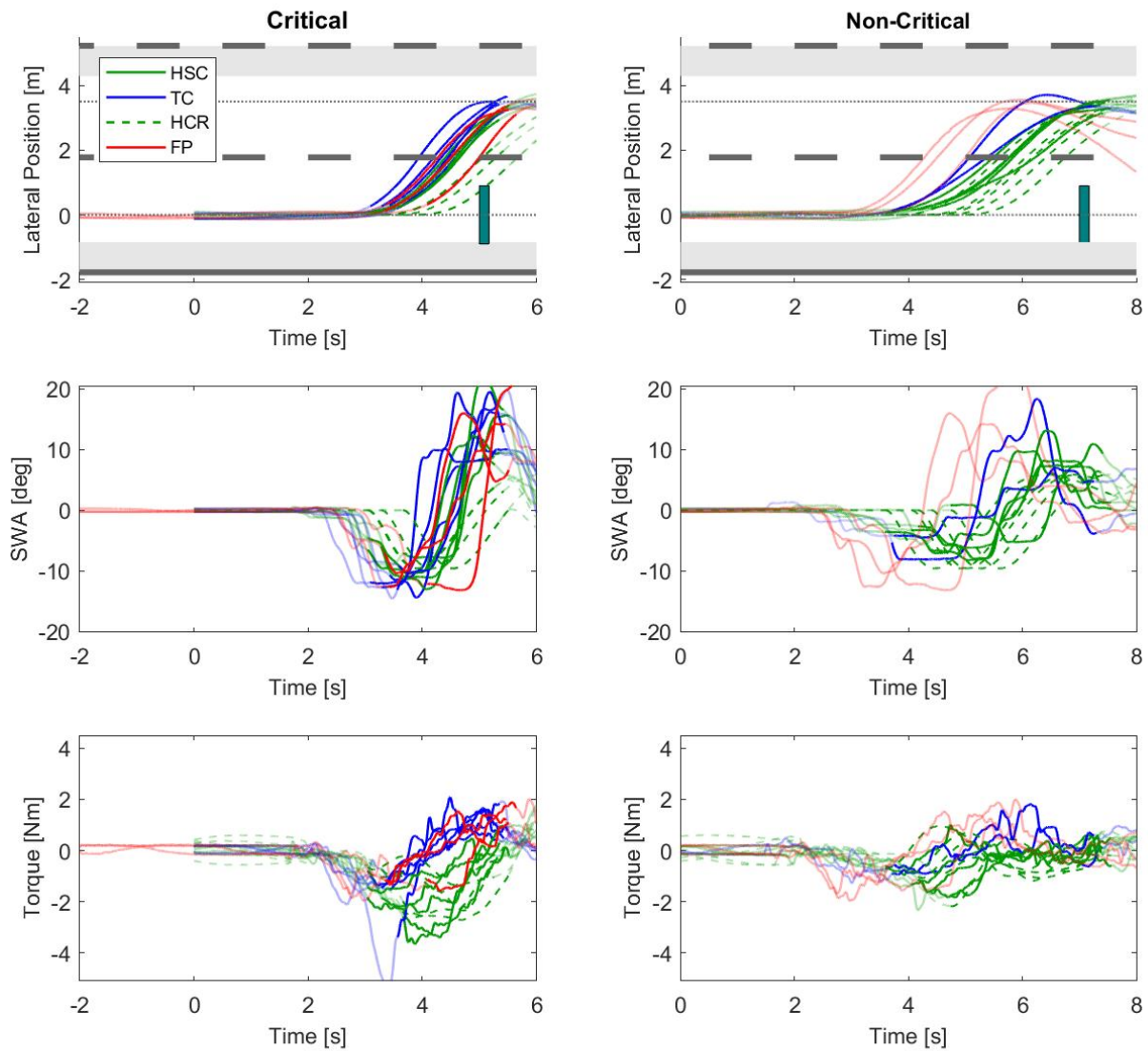


Figure (C.29) Raw data time traces of all critical (left) and non-critical (right) take-over maneuvers performed by one participant (Nr. 29) aligned at TOR. Top: lateral position, Middle: steering wheel angle, Bottom: Steering Torques. The highlighted area represents the analyzed period for the dependent variables from  $t_{start}$  to  $t_{end}$ . The falsely timed TOR during TC in (b) has been analyzed as a critical take-over maneuver, shown in (a). The time trace starts at the placement of the defect vehicle and shows no driver input until after the TOR. The vertical bar represents the defect vehicle with only its width to scale.

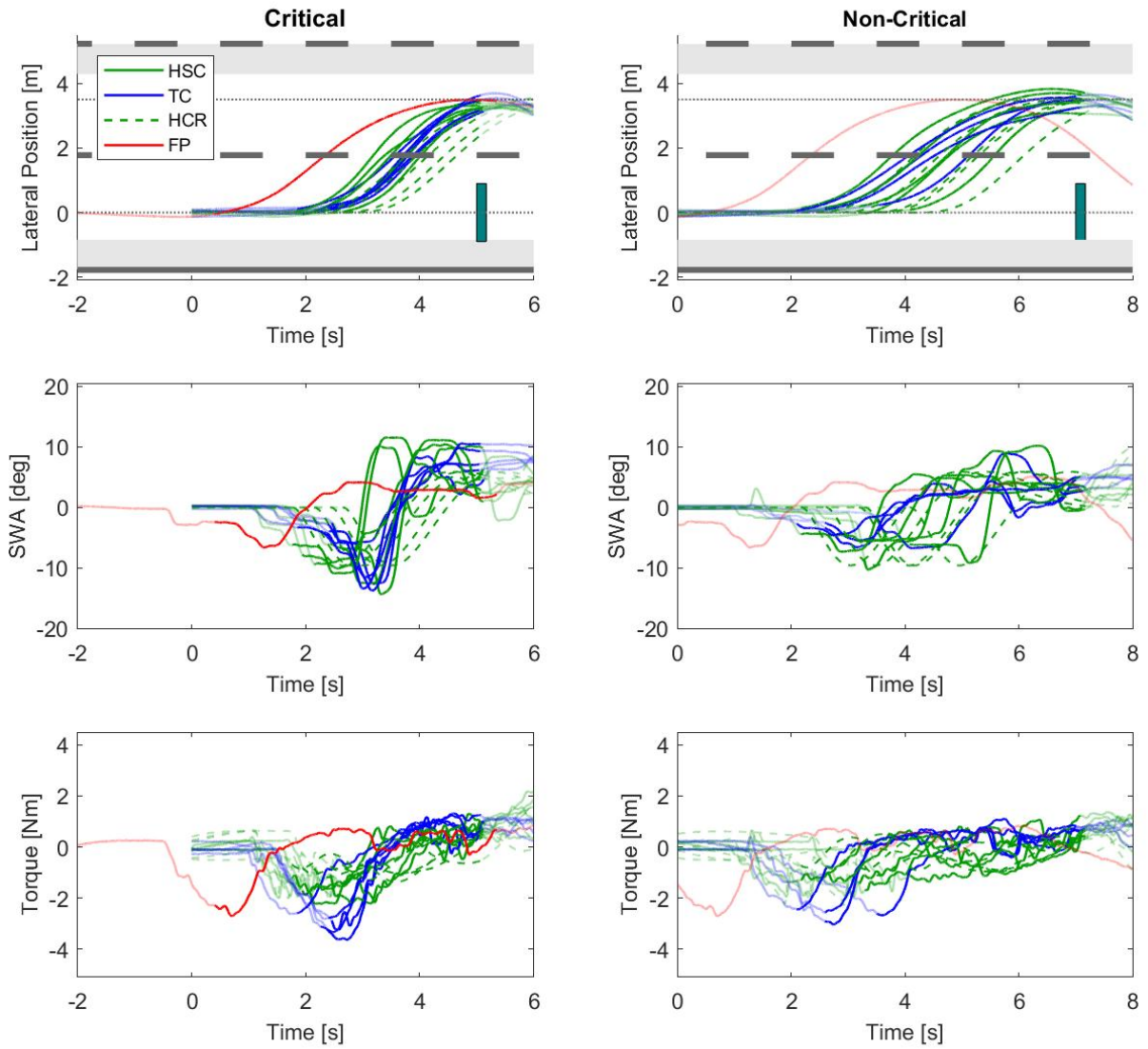


Figure (C.30) Raw data time traces of all critical (left) and non-critical (right) take-over maneuvers performed by one participant (Nr. 30) aligned at TOR. Top: lateral position, Middle: steering wheel angle, Bottom: Steering Torques. The highlighted area represents the analyzed period for the dependent variables from  $t_{start}$  to  $t_{end}$ . The falsely timed TOR during TC in (b) has been analyzed as a critical take-over maneuver, shown in (a). The time trace starts at the placement of the defect vehicle and shows no driver input until after the TOR. The vertical bar represents the defect vehicle with only its width to scale.

## C.2. Additional Results

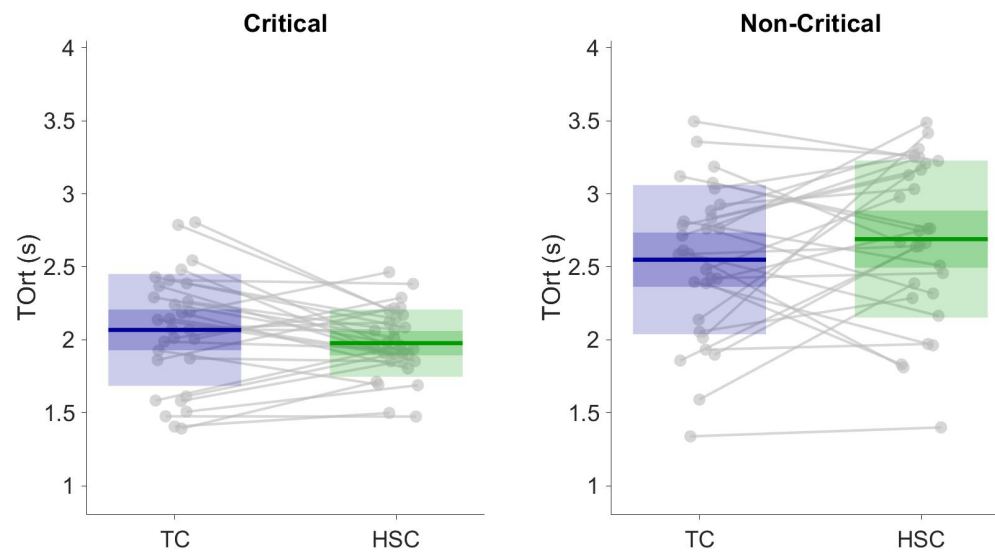


Figure (C.31) Results for the TOrt of the critical (left) and non-critical (right) take-over maneuvers. The mean is illustrated by the horizontal line within the shaded areas. The darker regions represent the standard error of the mean with a 95% confidence interval and the lighter shaded regions highlight the standard deviation. The dots represent each participant in one level of criticality, connected to a dot of the same participant in the other level.

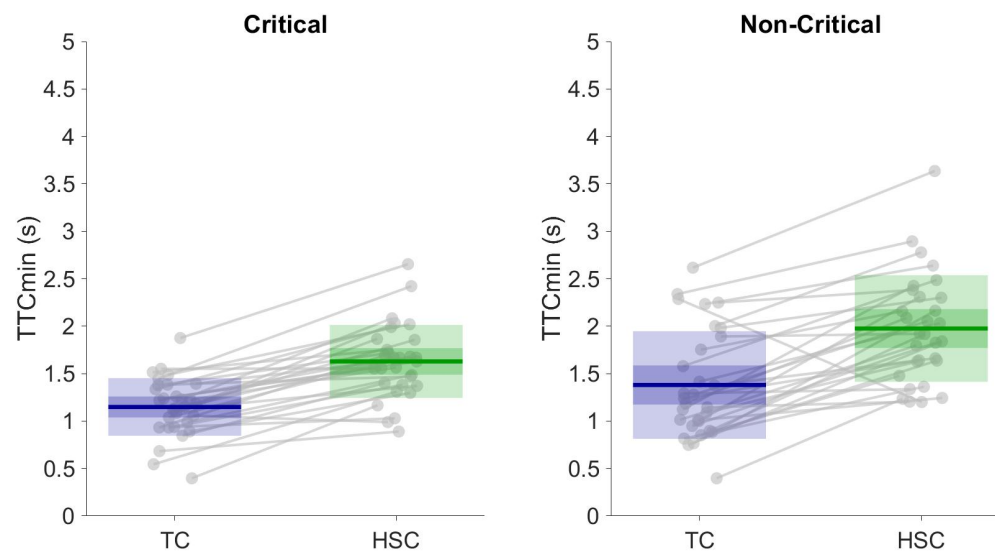


Figure (C.32) Results for the  $TTC_{min}$  of the critical (left) and non-critical (right) take-over maneuvers. The mean is illustrated by the horizontal line within the shaded areas. The darker regions represent the standard error of the mean with a 95% confidence interval and the lighter shaded regions highlight the standard deviation. The dots represent each participant in one level of criticality, connected to a dot of the same participant in the other level.

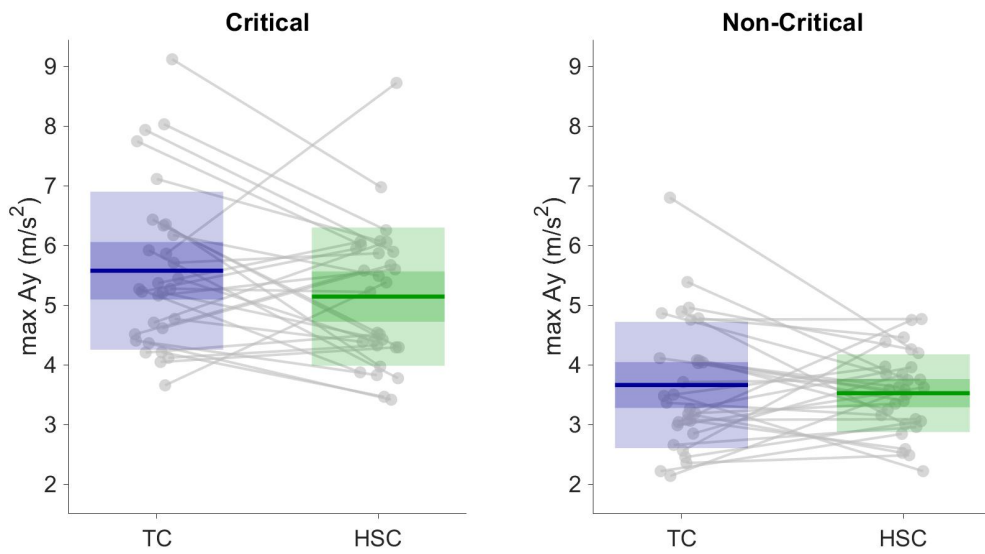


Figure (C.33) Results for the maximum lateral acceleration of the critical (left) and non-critical (right) take-over maneuvers. The mean is illustrated by the horizontal line within the shaded areas. The darker regions represent the standard error of the mean with a 95% confidence interval and the lighter shaded regions highlight the standard deviation. The dots represent each participant in one level of criticality, connected to a dot of the same participant in the other level.

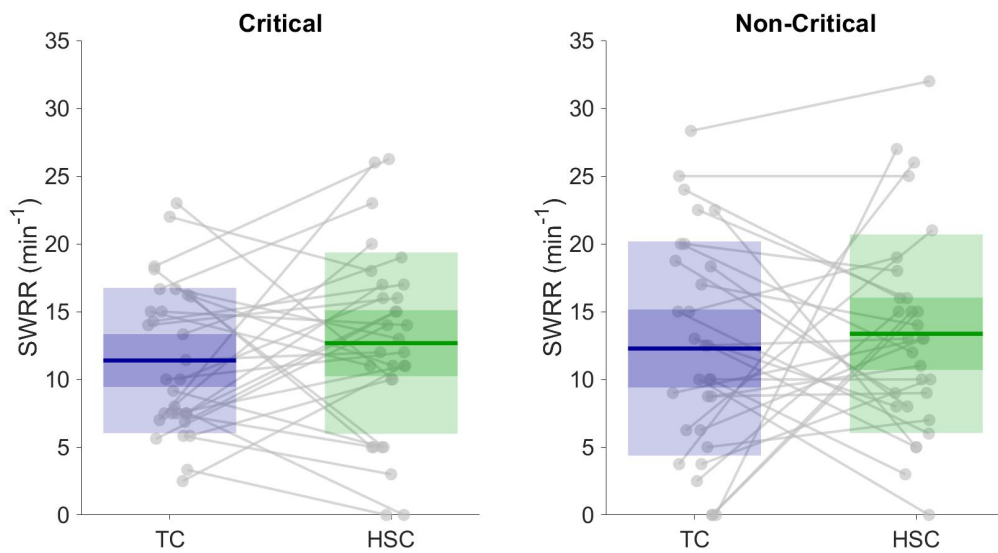


Figure (C.34) Results for the SWRR of the critical (left) and non-critical (right) take-over maneuvers. The mean is illustrated by the horizontal line within the shaded areas. The darker regions represent the standard error of the mean with a 95% confidence interval and the lighter shaded regions highlight the standard deviation. The dots represent each participant in one level of criticality, connected to a dot of the same participant in the other level.

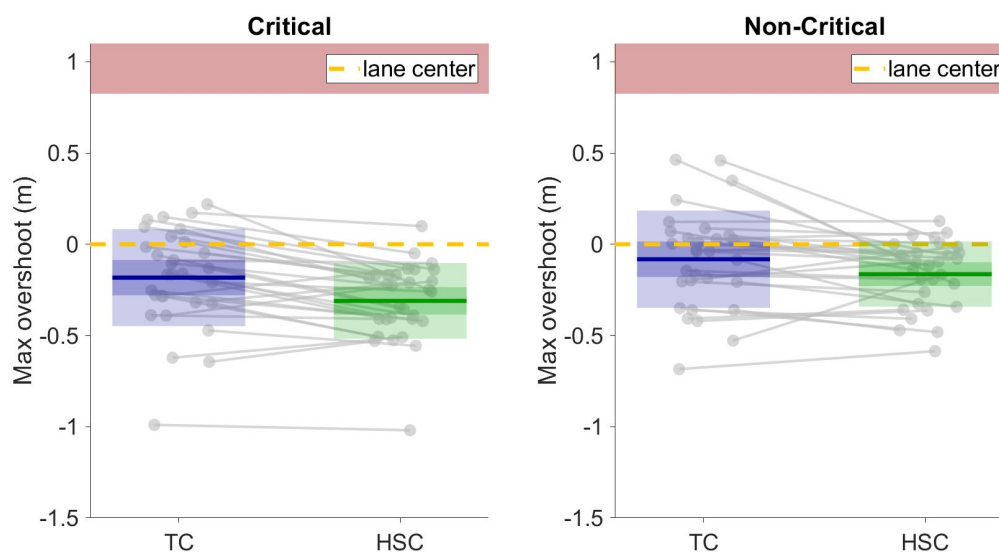


Figure (C.35) Results for the overshoot of the critical (left) and non-critical (right) take-over maneuvers. The mean is illustrated by the horizontal line within the shaded areas. The darker regions represent the standard error of the mean with a 95% confidence interval and the lighter shaded regions highlight the standard deviation. The dots represent each participant in one level of criticality, connected to a dot of the same participant in the other level. In the results of the obstacle clearance the yellow line represents lane center, and the red patch indicates the critical area for a lane departure.



# D

## Planning

At the start of this master thesis a Gantt chart was made to make a planning for all objectives, see figure D.1. The original goal was to finish the project before Christmas 2019. The project was divided into three main stages. The first stage consisted of a literature study on the take-over maneuver, during this phase the scope of this master thesis has been formed. The second phase was the actual research which was done at Cruden BV. The start of this phase included research on which approach to use for implementing control transition on the Cruden driving simulator. Two approaches were evaluated, an angle tracking control law and a force based control law. At the end of this phase it has been concluded to continue with a force based control law. This stage has not been included in this report, since it was not part of the research scope. The rest of the time spend at Cruden was used for the preparations of the experiment (e.g. implementation of HSC, Lane change algorithm and transition approaches in Matlab&Simulink and designing and building experiment environment). The implementation phase took longer than originally planned due to the issues discussed in appendix A. This caused the experiments to be postponed until the first of September. Originally a holiday was planned at the end of July before the start of the experiments. This has been moved to October due to the simulator not being available in October, and thereby eliminate the risk of not being able to complete the experiment. In the final week at Cruden, a start had been made on the data analysis. The rest of the data analyses and the documentation of the thesis have been done at the TU Delft. In the end the original goal will be achieved by defending this master thesis on the 23<sup>rd</sup> of December 2019.

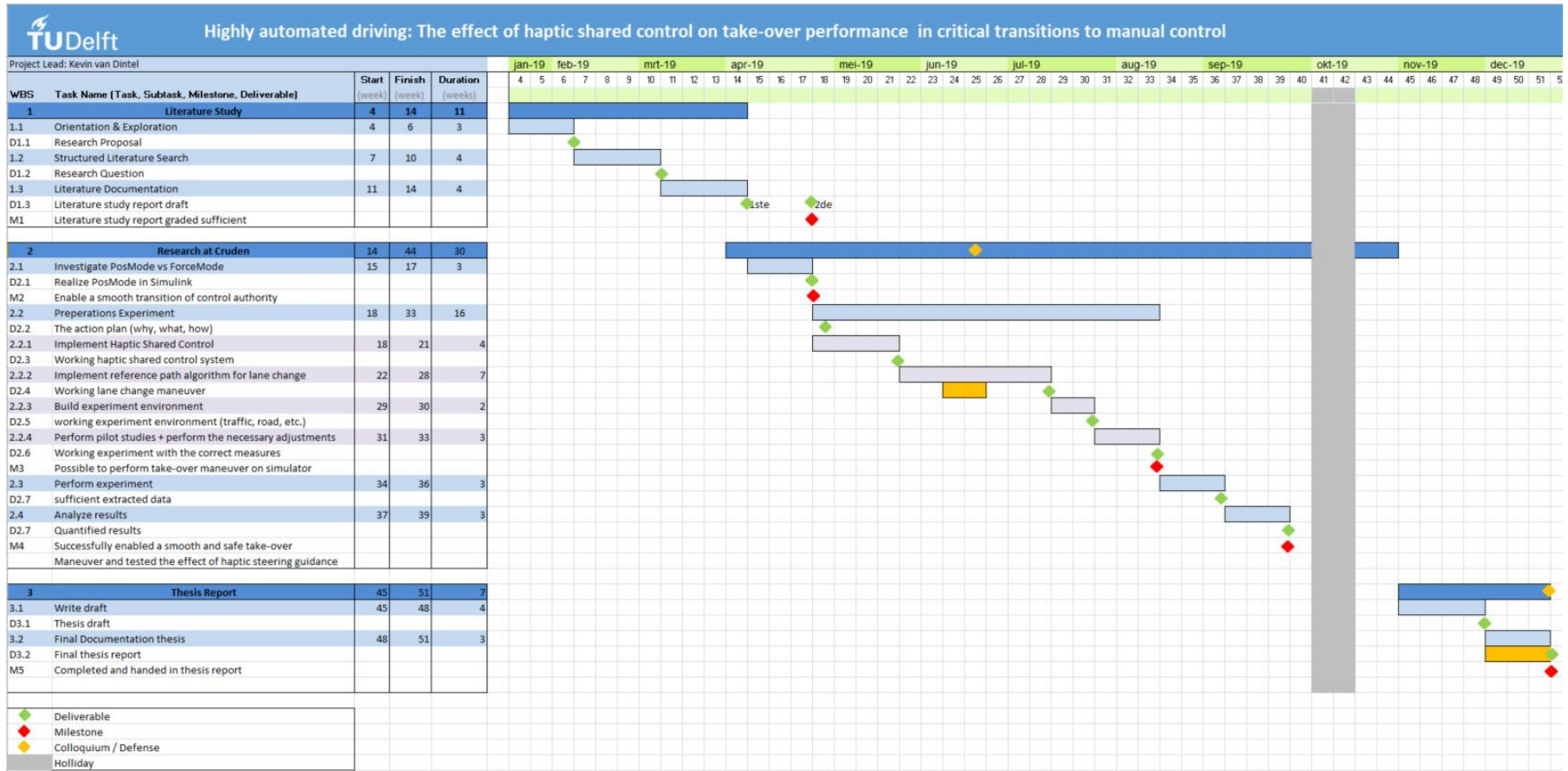


Figure (D.1) Gantt chart of the initial project planning.

# Bibliography

- [1] Edwin John Henry De Vries. Model-based brake control including tyre behaviour. 2012.
- [2] Said Mammar, Sébastien Glaser, and Mariana Netto. Time to line crossing for lane departure avoidance: A theoretical study and an experimental setting. *IEEE Transactions on Intelligent Transportation Systems*, 7(2):226–241, 2006. ISSN 1524-9050.
- [3] Kakin K Tsoi, Mark Mulder, and David A Abbink. Balancing safety and support: Changing lanes with a haptic lane-keeping support system. In *2010 IEEE international conference on systems, man and cybernetics*, pages 1236–1243. IEEE. ISBN 1424465885.
- [4] Marinus M. Van Paassen, Rolf Boink, David Abbink, Mark Mulder, and Max Mulder. *Four design choices for haptic shared control*, pages 237–254. 2017. ISBN 978-1-4724-8141-2. doi: 10.4324/9781315565712-12.
- [5] H.M. Zwaan. Adaptive steering wheel stiffness in driving with haptic shared control. Master's thesis, Delft University of Technology, <http://resolver.tudelft.nl/uuid:97ca461a-a7f6-420c-9c84-9dc168b57f50>, 2018.